Transtibial Prosthesis Insert to Accommodate Residual Limb Volume Change

Andre Raffla

Thesis submitted to the Faculty of Engineering
in partial fulfillment of the requirements for the degree of

MASTER OF APPLIED SCIENCE

in Biomedical Engineering
Faculty of Engineering
University of Ottawa
Ottawa, Ontario

May 2025

Abstract

Within the first year after amputation, individuals with lower limb amputations often require multiple prosthetic sockets to accommodate changes in residual limb volume and shape. This frequent need for new sockets arises as the limb matures, posing a challenge for both amputees and prosthetists. Digital manufacturing technologies offer promising solutions to streamline this process. This thesis presents the development and pilot evaluation of a novel transtibial prosthesis insert, designed to provide a good socket fit without the need to manufacture an entirely new socket.

The insert is created by digitally aligning the original socket shape with a newly designed socket shape based on the current limb morphology. This alignment allows for the digital creation of a 3D insert model that conforms to the original socket externally while matching the new limb shape internally. The insert is then 3D printed and integrated with the original socket to achieve proper fit.

Various materials were tested to identify appropriate material and 3D printing parameters. An insert prototype was subjected to mechanical tests in accordance with current transtibial prosthesis socket testing methods to ensure durability under typical prosthesis loads. Additionally, a pilot trial with a transtibial amputee was conducted to evaluate user experience and satisfaction.

Following testing, Ninjatek Cheetah Thermoplastic Polyurethane (NCT) was selected as the most appropriate material. The printing parameters were cubic print pattern and 35% infill. The results from mechanical testing and the pilot trial indicated that the insert is robust for use in daily activities, can accommodate residual limb volume change, and does not compromise on comfort and fit. This new approach offers an alternative to manufacturing a new socket, which saves time and costs for the end-user, prosthetist, and the health care system.

Acknowledgments

First and foremost, I would like to thank my supervisors, Prof. Edward Lemaire and Prof. Natalie Baddour, whose expertise, understanding, and patience were invaluable to my graduate experience. Your guidance, insightful comments, and constant encouragement made this thesis possible. I am grateful for your continuous support throughout the entire process.

I would also like to thank the uOttawa makerspace team for their assistance in 3D printing the initial prototype. Thanks to their insight and time, the prototype was made possible. I would like to thank Mr. Leo Denner for his countless hours assisting me with the Instron technologies used in this thesis, providing expertise in their operation. I would like to thank the uOttawa machine shop team (Mr. Paul Burberry and Mr. James Kent) for always machining all requested parts needed in this project, timely and in the highest-quality possible. I would like to thank Mr. Farshad Golshan for his assistance in 3D printing the final model. I would also like to thank the Ottawa Hospital Prosthetics team (Mr. Patrick Label, Mr. Daniel Maassen, Ms. Kaitlin Evans and Ms. Natalie Mainville). They were directly involved in many stages of the project including providing socket models for the prototype, preparing the prototype for testing, providing expertise on user needs and connecting me with candidates for the pilot trial. Without their time and effort, this project would have suffered immensely.

On a personal note, I would like to thank my family for their unconditional love and encouragement. To my parents, Nagui Raffla and Marianne Yanni, thank you for your endless support and for instilling in me the value of education. To my dear sister Clara Raffla, thank you for always believing in me and cheering me on. Lastly, I would like to thank my wonderful partner, Melody Salib, who supported me through every roadblock and breakthrough. She was my anchor during every storm, keeping me steady on my path to completing this thesis.

Thank you all for your contributions to this thesis. I could not have accomplished this without each and every one of you.

Table of Contents

Table of Figures

Table of Tables

Nomenclature

Abbreviations	Definition
2D	Two dimensional
3D	Three dimensional
ABS	Acrylonitrile butadiene styrene
AM	Additive Manufacturing
BSP	Bi-lateral symmetry plane
CAD	Computer aided design
CAE	Computer aided engineering
CF	Carbon fiber
CO_2	Carbon Dioxide
CT	Computed tomography
FDM	Fused disposition modelling
ISO	International Organization for Standardization
LabVIEW	Laboratory virtual instrument engineering workbench
MBB	Minimum bounding box
MJF	Multi-jet fusion
MRI	Magnetic resonance imaging
NCT	Ninjatek cheetah thermoplastic Polyurethane
PCA	Principal Component Analysis
PEQ	Prosthesis evaluation questionnaire
PLA	Polyactic acid

PP	Polypropylene
S_b	Ankle joint specific offset
SLS	Selective laser sintering
TOHRC	The Ottawa Hospital rehabilitation center

Chapter 1: Introduction

Transtibial amputation marks a turning point in a person's life, with the loss of a limb below the knee bringing about continuous changes in the body's physical state well after the initial surgery. Among the most critical of these changes is limb volume change. In the post-amputation phase, the residual limb typically undergoes a decrease in volume as swelling decreases and healing progresses. This reduction often necessitates multiple adjustments to the prosthetic socket or the creation of entirely new sockets as the initial prosthesis becomes loose, reducing comfort and mobility.

The need for repeated adjustments not only adds to physical discomfort but also imposes a financial and emotional burden on the amputee. In response to these challenges, this thesis details a novel device that can be quickly and cost-effectively produced specific for each amputee. This innovative insert approach streamlines the refitting process, reducing the need for frequent prosthetic socket replacements and enhancing the overall rehabilitation experience for transtibial amputees.

1.1 Rationale

With many advancements in lower limb prostheses, lower limb amputees are now able to enjoy a much-improved quality of life and health compared to decades ago. Nevertheless, reduction in residual limb volume and changes in limb shape within the first year of amputation usually leads to an ill-fitting prosthesis. Amputees may require a new socket, or a full prosthesis change 3 to 5 times within the first few years [1]. Since the socket adjustment and fitting process can be labor-intensive, time consuming, and costly, both the amputee and the health care system would benefit from a reduction of any of these factors. A possible

solution is to develop an automated or semi-automated, cost- and time- effective process to readjust the socket shape and size.

Maintaining an appropriate socket shape is essential to ensure the highest quality of life. In some Canadian provinces, the person covers all or a substantial portion of the cost for sockets and prostheses, with the remainder being subsidized by the government [2]. This can make prosthesis acquisition financially burdensome, thereby leading many people to delay refitting as long as possible to save money and time. The current process for getting a new socket (casting or scanning, socket design, fabrication, initial fitting, iterative adjustments, final socket fabrication, and final fitting) is not only burdensome for the person but is difficult and time consuming for prosthetists. Thus, a cost effective and faster socket shape adjustment and fitting process would ensure better quality of care, the best allocation of resources to the healthcare system, and help alleviate caregiver workload.

A well-fitted socket helps to provide safe and efficient mobility while using a prosthesis. People using an ill-fitted prosthesis for elongated periods often report pain, discomfort and an inability to perform daily tasks [3].

1.2 Objectives

The objective of this thesis is to develop and perform a pilot evaluation of a 3D printed lower limb prosthesis insert. The insert should be inexpensive, easy to design, and quick to fabricate. The insert shape should be custom designed for every socket using a full- or semi-automated process.

1.3 Thesis Contributions

This thesis presents a framework for the development and evaluation of a novel transtibial prosthesis device called an “insert”. The key contributions include but are not limited to design and development of an insert from two 3D shapes, mechanical testing of inserts and transtibial sockets, and a pilot clinical evaluation.

The thesis provides an automated method to align two 3D shapes allowing for further manual adjustment. The method for automated alignment reduces the time and effort required for an initial alignment, providing a quick and efficient starting point. Integrating manual adjustments further allows designers to fine-tune the alignment, ensuring that the final inter-shape positioning is satisfactory. The thesis also provides a method to create a 3D model from the difference between two aligned 3D shapes. This method allows the insert to conform to an amputee’s old socket externally and their new limb internally. Finally, the thesis provides an analysis of different materials and 3D printing settings, leading to an evidence-based recommendation for insert materials and infill settings.

Regarding mechanical testing, the thesis provides a complete comprehensive method to mechanically assess the insert under various loading conditions. Since the insert was tested in a socket-insert system, the methods used for mechanical testing can also be used to test other transtibial prosthetic sockets.

The thesis provides the results of a pilot evaluation with a prosthesis user wearing an insert. This evaluation provides real-world feedback on how the insert performed in daily use. Quantitative data on gait performance, stability, and energy efficiency offer a measure of the insert’s performance compared to the performance of a regular socket. Qualitative data from participants on comfort, ease-of-use, and overall satisfaction offer insight into user experience, guiding further improvements to meet user needs more effectively.

Chapter 2: Literature Review

Additive Manufacturing (AM) is an integral part of many industries such as, automotive, military, telecommunications and computer industries, allowing many novel innovations that were previously not feasible. This is particularly true in the biomedical engineering field due to the need for highly customized equipment and devices [4-8]. Figure 1, for example, shows a transtibial prosthesis designed with AM. The use of AM in prosthetics and orthotics commonly starts the production process by using 3D scanning technologies to collect the person's morphology. Then, person-specific designs are created using computer aided design and engineering (CAD-CAE) tools. Finally, a prototype may be made using an AM machine. AM usage thus offers an alternative in the orthotics-prosthetics sector, along with novel 3D acquisition procedures [8].

Figure 1: Prosthesis designed using computer aided design and fabricated using additive manufacturing [9]

This thesis concentrates on the application of AM in prosthetics, specifically transtibial prosthetics. The following section reports on socket fitting techniques and technologies, manufacturing processes, shape alignment algorithms, and socket testing protocols. A prosthetic socket is the interface between the prosthetic components (joint, connectors, foot, etc.) and the person's residual limb. Since all ground reaction forces are transferred to the body via the socket, socket design is essential for function, comfort, and limb health [10].

2.1 Socket Manufacturing

Detailing the limb morphology is crucial for prostheses development using AM. To achieve this, different tools have been used such as computed tomography (CT), 3D scanners, and computer aided design (CAD).

2.1.1 CT Scanning

CT is an effective tool for diagnostics and surgical planning. Traditionally, images are captured in either the axial or transverse planes [8]. Modern CT scanners can create volumetric reconstructions for 3D representations by recording images along many planes [8]. CT has been recommended by numerous authors to create prosthetic and orthotic devices [11-15]. One of the earliest recommendations was in 1998 [11], where volume accuracy of over 97% was obtained in spinal orthosis CT scans. CT or magnetic resonance imaging (MRI) scanning was recommended as a time-effective approach to obtaining torso shape without compromising accuracy, ease of use, or cost [11]. In another instance [16] CT in conjunction with AM was used to create diabetic insoles. Peak plantar pressure was reduced by 33.67% and pressure and tissue tension were correlated along the plantar foot with the therapeutic effect of footwear and specially constructed orthotic inserts [16]. When producing silicone ear

prostheses using 3D printing [13], CT and AM (using polylactic acid or polylactide, PLA, resolution 100 μm) differed by 0.1% between the manufactured prosthesis and the objective model. Liacouras et al. [14] developed methodologies for building transtibial prosthetic sockets, using CT to acquire residual limb morphology. Furthermore, the CT data enabled prosthetic socket finite element analysis to determine the structural stresses and strains at the socket as well as contact pressure at the fibula head [14]. Among the biggest benefits of CT is the high picture resolution between tissues, together with the ability to boost contrast and lower noise [8]. However, radiation exposure exists, with the exposure directly related to scanning time, and the partial pixel effect (i.e., various densities sharing overlapping pixels) causes blurred boundaries that makes some images difficult to use [15].

2.1.2 3D Scanning

3D scanning has emerged as the most convenient and comfortable method for capturing human topography or external limb contour [8]. To establish the desired shape, 3D scanning systems use light-based technologies to locate points that make up the object's surface in space. Computer software is then used to obtain a CAD model by reconstructing surfaces from the point cloud.

3D scanners can use single scans for reconstruction, structured light technologies, lasers, and various stereo reconstruction techniques [17], [18]. Laser and structured light technologies are most frequently utilized to recreate human body shapes [18]. The laser approach uses a hand-held instrument to produce a laser dot or line [8]. A sensor, typically a charge-coupled or a position-sensitive device, measures the distance between the scanner and the surface [8]. Data is gathered with respect to an internal coordinate system for static objects. In dynamic situations, the scanner's position is used to create the point cloud [8]. In structured

light techniques, pre-defined light patterns are projected onto the object using a projector-camera system [8]. The inability of this technology to capture certain topography areas of the human body with complex folds and creases is a limitation; for example, between the fingers when the hand is in a neutral posture, back of the knee when bent, or the armpits [8]. Nevertheless, noise in the images captured is decreased and the information gathered is more accurate [8]. To develop a standardized, clinically valid procedure, 3D anatomical data gathering techniques were examined and laser scanning offered the best combination of cost, resolution, speed, accuracy, patient safety, cost, and overall efficiency for collecting ambiguous data [19].

Other technologies include white light scanning, blue light scanning, and polarization 3D imaging. White light scanning employs line shadows that are cast from a 2D lens onto a 3D surface [20]. Cameras capture the variations in these lines as they contour across the object, compiling point clouds that are combined to form a 3D image [20]. Enhancing the capabilities of white light, blue light scanning incorporates a narrower wavelength, reducing interference from ambient lighting, thus offering superior precision [20]. Polarization 3D imaging utilizes the reflective polarization properties of surfaces to uncover detailed textural information [21], distinguishing between specular and diffuse reflections to enhance the accuracy of surface texture and geometry characterization [21].

In addition to data file sizes being substantially smaller with 3D scanning than with magnetic resonance imaging (MRI) and CT, processing time was also less [18]. Varied 3D scanners may have different recording times and resolutions, ranging from 3-5 minutes and 0.1 mm for highly accurate systems to a few minutes and 1.0 mm for inexpensive devices [22]. Inexpensive hardware and software, a low learning curve, availability, accessibility, and efficiency are further benefits of 3D scanning techniques [18].

2.1.3 CAD

Computer-aided design (CAD) software has been recommended by a number of authors as a way to improve imaging results by adjusting data points to better describe a 3D object [23], [24]. Eldeeb recommended combining CAD with CT scanning to create an orthosis model [11]. Mavroidis et al. [25] developed patient-specific foot orthoses using 3D laser scanning and patient anatomy surface data was optimized using CAD software. Comparing the prototype to a commercial foot orthosis, the prototype more accurately fit the person's anatomy [25]. CAD has been used successfully in recent works to produce an upper limb orthosis [26] and a lower limb orthosis [27]. Nevertheless, while the use of 3D scanning along with CAD has become more common, there is a need for further research in the field and an establishment of standards to increase uniformity in the technologies available [24]. Furthermore, current technologies are not adopted by developing countries due to the gap in capital sources and knowledge [23]. Research would facilitate reducing the cost of acquiring and operating the technologies allowing its implementation in developing countries.

2.2 Additive Manufacturing (AM)

Over the years, many AM techniques have been developed along with various ways to categorize these techniques. Currently, AM techniques are classified according to the method the material is applied [8]. The most common techniques are fused deposition modelling (FDM), selective laser sintering (SLS), and multi jet fusion (MJF) (Figure 2).

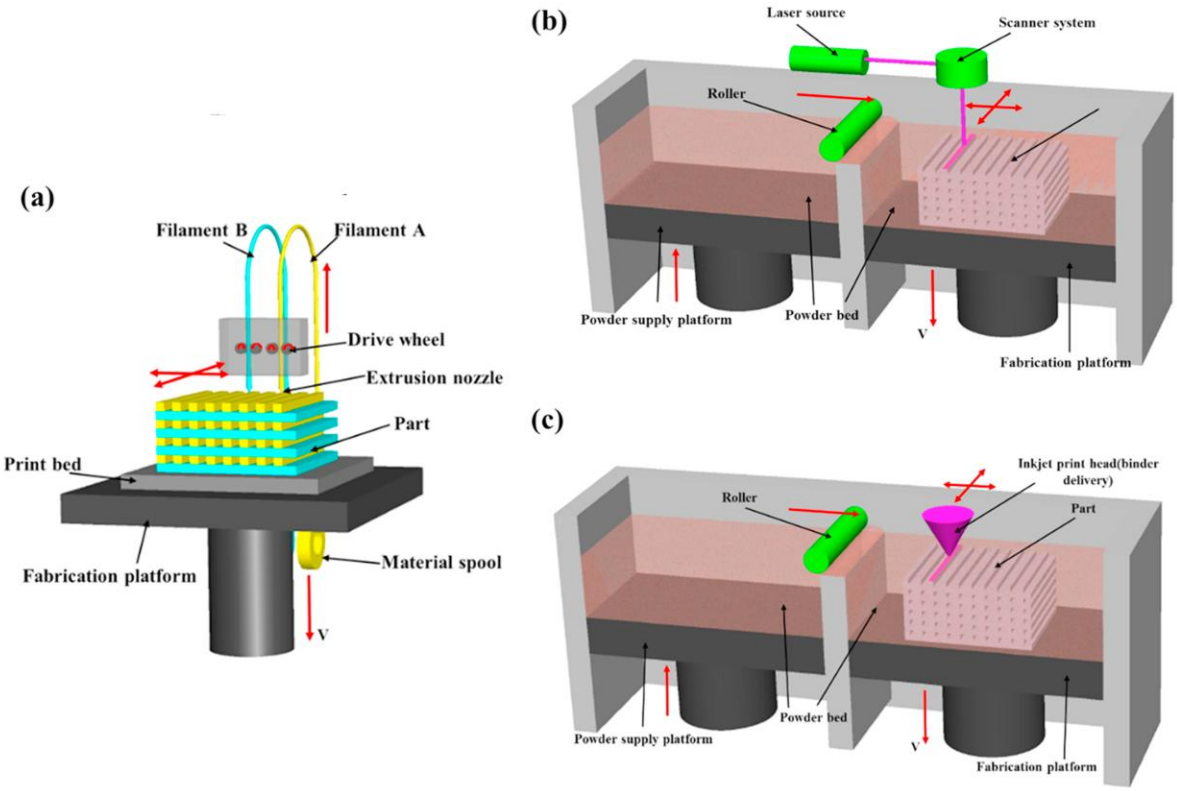

Figure 2: Diagrams describing (a) FDM (b) SLS (c) MJF [28]

2.2.1 FDM

For each layer of objects made using FDM, a semi-molten material is extruded through an extrusion head that moves along the x- and y- axes [29]. The moveable extrusion head can have one or two extrusion nozzles, for depositing build or support material. Typically, the extruder head fills the delimited zone created by the previous extrusion by adhering to a predetermined pattern after first extruding the perimeter of each layer. The support platform descends after the layer is finished, and another layer is extruded. Layer after layer, the technique goes on until the item is finished. FDM technology uses inexpensive materials, which is the main benefit. The earliest references found that used FDM for prosthetics was in 1993, where Rovick [30] aimed to reduce the required manual labor when producing a prosthetic socket.

2.2.2 SLS

By employing a CO_2 laser to selectively fuse powdered polymer-based materials, such as nylon/polyamide, the SLS process produces 3D solid objects [31]. To create a 2D profile, a CO_2 laser moves across the powder bed in the x- and y- axes, selectively sintering designated portions [31]. The platform descends, a fresh layer of powder is applied, and the sintering procedure is repeated one layer at a time [31]. This procedure is also referred to as powder-based fusion. Some of the earliest adopters of this technique for prosthetics are Rogers et al. [32], who showed that SLS created better contouring sockets than traditional methods, particularly in the distal end [32].

2.2.3 MJF

Powdered-based fusion is a recent advancement in 3D printing. A build platform is first covered with a powder layer [8]. Second, by adhering to a patterned layer in the x-y plane, a liquid binder is selectively deposited by an inkjet printhead [8]. As opposed to SLS, this leaves the powders in a semi-solid state. Heat is then applied to strengthen the bonds, before the platform descends and the following powder layer is spread [8]. In a comparative study between SLS and MJF [33], parts printed with MJF had similar tensile strength in the x and y orientation compared to those printed with SLS, and tensile strength 25% higher in the z orientation. MJF has been used in orthotics and prosthetics to create a foot prosthesis [34] and a hand prosthesis [35].

2.3 Comparing Socket Shapes

With the development of AM techniques, many applications developed a need to compare 3D socket shapes [36]. Shapes can be compared for assessing limb changes over time, socket manufacturing analysis, socket liner design, or creating a socket insert. Substantial work has been done in the field and, while principal component analysis is currently the most used algorithm, no algorithm accurately aligns all 3D shapes.

Three main processes are often involved in 3D object matching and retrieval: object normalisation, feature extraction and object representation, and object comparison. The first stage typically translates object centroids to the 3D coordinate frame origin, normalises point variances on the objects, and aligns principal axes obtained through Principal Component Analysis (PCA) [37], [38]. Many PCA variations have been developed over the years, such as, probabilistic PCA, kernel PCA, robust PCA, weighted PCA, generalized PCA, and Laplacian PCA (Figure 3) [39]. The second stage collects numerous features from the objects and expresses them in a variety of ways, including histograms, 2D spherical maps, 3D grids, and abstract representations based on the extracted features [37]. For efficient comparison, the third stage often uses inter-shape distance measurements such as the Euclidean distance.

The above-mentioned normalisation procedure has some shortcomings. PCA-based orientation alignment is not robust because PCA is sensitive to object point distributions. Objects of comparable shape could be misaligned [38]. Furthermore, this technique ignores differences in the 3D aspect ratios. Different objects with similar shapes could have different aspect ratios for the three spatial dimensions. Normalization by the same scaling factors results in misalignment of their corresponding sections (Figure 4) [40]. All these misalignments can exaggerate the contrast between objects with comparable forms. As a result, relevant features

(i.e., features in common between objects of the same category) may not be matched [40]. Consequently, appropriately normalising the objects is critical.

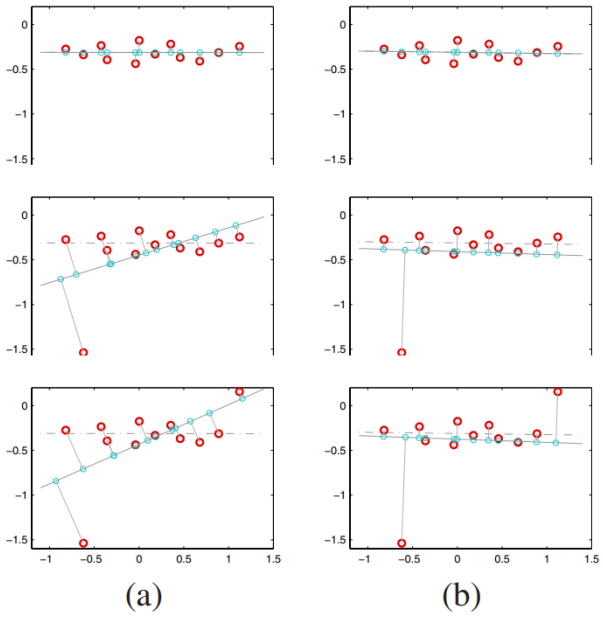

Figure 3: Principal components found using (a) PCA (b) LPCA

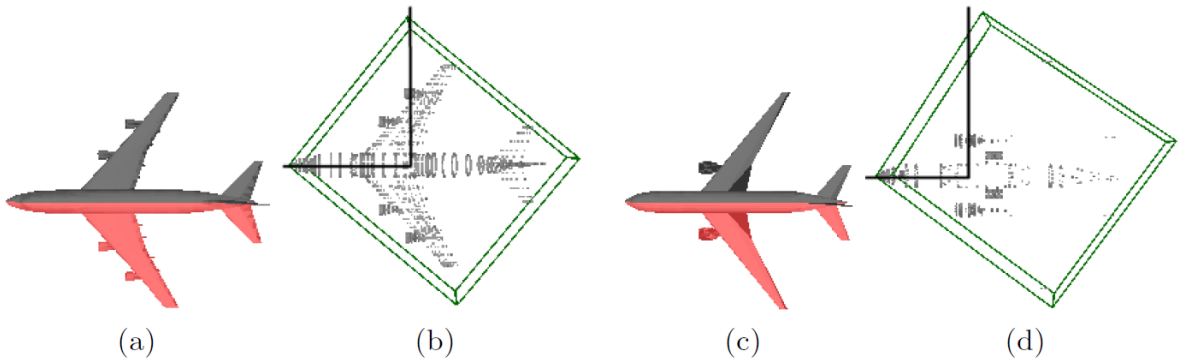

Figure 4: (a,c) show two 3D objects with a similar shape but different aspect ratio. (b,d) show misalignment due to the difference in the 3D aspect ratios of the first principal component axes

When applicable, scaling the objects according to their 3D aspect ratios is a simple enhancement over the usual normalising method. This raises the issue of which coordinate system should be used to compute the 3D aspect ratios. Measuring 3D aspect ratios along the

PCA axes is one option. However, this approach is not robust due to its dependency on PCA [40]. An alternate way is to compute the minimum volume bounding boxes (MBB) [41], and then normalise the objects based on the MBB axes and widths, but this was found to be less robust than PCA [40]. Furthermore, for prosthetic applications, scaling is not an option since scanned dimensions are critical for creating an appropriate device.

Another method utilises bilateral (i.e. left-right) symmetry planes [40]. Many natural and man-made objects have bilateral (i.e., left-right) symmetry. The BSP divides an object into two halves (reflectional symmetry) where, each half is a mirror reflection of the other about the BSP. Furthermore, the BSP contains the primary axis that defines the top object boundary. As a result, by normalising objects according to the major axes and 3D aspect ratios set on the BSP, the semantically relevant components, such as the head, body, and legs, can be aligned.

PCA or MBB alone are insufficient for calculating an object's BSP [40]. In terms of position and 3D orientation, the PCA and MBB planes (i.e., planes normal to the PCA/MBB axes) may not be aligned with the BSP plane [40]. Simply using PCA and MBB does not make it easier to establish the closest plane out of three to the object’s BSP [40]. Further, the best fitting BSP may not pass through the item’s centroid if the item is not perfectly bilaterally symmetric [40]. To compute an object's BSP, the algorithm must first compute the correct 3D orientation and position of a plane that divides the item into two bilaterally symmetric pieces. Further research and improvements are needed on the algorithm suggested in [40] to definitively say that BSP is a better than PCA at object normalisation (Figure 5).

Figure 5: Sample BSP results. Successful cases (Rows 1-3). Failure cases (Row 4) [40]

2.4 3D Printed Transtibial Sockets

AM of 3D printed sockets may reduce the period between amputation and receiving the initial prosthesis or receiving a new socket after socket difficulties, which may improve patient outcomes [42], [43]. AM may also be relevant for managing patients with unstable limb volume who require multiple socket changes. Furthermore, the cost of a 3D printer and 3D printing filament materials can be lower than the cost of traditional manufacturing methods [44], [45], [46].

One material that can be used for 3D printed orthopedic devices is polylactic acid (PLA). PLA is biocompatible and has no negative metabolic effects [47], [48]. Furthermore, due to its semi-crystalline form, PLA has a lower melting point (150-162°C) [49], higher compressive strength (70 MPa) [50], and lower thermal expansion (78 m/m-K) [51] than acrylonitrile butadiene styrene (ABS), another typical 3D printing material in FDM processes. Accordingly, PLA could provide specific advantages for prosthetic sockets, such as increased durability and strength.

Another material used for 3D printed devices is polypropylene (PP), which is preferred due to its lower cost and greater durability compared to other typical 3D printing materials, such as ABS or PLA. However, just two studies examined used PP, and any strength advantages are inconclusive [52], [53]

Carbon fiber (CF) was extensively employed in 3D printed experiments, since CF has high strength, is lightweight, and is used in traditional socket manufacturing. When compared to PLA alone, composite 3D printed sockets (i.e., adding carbon fiber particles to PLA) had a 31.5% increase in ultimate failure force (Figure 6) [50]. Carbon added to PLA boosted bending modulus by approximately 208% and maximum bending strength of material samples by 36%, when compared to PLA alone (Figure 6) [54]. These qualities are important for socket strength because the load line is anterior to the knee and causes a bending moment in the socket [50].

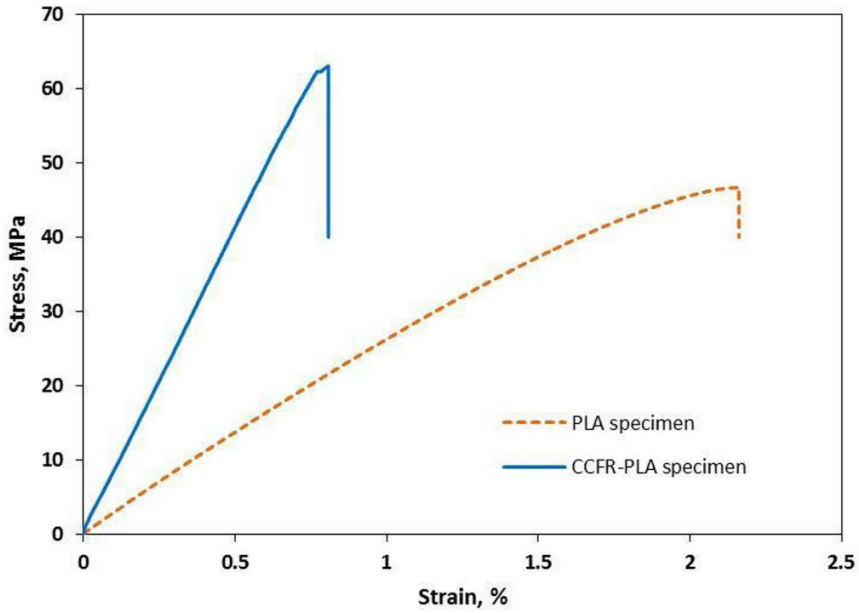

Figure 6: Stress versus strain graph comparing sockets made with PLA and sockets made with a PLA-CF composite

2.5 Conclusion

Through this review, it was shown that AM has catalyzed many advancements in the design and production of prosthetics and orthotic devices. The methods discussed provide precision and customization, crucial for the development of patient-specific devices that enhance wearer comfort and functionality [8], [28], [33]. Moreover, the integration of diagnostic and modification tools, such as 3D shape comparison algorithms, has further refined the production of prosthetic and orthotic devices, ensuring better fit and treatment outcomes [11], [14], [16]. The shift from traditional methods to AM offers a sustainable, cost-effective solution for prosthesis design and opens the door for many advancements in the field.

Chapter 3: Design Requirements

This thesis developed and evaluated an anatomically conforming transtibial socket insert used to compensate for residual limb volume loss. Note that the insert is not a prosthetic liner (i.e., interface between residual limb and socket to facilitate load transfer and suspension) but a device that changes the interior shape and volume of the prosthetic socket. The amputee can wear a liner when using a socket with an insert.

This insert must be custom designed for every person and socket using full- or semi-automated processes. Furthermore, the insert must be easy and quick to fabricate and remain as comfortable as the original socket. Fabrication process including any computational work should not exceed 4 days. Using a new socket as the comparator, the insert should be inexpensive and take less time to design, manufacture, and fit.

The design should be modifiable before fabrication, at the prosthetist's discretion, to ensure the best outcomes. The processes developed to produce the insert should be easy to learn to allow technicians, prosthetists, other clinicians, industry experts, and researchers to quickly develop custom inserts to assist them in their applications. Furthermore, processes should be modular to allow improvements to the fabrication pipelines as research and technologies advance and become available. Materials and fabrication processes should be readily available, and components should be cost-effective and easily procured (i.e., avoid specialty components if possible).

The insert fabrication process allows most prosthetic centers to adopt and most researchers to develop and improve. As such, open-source software is preferred, and readily available tools should be sufficient to digitize the residual limb models. The insert should be applicable for adults with a body weight up to 100 kg.

The model insert, in conjunction with the corresponding socket, must withstand lab testing with critical loads without damage, including loads corresponding to socket testing as described in the literature [55], [56], [57], [58]. In particular, a socket-insert system should withstand a proof static load of 2240 N, an ultimate static load of 4480 N, and cyclic testing for 1,000,000 cycles [59].

3.1 Design Summary

In summary, the insert design criteria are:

- Custom design:
    - Adaptable to many residual limb shapes.
- Fabrication:
    - Use readily available 3D printing material and equipment and easily sourced components and software.
    - Semi- or fully- automated process.
    - Easy to learn and train.
    - Modular to allow for future improvements.
- The insert must survive all load and test procedures:
    - Proof Static Test: 2240 N, held for 30 s at both heel and forefoot positions.
    - Ultimate Static Test: 4480 N, held for 30 s at both heel and forefoot positions.
    - Cyclic Test: 1000000 cycles alternating between 50 N and 1330 N, at each heel and forefoot, followed by static proof test of 2240 N, for 30 s.
    - Pilot Trial: Positive qualitative feedback required from a prosthesis user and the prosthetist.

Chapter 4: Insert Design

4.1 Literature Proof-of-Concept

The concept of an insert is new to the world of prosthetics and therefore only two papers were found at the time of this review. The first was written by Sanders et al. [60] and briefly mentions inserts as a future possibility. Nickel et al. [61] is more recent and relevant, where one participant's well-fitted socket was used as a base model for the insert. The insert model was created by scanning the original socket and a new socket that was expanded by 10 ply, and then creating a digital object for 3D Printing (95 A TPU). Socket-insert performance was compared to the well-fitted socket and loose-fitted socket.

Using the loose-fitted socket, the participant had a 6.6% reduction in walking distance compared to the well-fitted socket. Only a 0.6% reduction in walking distance occurred when using the socket-insert compared to the well-fitted socket. Furthermore, the participant reported a socket comfort score of 8 and had positive comments such as "I feel level" and "I think it is just as good as my existing socket". This study stands as a strong proof-of-concept of the insert showing its potential benefits and user satisfaction.

Nevertheless, the study had several limitations. First, the study did not investigate the effects of changes in residual limb shape or suggest a method to design an insert given a change in shape. Second, the study lacks a mechanical test and is limited to only 1 participant. This thesis addresses these limitations.

4.2 Modelling the Insert

This section of the thesis is focused on modelling the insert. A 3D model is obtained by combining scans of the old socket and a rectified CAD model of the current limb that has experienced extensive volume reduction. These two models are aligned using software and

modified at the designer's discretion to ensure that no protrusions are present, and the alignment is satisfactory. The insert is then modelled compromising of the negative difference between the two models. Post processing includes filling in gaps if needed, trimming the bottom of the insert to prepare the insert for socket installment, and smoothening the interior and exterior to ensure comfort for the person wearing the insert.

Slicer 3D open-source software was used to align the 3D shapes [62]. Slicer 3D is free to download, with many plugins and features critical for this design. Moreover, any improvements to design functions can be converted to a plugin and immediately implemented worldwide. This software is commonly used in dentistry and diagnostic imaging [63]. A 2020 study found Slicer3D to have a matching percentage higher than 90% compared to manual segmentation when obtaining volumetric renderings of the mandible [64]. Another study concluded no significant difference in accuracy with Slicer 3D compared to commercial software in the volumetric assessment of post regenerative endodontic procedures, with Slicer 3D performing the task approximately 3 min faster [65]. The CMFreg extension was used for 3D object alignment and shape comparison [66]. While CMFreg was originally developed to assess craniofacial changes over time [66], the algorithm provided a good first alignment of two residual limb scans before being manually adjusted by a prosthetist. Post-processing was also performed almost entirely on Slicer3D, apart from smoothening which was performed on Fusion360 software.

A step-by-step picture guide to producing insert models can be found in Appendix A. Deidentified models were kindly provided by The Ottawa Hospital Rehabilitation Centre (TOHRC) to develop the insert used for mechanical testing.

4.2.1 Design Process

The design process would generally consist of the following steps:

- Import the rectified models of a person's residual limb into Slicer3D software
- Align using CMFreg registration. Alignment can be made using 'Surface Registration' or 'Fiducial Registration'
    - 'Surface Registration' uses PCA to align the models. This is best used when the two shapes closely resemble each other
    - 'Fiducial Registration' uses PCA along with landmarks, specified by the designer, to align the models. This is best used when not only the volume has changed, but also the shape of the residual limb
- Convert models to segments
- Convert segments to binary labelmaps
- Use the 'Transform' feature to manually adjust the alignment as necessary
- Fill-in the segments to create solid structures using the 'Smooth' tool, located under 'Segment Editor: Logic Operator'
- Import filled-in segments to one segment folder
- Subtract the inner segment from the outer segment to create a model of the negative space using the 'Subtract' feature found under 'Logic Operator' in the 'Segment Editor' tab
- Use the 'trim' feature found under segment editor to remove any unwanted protrusions
- Convert insert segment to model
- Export model as a STL file

- Import STL file to Fusion360
- Use the ‘Smooth’ feature under the mesh tab to output the final model

Chapter 5: 3D Printing Material and Settings

Additive manufacturing was selected for creating the inserts since complex geometries can be manufactured in a cost-effective manner. While AM can be slow to produce large quantities of a design, this is not a major constraint since inserts are customized to each person and only need to be produced one-at-a-time. Furthermore, many AM techniques and equipment require minimal training, reducing the need for long training sessions for prosthetists, and ensuring consistent results can be achieved.

For initial testing, AM was performed at uOttawa Makerspace. FDM was chosen over other processes due to its availability and accessibility when translating the project into practice. To choose the initial print settings to test the insert, a preliminary study was performed. Small rectangular blocks, fabricated with varying thicknesses and materials, underwent mechanical testing. Following consultation with a certified prosthetist, the insert was anticipated to accommodate thicknesses between 3 mm and 7 mm at any given point. Consequently, each material and 3D print setting were assessed at these two extremities.

5.1 Methods

Two materials were selected as initial candidates for testing: Nylon and Ninjatek Cheetah TPU (NCT). These materials ensure elasticity to effectively absorb loads while maintaining an accessible 3D printing process. Three distinct print patterns were evaluated: line, cubic, and triangle. Additionally, infill percentages were tested in 10% decrements, commencing with a maximum infill of 60%, as recommended by the uOttawa 3D printing technician (Figure 7). The objective of varying infill percentages was to reduce weight and material required in producing the insert while ensuring resilience under loading conditions.

This approach also aims to minimize printing time and mitigate the risk of print failure.

Figure 7: Six 3D-printed NCT blocks with 40%, 50% and 60% infill (3mm and 7mm thickness).

Blocks were tested in direct compression and loaded based on the socket-insert static loading sequence (Figure 8). An Instron 68FM-100 test machine was used for all mechanical tests in the material selection phase. Blocks were loaded with 3 different loads (1024 N, 2240 N, 4480 N), at a 200 N/s loading rate, and maintained using the creep function for 30 s before unloading at -200N/s [55], [56], [57], [58], [59]. In between each load, blocks were left to rest for 15 min.

To pass testing, blocks needed to withstand the ultimate load while maintaining elastic properties. Furthermore, to reduce variation in user's experience, blocks should not exceed 10% compression at the proof static load.

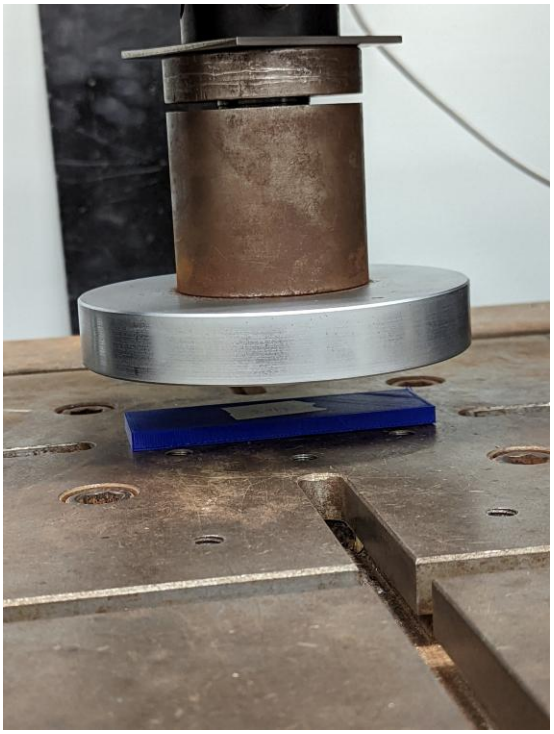

Figure 8: Block compression test setup.

5.2 Results

5.2.1 Print Material

To compare the different printing materials, blocks were printed with a 7 mm thickness, a triangle print pattern, and a 60% infill. The results of both proof static tests and ultimate static tests are presented in Figure 9 and Figure 10.

Nylon exhibited superior performance compared to NCT. During the proof static load test, nylon demonstrated a compression resistance 26.64% higher than NCT. During the ultimate static load test, nylon exhibited a compression resistance 45.24% greater than NCT. However, during the ultimate static load, NCT experienced a total compression of 6.26% or 0.44 mm. Comparing the proof and ultimate tests of the same material, at the same load, yielded similar compression. This indicated that both Nylon and NCT maintained elastic properties following the proof static test. Furthermore, there were no sudden jumps in the

results, further indicating that both materials did not fail before reaching the ultimate load. Both samples were under 10% compression at the proof static load.

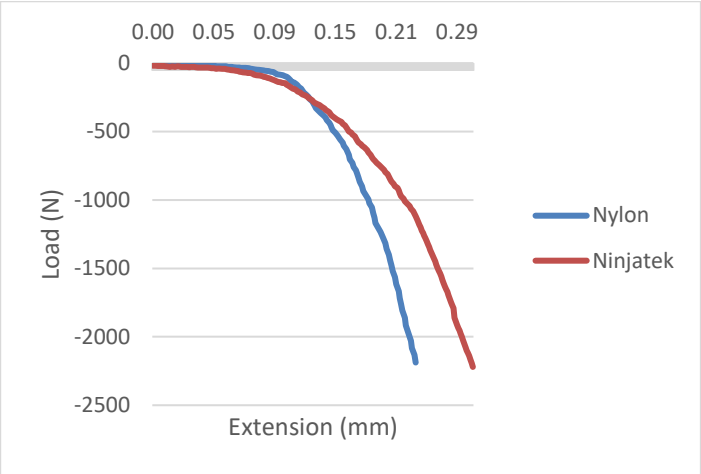

Figure 9: Proof test for triangle print pattern at 60% infill

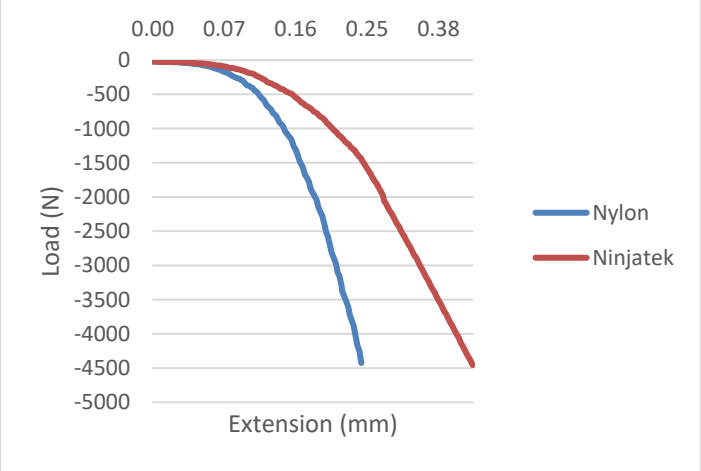

Figure 10: Ultimate test for triangle print pattern at 60% infill

Since the residual limb has boney areas that can result in high contour areas, a flexible material is required to allow the prosthetist to press fit the insert into the socket. Given that NCT performance was deemed suitable for the insert application and considering that TPU is more flexible, and is generally more cost-effective than Nylon, NCT was selected as the material for the insert.

5.2.2 Print Pattern

To examine printing patterns, the infill percentage was set at 60%, and the cube thickness was maintained at 7 mm. Blocks were printed using NCT. Proof and Ultimate static testing were conducted on all three blocks manufactured with line, cubic, and triangle fill patterns.

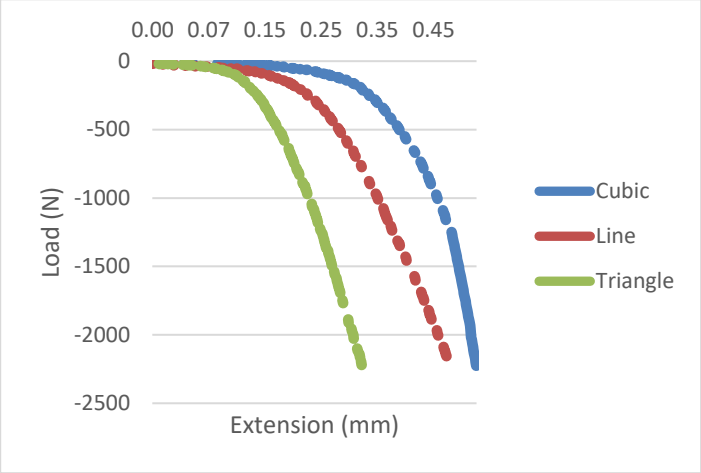

Figure 11: Proof test for cubic, line and triangle print pattern at 60% infill

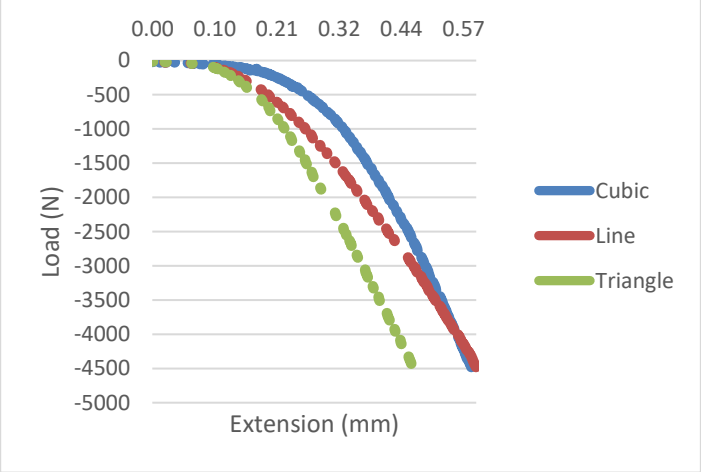

Figure 12: Ultimate test for cubic, line and triangle print pattern at 60% infill

As illustrated in Figure 11 and Figure 12, blocks printed with the triangle pattern exhibited the most favorable performance compared to those printed with the cubic and line patterns. Using blocks printed with the cubic pattern as a baseline, at the proof load, blocks printed with the line pattern had 13.78% better compression resistance while blocks printed with the triangle pattern had 42.21% better compression resistance than the line pattern. Moreover, at the ultimate load, blocks printed with the triangle pattern had 21.89% better compression resistance than the cubic pattern. Interestingly, blocks printed with the line pattern failed before reaching the ultimate load, as indicated by the sharp increase in the extension as the load increased. Blocks printed using the cubic and triangle pattern showed elastic performance from the proof to the static load without any sharp increases in the extension suggesting that both materials withstood the ultimate load without failure. Furthermore, all the blocks experienced compression below 10% at the proof static load.

The superiority of the triangle print pattern in z-compression was expected since 2D patterns, such as the triangle, print all layers in the same direction, thereby better withstanding loads in that direction [67]. However, for the insert application, loads will be applied in various directions. 3D patterns, such as the cubic pattern, print layers in an isotropic sequence, sacrificing z-performance but allowing the print to equally withstand loads from all directions [67]. For this reason, and since all print patterns performed adequately for the insert application, the cubic print pattern was selected for the insert.

5.2.3 Infill Percentage

To evaluate the infill percentage, blocks with 10%, 20%, 40%, 50%, and 60% infill were subjected to testing. NCT material and the cubic print pattern were used. Given that this was the last material testing stage, 3mm blocks were used in order to evaluate 10% compression at proof load criteria.

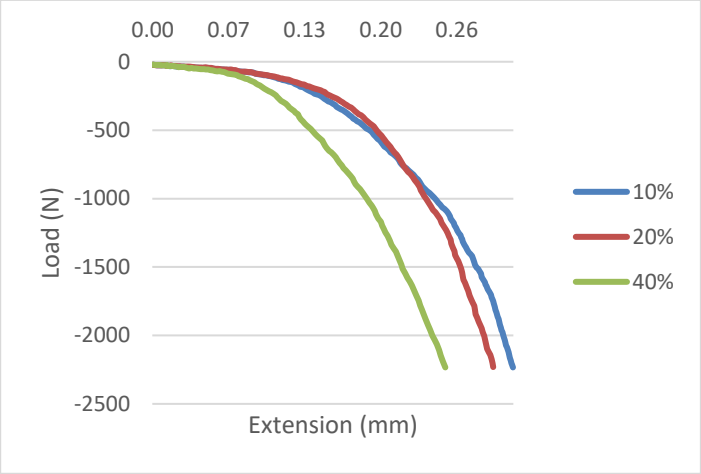

Figure 13: Proof test for cubic pattern at 10%, 20%, and 40% infill

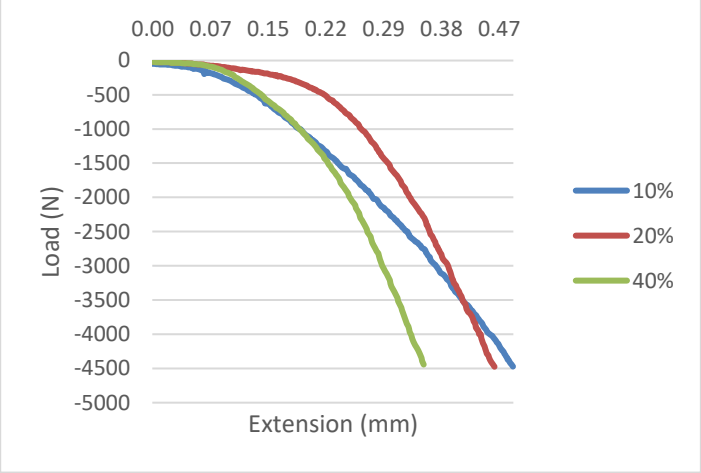

Figure 14: Ultimate test for cubic pattern at 10%, 20% and 40% infill

As shown in Figure 13 and Figure 14, blocks with 20% and 40% infill withstood the ultimate load without failure. The block with 10% infill failed during the proof test, which explains the unusual spike in extension at higher loads in the ultimate test. At the proof load, the block with 20% infill had a maximum compression of 0.31 mm (10.33%) and the block with 40% infill showed a maximum compression of 0.25 mm (8.33%). At the ultimate load, the block with 20% infill had a maximum compression of 0.46 mm (15.33%) and the block with 40% infill had a maximum compression of 0.34 mm (11.33%). Based on these numbers, an infill between 20% and 40% would be appropriate for the insert application. Our research team chose 35% infill for the insert model to ensure compression at the proof load is under 10%.

Based on the sample tests results, the insert 3D printing specification for the remainder of the thesis was NCT with a cubic print pattern and 35% infill percentage.

Chapter 6: Insert Mechanical Testing

The insert should undergo both static and cyclic tests to ascertain its ability to endure the usual biomechanical forces experienced by the lower leg.

6.1 Literature

Currently, there are no testing standards for prosthetic socket inserts. To provide a comprehensive framework for mechanical testing in this thesis, the methods described in [55-59] were consulted since these papers describe a testing methodology for transtibial prosthesis sockets. These are suitable references due to the correlation in function between an insert and a socket. Testing a socket-insert system using a custom-made socket, made using the commercial processes, and a literature-supported protocol for socket testing guarantees the insert is subjected to appropriate static and cyclic loading conditions. The methods described in the literature replicate stance phase, where body weight is supported [55]. Tests include proof static test, ultimate static test, and cyclic test [59].

6.1.1 Orientation

Figure 15 shows the typical test orientation for transtibial prosthetic sockets. Both the knee joint centre and the ankle joint centre are defined as points that lie on the same vertical axis (u), defined as an axis passing through points equally distant from the foot's medial and lateral sides, and 0.25 mm (foot length) from the calcaneal tuberosity edge or equivalent. The ankle joint is located 80 mm from the toe loading plane or equivalent. The forefoot loading point is equally distant from the foot's medial and lateral sides, with a specific offset (S_B) from the ankle joint centre (Figure 16). S_B is defined by the prosthetic user's weight [59]. The longitudinal axis of the foot is defined by the ankle joint centre and S_B.

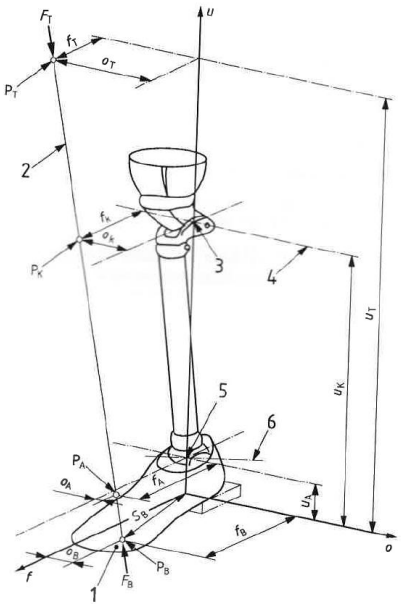

Figure 15: Test loading orientation: 1) left foot, 2) loading, 3) effective knee-joint centre, 4) effective knee-joint centreline, 5) effective ankle-joint centre, 6) effective ankle-joint centreline, $P_{K)}$ knee load reference point, P_A) ankle load reference point, P_B) bottom load application point, P_T) top load application point [59]

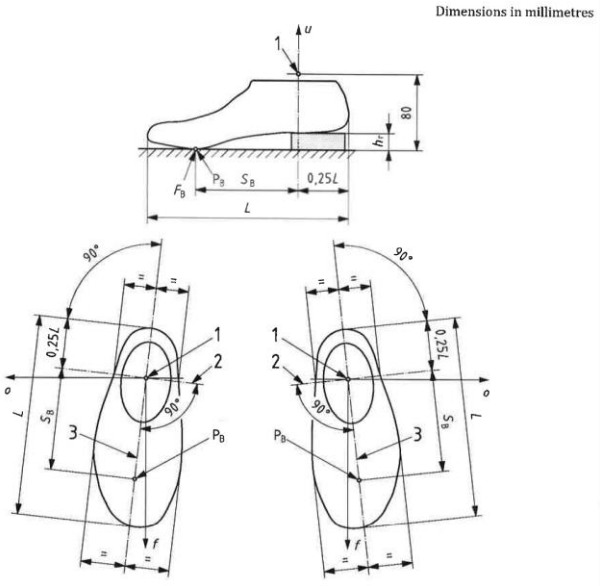

Figure 16: Foot coordinates and axes: 1) effective ankle-joint center, 2) effective ankle-joint centerline, 3) longitudinal axis of foot, h_r) heel height, L) foot length, S_B) combined bottom offset of bottom load application on forefoot from u-axis [59]

When testing the heel, the load is applied at a 15° (α) angle from the vertical axis and forefoot load is applied at a -20° (β) angle from the vertical axis. The longitudinal axis of the foot must be -7° (γ) from the forward horizontal axis.

6.1.2 Test Load Conditions

The loading conditions are determined by user weight ranges: P3 is for individuals weighing less than 60 kg, P4 for 60 to 80 kg, and P5 for 80 to 100 kg [56]. The ISO 10328 test standards also encompass people whose weight exceeds 100 kg, accommodating loads of up to 175 kg. In this thesis, an analysis was conducted on the P5 criteria (Table 1) since the average Canadian adult male weighs 87.3 kg [68]. Consequently, the loads applied on the insert should accommodate a wide range of potential insert users. Based on the established standard, S_B (i.e., forefoot loading point offset) at P5 is 130 mm [59].

Table 1: P5 Loads [55]

Test name	**Force (N)**
Proof static test	2240
Ultimate static test	4480
Minimum cycle load	50
Maximum cycle load	1330
Final static load	2240

6.1.2.1 Proof Static Test

The purpose of the proof static test is to subject the device to a larger load than what the device would typically encounter, simulating rare occurrences that may happen during its usage. The load is initially applied at the heel at a consistent rate ranging from 100 to 250 N/s. Subsequently, the load is maintained in position for 30 (±3) seconds. A consistent and uniform forefoot load is then administered, maintaining the same magnitude, range, and duration. To

successfully meet the requirements, the device must be free from any type of deformation or structural impairment during the entirety of the testing's duration and inclination [59].

Given that lower limbs can experience high stresses, such as during running or jumping, any replacement component must be capable of withstanding comparable loads. Adult males running at 6 m/s can experience loads of up to 2.38 times their body weight [69]. Furthermore, these loads can be higher during jumping. Therefore, a static proof load of 2240 N is reasonable.

6.1.2.2 Ultimate Static Test

The ultimate static test simulates a single catastrophic event. The goal of this test is to determine the device's maximum sustainable load within predefined limitations before it becomes unusable. The load is applied at a steady rate of 100 to 250 N/s. The force is increased until failure or reaching the upper limit of 4480 N. If the sample survives, the forefoot is loaded in the same way. To pass this test, the device must remain functional after exceeding the upper limit in both the heel and forefoot loading circumstances [59].

6.1.2.3 Cyclic Test

The cyclic test replicates operational performance during typical prosthesis usage scenarios. The test consists of two components: an initial cyclic load test and a subsequent final static test, both aimed at verifying the device's continued operational efficacy. In the ideal cyclic load test, the heel and forefoot are subjected to alternating loads in a pulsing manner [55]. Figure 17 illustrates typical walking behaviour, wherein the heel is loaded followed by the forefoot. The heel and forefoot load functions were engineered to exhibit comparable characteristics, albeit with a deliberate delay in the forefoot load to replicate the process of load transfer that occurs during midstance.

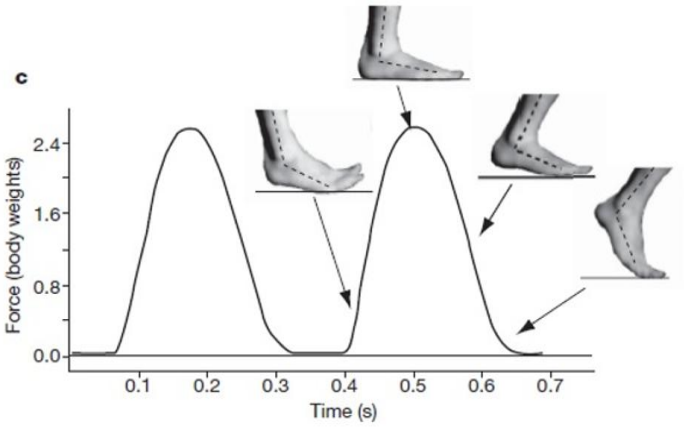

Figure 17: Gait cyclic behaviour force-time graph [70]

The testing apparatus is expected to stabilise at the specified frequency of 1.5 Hz, while being subjected to a 69 N applied force, which corresponds to 10% of the maximum cyclic value. After reaching the required loading frequency, 2 million cycles are completed (1 million repetitions on the forefoot and heel components each), or until device failure occurs. If the device remains intact throughout the cycle test, a static proof test is subsequently conducted at the heel region. This test is performed at a consistent rate, varying between 100 and 250 N/s. A load of 2240 N is exerted for 30 (±3) seconds. Subsequently, the forefoot undergoes loading in a similar manner [59].

6.2 Socket-Insert Preparation

The insert was initially 3D-printed using the settings determined in the preliminary study with the blocks and the default settings for TPU shore hardness 95A found on the Ideamaker slicing software. Had the insert failed 3D printing or mechanical testing, 3D print settings would have been adjusted and testing would have been repeated. No modifications to the print settings were needed, as shown in the sections below. A complete description of the print settings can be found in Appendix B. To test the insert, a socket-insert system was used. Socket and CAD models were provided by the Prosthetics and Orthotics department at

TOHRC. A pylon was attached via a pyramid adaptor and a mandrel was fixed using plaster. Pylon length was adjusted to ensure that the knee center was 500 mm above the zero-reference plane [71]. Since the ankle joint centre was required to be 80 mm above the zero-reference, the pylon was made to be 420 mm from the knee center (Figure 18). The knee center was estimated by a trained technician.

Before applying the plaster in the socket-insert, 5 cm of foam was placed in the distal portion of the socket-insert to allow this portion to deform freely under load [56], [59], [71]. The mandrel was aligned with the pylon using a typical alignment jig and laser (Figure 19). Once the plaster had hardened, a 3/8th inch hole was drilled in a coronal plane rotated 7º laterally [56], [59] to account for the toe out effect.

Figure 18: Socket-insert in the alignment jig. A tape measure identified the mandrel lock-pin location.

Figure 19: Socket-insert in the alignment jig. Laser is used to align the mandrel and the pylon.

6.3 Jig Preparation

Static testing was done using an Instron 68FM-100 and cyclic testing was done using an Instron 1332. Jigs were designed for testing to ensure appropriate loading points for the socket-insert. Jigs were made with cold-rolled steel. Attachments between the plates, the Instron machines, and the socket-insert were made using lock pins except for the bottom plate, which was attached to the pylon using a 10 mm screw. The bottom plate had a length of 130 mm from the ankle joint center to the toe loading point and a length of 23.75 mm to the heel loading point. The base plate had a thickness of 80 mm at the toe loading point, and 60 mm at the heel loading point. To factor in the different angles for each loading condition, the heel loading top plate had a length of 115.07 mm, and the toe loading top plate had a length of 65.85 mm from the connection point with the Instron to the connection point with the mandrel. The top plates were designed with a rod attached at angles corresponding to the loading

condition, 15º for the heel loading plate and 20º for the toe loading plate. To accommodate different attachments in each Instron, a sleeve was designed to achieve an appropriate lock pin hole size. To apply a point force, the base plate sat on a metal ball fixed in place via a sleeve (Figure 20). Jig designs can be found in Appendix C.

Figure 20: Bottom half of the testing setup in toe-loading configuration. Shown is the distal portion of the socket-insert, pylon, and bottom plate resting on the metal ball.

6.4 Static Testing

Static testing was performed on an Instron 68FM-100 and data was collected via Instron's native BlueHill 3 software and extracted to an Excel file. The combined socket-insert system was loaded with forces up to 4480 N at 200 N/s. Subsequently, each load was sustained using the creep function for 30 s, after which the load was gradually released at a rate of -200 N/s and left to rest for 15 min before proceeding with the next load. To find the initial

zero position, the socket was preloaded to 50 N. Three different loads were used, an initial load of 1024 N, the proof static load of 2240 N, and the ultimate static load of 4480 N. The system was initially loaded in the heal configuration at 15º, and then in the toe loading configuration at 20º.

6.5 Cyclic Testing

An Instron 1332 (Figure 21) was used for cyclic testing. Frequency was set at 1.5 Hz and the input load was set to vary from 50 N to 1330 N. Data was collected using LabVIEW software provided by uOttawa. Due to limitations from testing equipment available, and since toe loading is considered to have more stresses involved [58], [71], cyclic testing was only done in the toe loading configuration. The test was run for 1,000,000 cycles.

Figure 21: Instron 1332 controller.

6.6 Results

6.6.1 Insert Static Testing

The socket-insert maintained elastic properties throughout static testing, as shown in Figure 22 and Figure 23 by the overlapping graphs of the initial, proof, and ultimate loads. To reach the ultimate load, approximately 48 mm displacement was needed in the heel

configuration, and approximately 20 mm was needed in the toe configuration. The difference in displacements was expected since the socket-insert system experiences larger stress in the toe configuration, which means higher loads experienced for the same displacement.

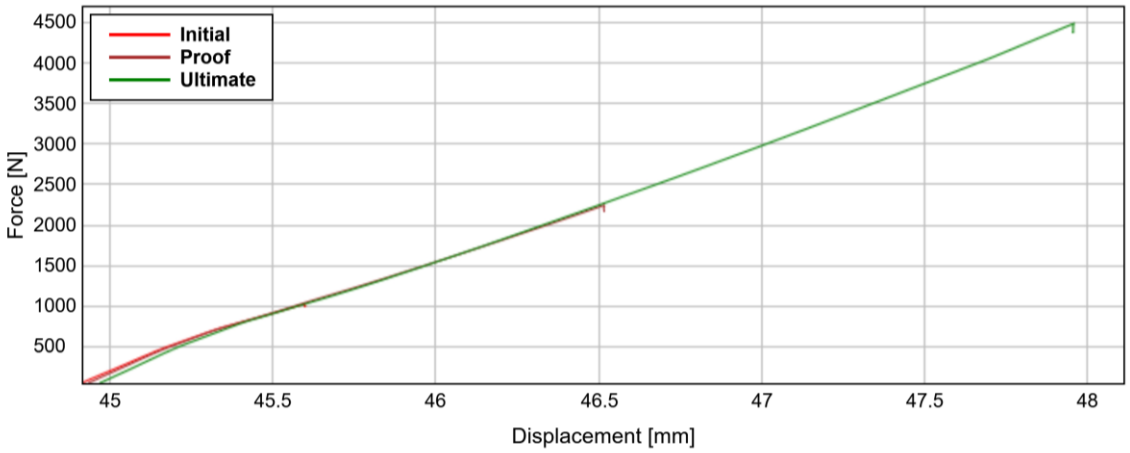

Figure 22: Heel static testing results

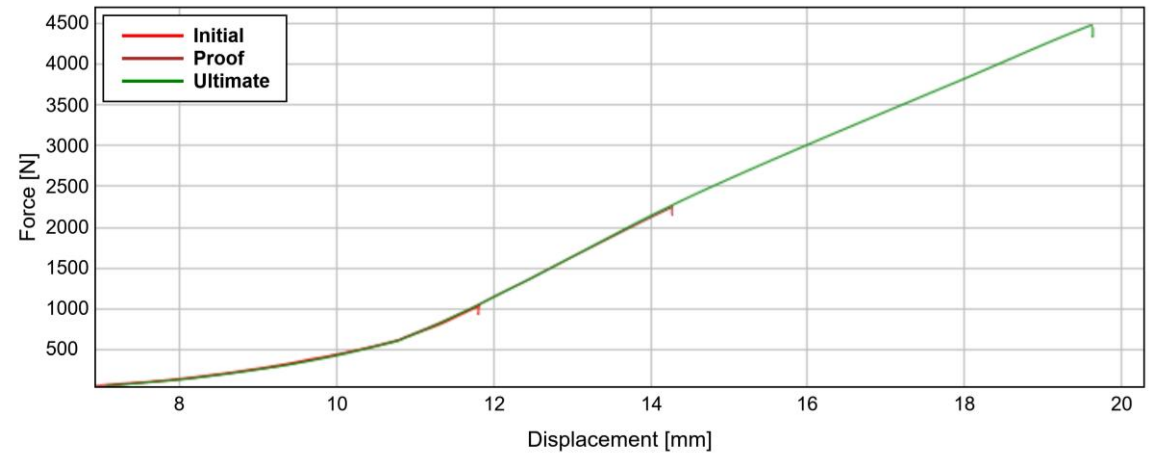

Figure 23: Heel static testing results

6.6.2 Insert Cyclic Testing

During cyclic testing, peak vertical displacement and load were sampled at one-minute intervals (latest maximum vertical motion and load peak within each 1-minute window). Both positive and negative peaks were plotted to demonstrate the amplitude for load (Figure 24) and vertical displacement (Figure 25).

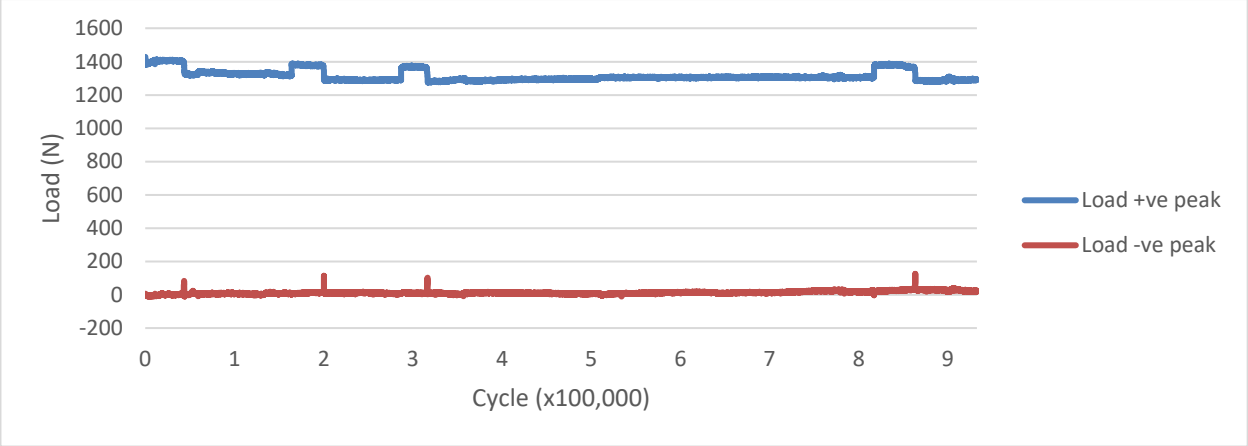

Figure 24: Maximum and minimum loads induced during cyclic testing.

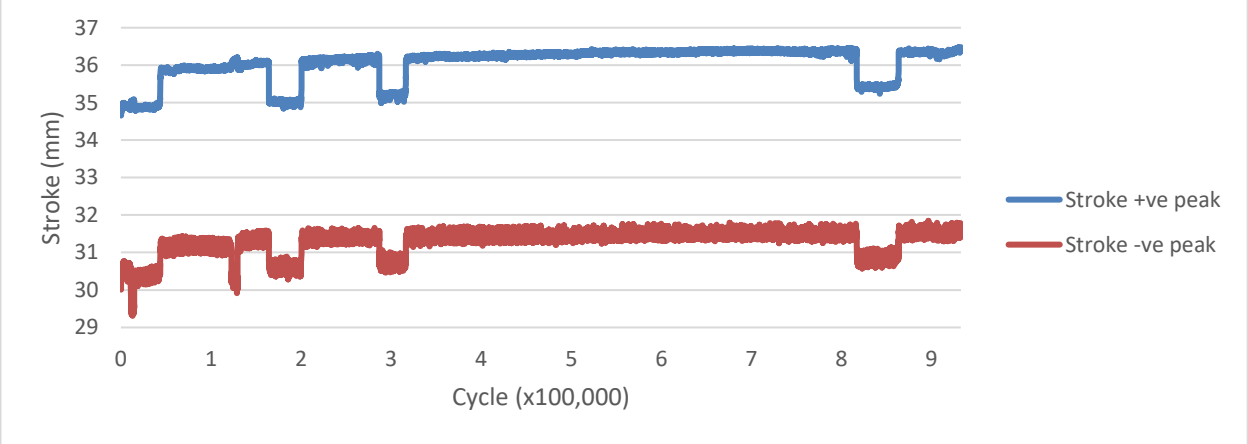

Figure 25: Maximum and minimum vertical displacement (strokes) during cyclic testing.

To maintain a constant load amplitude, the Instron machine aimed to generate specified loads by exerting pressure on the bottom loading base. Consequently, the load remained stable with minimal variation. Nonetheless, slight variations occurred during testing due to minor adjustments to the load control panel to ensure the load amplitude was within its intended range. However, given the infrequency of these adjustments, the testing procedures remained unaffected. As seen in Figure 25, the stroke also remained mostly consistent, which showed that the socket-insert could withstand cyclic loading. While the amplitude remained constant, peak stroke slightly increased over the 1,000,000 cycles. Initially, stroke peaks ranged from 30.7 mm to 34.9 mm following initial adjustments, and by the end of the test, range increased

to 31.5 mm to 36.4 mm. This rise amounted to approximately 0.6 mm over the 1,000,000 cycles. Initially, the amplitude increased by 0.4 mm in the first 100,000 cycles, followed by a 0.2 mm gradual increase for the remainder of the test. The gradual increase is explained by the larger displacement needed over time to maintain the same load, likely due to microscopic fatigue-induced deformations. A 0.6 mm change in insert thickness should have little or no effect on socket fit.

In summary, the socket-insert demonstrated robust fatigue performance, with most components remaining unaffected or undamaged by the testing process. Figure 24 and Figure 25 illustrate that the applied load was largely consistent, indicating that the insert effectively endured cyclic loading. Notably, the steel mandrel used to attach the socket-insert to the testing equipment was slightly bent at the connection point (Figure 26). Nevertheless, this deformation did not affect testing and should not be a concern for the insert.

Figure 26: Socket-insert in toe loading configuration. Mandrel is highlighted in yellow. Bending location is highlighted in red

Chapter 7: Pilot Trial

7.1 Methodology

Three male adults with transtibial amputations were recruited from the Prosthetics and Orthotics Service at TOHRC. They required a new socket due to limb volume changes, as identified by a staff prosthetist, and who had their original sockets designed using digital techniques. Inclusion criteria were people greater than 19 years of age and K level 3 or 4 (i.e., community ambulator or better). Exclusion criteria were people with cognitive issues that may have difficulty following instructions.

Prior to getting a new socket, each participant completed the Socket Comfort Score [72] and Prosthesis Evaluation Questionnaire (PEQ) [73] for their current socket. Participants then performed a 2-min walk test, with a smartphone on a belt at the posterior pelvis to capture acceleration and angular velocity data [74]. The 2-min walk test involves measuring the distance a person can cover walking continuously for 2 min [75].

A prosthetist scanned the participants' residual limb and created a new socket shape using CAD. Both original socket and new socket 3D CAD files were used, with the assistance of the prosthetist, to design and fabricate the corresponding insert. Standard socket fitting procedures followed to achieve a successful fit (i.e., included iterative revisions to the insert as necessary).

When an acceptable fit was achieved, the participants wore the socket for at least one week before returning to TOHRC for a checkup by the prosthetist and, when no further revisions were required, completed the Socket Comfort Score [72], Prosthesis Evaluation Questionnaire (PEQ) [73], and 2-min walk test [75] with the new socket-insert. Qualitative

feedback on the fitting process and prosthetic performance was also captured from the participants and prosthetist.

Results from the questionnaires and 2-min walk test were compared between original and new insert enhanced sockets using descriptive statistics.

7.2 Results and Discussion

7.2.1 Participant A

When first recruited, the participant was using a pin-lock patella tendon bearing socket and 17 ply socks to compensate for his residual limb volume change. Fiducial registration was used to align his old limb shape to his new limb shape since there were substantial changes to the residual limb shape. An iterative process was needed to create the insert because the first version misaligned the pin with the socket, thereby not allowing the liner to engage. To resolve this issue, central alignment of the insert's distal end was prioritized to allow the pin to sit square in the socket, allowing regular pin engagement (Figure 27). Furthermore, the prosthetist requested that certain areas of the insert be 3D printed with 100% infill to allow for the prosthetist to sand down the area without exposing the inner lattice structure. Sanding down these areas as needed allowed the prosthetist to alleviate any pressure that users experienced. This was easily achieved through the slicer software by creating 'modifiers' and adjusting the print settings within those 'modifiers'. The specific areas were below the patella tendon, along the tibia crest, and the distal end of the insert. These areas are common pressure points in transtibial prosthetics. This step was repeated for all the other participants.

The participant used the insert for 3 weeks before returning the TOHRC for final testing. The participant initially reported a SCS score of 9 when using his old socket with socks but reduced this score to 8 when using the insert instead of socks. His main complaint

was the time needed to put the socket-insert on after long periods of rest, such as after sleep or after showering. He claims that it could take 10-15 min of him trying to wiggle his liner into the socket in the morning to engage the pin. This is reflected in the PEQ since the only change in scores were in questions related to donning the prosthesis. The prosthetist suggested that this problem might have been caused by the striations of the 3D printed layers. A potential solution would be to prepare the insert with a lower layer height, providing a smoother interior, although this would increase insert print time and subsequently might also increase the number of failed prints, which could increase costs. The participant was able to walk three extra meters (212m à 215m) in the 2-min walk test, which is below the minimum detectable change of 42.5m [76]. This suggested that the insert performed adequately. The insert showed no signs of damage and participant chose to keep the insert as a back-up solution if any problems would arise with his long-term prosthesis.

Figure 27: Socket insert with the distill opening centralised about the pin

The participant noted that having the insert did have some benefits such as the ability to wear jeans, which he did not feel comfortable doing when he was using socks to compensate for the volume change since the socks would roll up and annoy him. Furthermore, participant noted: “once it’s on, I have no issues or pain at all.” The prosthetist’s feedback was that this is an overall positive project and recommends research into smoothening the inside as the next step.

7.2.2 Participant B

Participant B had a very similar experience to participant A. When he was first recruited, the participant was also using a pin-lock patella tendon bearing socket with 18 ply socks to compensate for his residual limb volume change. Surface registration was used and manual adjustments were made to accommodate pin positioning. No iterations were needed and the insert was 3D printed. Uniquely, this participant experienced large daily fluctuations in his residual limb volume. Therefore, the prosthetist requested that the participant start his days without the insert and to use the insert after his residual limb has shrunk in size, around noon. Unfortunately, the participant lacked the ability to easily remove and re-insert the insert in the socket. To resolve this, the prosthetist attached hooks to the side of the insert (Figure 28) that provided the participant with the grip he needed. Moreover, this participant was complaining of pain in his non-amputated knee which affected his walk scores.

The participant used the insert for 2 weeks before returning to TOHRC for final testing. The participant initially reported a SCS score of 7 when using his old socket with socks, which remained unchanged when describing his experience with the socket-insert. Initially, the participant reported a very positive experience with the insert and had no complaints. This was also reflected in the PEQ where the participant did not have any notable changes when

comparing his experience with and without the insert. When asked about his experience donning and doffing the insert-socket, the participant noted that he required a couple of extra seconds to put the socket-insert on, but these extra seconds did not matter to him. Finally, the participant had an 8.5 m (75.9m → 67.4m) reduction in walking distance. This reduction was below the 2MWT minimum detectable change and can be explained by the worsening of his non-amputated knee.

Figure 28: Participant B insert with hooks attached

7.2.3 Participant C

The third participant was a bilateral amputee. The participant used a total surface bearing prostheses with 27 ply socks on his left leg and 21 ply socks on his right leg. This person was unique in that he had a well-fitted socket that cracked and needed repairing. Therefore, he was reverting back into his old sockets, which explained the large number of socks he was using. Challengingly, the well-fitted sockets had different shapes than the old sockets that were used for testing. Furthermore, considering the positive results that were observed from the first two participants, the prosthetist wanted to test a different method to obtain the inner model needed for insert design. The left insert was designed using surface registration with no modifications to the design process. For the right insert, the prosthetist took tape measurements of the participant's limb in one-inch intervals rather than rescanning the limb. Using the old scan of the limb as a base, the prosthetist used CAD adjusted the circumference of each interval according to his measurements. According to the prosthetist, this is common practice when making prostheses. This method to obtain the insert's inner model could potentially save the prosthetist time and not require additional scanning sessions with the patient. According to the prosthetist, a 3-6% reduction of the tape measurements is needed. Nevertheless, the first reduction chosen produced an insert that was small and did not fit the participant, therefore another iteration was made. Unfortunately, due to the number of different inserts that were needed to be manufactured along with difficulties to set up appointments with the participant, the process to make the 2 inserts was almost 2 months. This period is important since the limb can change in shape and size during that period. Evidently, by the time both inserts were ready for the participant, the participant's limbs had further shrunk, and 5 ply socks were needed in tandem with the left insert. Furthermore, before taking

the inserts home, the participant noted that he felt some pressure on the right side. This pressure was in an area that required padding when the participant was using his old socket (Figure 29), but he no longer needed padding on the new socket that he had been using. Since the participant did not note any pain, the prosthetist believed that this pressure is due to the changed shape and that the limb will adjust to the shape of the old socket. Also, the prosthetist scheduled a phone follow up with the participant after a couple of days to ensure that he no longer felt the pressure.

Figure 29: Participant C sockets and inserts. The concave area of the insert needed for the padding is visible on the right leg insert (pictured on the left)

After a couple of days of use, the participant called the prosthetist back and reported that the pressure on the right side had worsened and caused a scar. The participant stopped

using the right insert completely and used socks instead from that point. In the one-week appointment after the participant took the inserts, the participant noted that he felt an imbalance when using the insert on only the left side and switched to socks on the left side. To avoid further harm to the participant, the walk-test with the inserts was not performed and the participant was fitted with the repaired socket and testing with this participant stopped.

While results with this participant were not positive, they can be attributed to the new clinical design method. Further testing will be needed to monitor if other participants have a similar experience. Nevertheless, the participant noted that he was happy with the left insert and had the inserts been made with the correct shape and in a timely manner, the results would have likely been positive.

Chapter 8: Conclusions and Future Work

In this thesis, a novel process for fabricating 3D printed inserts was designed and evaluated for both strength and function. The insert is a viable solution to compensate for long-term residual limb volume change. The insert met all the design criteria, successfully passed load testing, and showed positive results in a pilot trial. The current design process produced inserts that are robust; however, future work is still needed to improve the design and functionality.

8.1 Design Criteria

The final insert design met all the design criteria outlined in Section 3.1. The semi-automated process allowed the fabrication of inserts custom made for each amputee. Inserts can be fabricated, including all computational work involved, within 3 days of obtaining the residual limb scans including 40-50 hours needed to 3D print an insert. The only non-fixed cost involved with the inserts is the cost of the 3D printing filament. On average, fabricating a single insert costs around $23 CAD. Assuming a patient might need a maximum of 2 iterations for an insert, the total cost per patient would be $69 CAD. This is a small cost compared to the cost of obtaining a brand-new socket.

Furthermore, the design process allows the designer to make manual adjustments to the alignment and design an insert from scratch in less than an hour. The main software used in the design was Slicer3D which is an open-source software free to download making this design process accessible around the world. Furthermore, Fusion360 was used to smoothen the final model and is highly adopted within prosthetic clinics. Shore 95a TPU is available for purchase from popular retailers such as Amazon and Digitmakers.

The insert was able to withstand all load testing according to ISO 10328. The insert did not exceed its elastic modulus up to the ultimate loads and showed stable performance in the cyclic test. The pilot user evaluation also returned positive results. The only drawback from using the insert was the effort needed to engage the liner into the socket, which could be resolved with a smoother inner surface.

8.2 Summary of Contributions

The principal contribution of this thesis was the design and evaluation of a novel process to fabricate an insert to compensate for long-term volume change. Specific thesis contributions were:

1. Successful use of open source Slicer3D software for prosthetic insert design.
2. Developed a process to automatically align two 3D shapes with the added optionality of manual adjustments.
3. Developed a process to create a CAD design of the space between two 3D shapes.
4. Determined appropriate insert material and 3D printing settings.
5. Implemented a complete and comprehensive method to mechanically test inserts and transtibial sockets.
6. Completed an insert pilot trial with three prosthesis users, which guides further development.

8.3 Future Work

While the design process recommended in this thesis proved to fabricate inserts that meet the design criteria. The process could be improved by using different prosthetic design methods to accommodate the end user. For example, Slicer3D could be used to apply a uniform volume adjustment to the old socket shape thereby not requiring a separate socket

scan (less time for prosthetist and prosthesis user, less rectification, 3D shape alignment, etc). Alternatively, a Slicer3D plugin could be developed to further automate many of the processes and make it easier for new users to implement the insert workflow.

Mechanical testing with a series of inserts could be performed to evaluate 3D printing variability. Furthermore, in order to accurately determine the effects of different 3D print settings, a method to accurately measure the thickness of the inserts before and after testing will be required. Moreover, testing with different layer heights, print speeds, and temperature is needed to fabricate inserts with a smoother surface. A smooth surface should facilitate donning and doffing the prosthesis.

A clinical trial with an appropriate population sample would provide evidence on socket insert performance and is needed to ensure inserts are ready for clinical adoption.

References

[1] M. N. Rush, E. Hagin, J. Nguyen, V. Lujan, R. A. Dutton, and C. Salas, “Design for transtibial modifiable socket for immediate postoperative prosthesis,” Feb. 2019.

[2] C. W. Howard, D. K. Saraswat, G. McLeod, A. Yeung, D. Jeong, and J. Lam, “Canada’s prosthetic coverage: A review of provincial prosthetic policy,” 2019, *Canadian Online Publication Group*. doi: 10.33137/cpoj.v2i2.33489.

[3] S. Turner and A. H. McGregor, “Perceived effect of socket fit on major lower limb prosthetic rehabilitation: A clinician and amputee perspective,” *Arch Rehabil Res Clin Transl*, vol. 2, no. 100059, 2020.

[4] D. Espalin, K. Arcaute, D. Rodriguez, F. Medina, M. Posner, and R. Wicker, “Fused deposition modeling of patient-specific polymethylmethacrylate implants,” *Rapid Prototyp J*, vol. 16, no. 3, pp. 164–173, 2010, doi: 10.1108/13552541011034825.

[5] M. K. Thompson *et al.*, “Design for additive manufacturing: trends, opportunities, considerations, and constraints,” *CIRP Ann Manuf Technol*, doi: 10.1016/J.CIRP.2016.05.004.

[6] I. Gibson and A. Srinath, “Simplifying medical additive manufacturing: Making the surgeon the designer,” *Procedia Technology*, vol. 20, pp. 237–242, 2015, doi: 10.1016/J.PROTCY.2015.07.038.

[7] S. Singh and S. Ramakrishna, “Biomedical applications of additive manufacturing: Present and future,” *Curr Opin Biomed Eng*, vol. 2, pp. 105–115, 2017, doi: 10.1016/j.cobme.2017.05.006.

[8] J. Barrios-Muriel, F. Romero-Sánchez, F. J. Alonso-Sánchez, and D. R. Salgado, “Advances in orthotic and prosthetic manufacturing: A technology review,” *Materials*, vol. 13, Jan. 2020, doi: 10.3390/MA13020295.

[9] The Engineer, “This 3D printed exo-prosthetic leg Is a work of art,” Wonderful Engineer. Accessed: Jan. 16, 2024. [Online]. Available: https://wonderfulengineering.com/this-3d-printed-exo-prosthetic-leg-is-a-work-of-art/

[10] S. Kapp and D. Cummings, “Transtibial amputation: Prosthetic management.” Accessed: Nov. 11, 2024. [Online]. Available: www.oandplibrary.org/alp/chap18-02.asp

[11] H. O. Eldeeb, “Computerized manufacturing of orthotic devices using CT/MR scanning,” Doctoral Dissertation, University of Miami, Coral Gables, 1998.

[12] K. C. Tan, K. F. Lee, and S. L. Lye, “Automation of prosthetic socket design and fabrication using computer aided design/computer aided engineering and rapid prototyping techniques,” *Proceedings of the 1st National Symposium of Prosthetics and Orthotics, Singapore*, pp. 19–22, Oct. 1998.

[13] B. O. Artioli, M. E. Kunkel, and S. N. Mestanza, “Feasibility study of a methodology using additive manufacture to produce silicone ear prostheses,” *IFMBE Proc*, vol. 68, no. 3, pp. 211–215, 2019, doi: 10.1007/978-981-10-9023-3_38/FIGURES/3.

[14] P. C. Liacouras, D. Sahajwalla, M. D. Beachler, T. Sleeman, V. B. Ho, and J. P. Lichtenberger III, “Using computed tomography and 3D printing to construct custom prosthetics attachments and devices,” *3D Print Med*, vol. 3, no. 8, 2017, doi: 10.1186/s41205-017-0016-1.

[15] M. Diwakar and M. Kumar, “A review on CT image noise and its denoising,” *Biomed Signal Process Control*, vol. 42, pp. 73–88, 2018, doi: 10.1016/j.bspc.2018.01.010.

[16] L. Tang *et al.*, “Functional gradient structural design of customized diabetic insoles,” *J Mech Behav Biomed Mater*, vol. 94, pp. 279–287, 2019, doi: 10.1016/j.jmbbm.2019.03.003.

[17] F. Górski *et al.*, “Automated design of customized 3D-printed wrist orthoses on the basis of 3D scanning,” *Mechanisms and Machine Science*, vol. 75, pp. 1133–1143, 2020, doi: 10.1007/978-3-030-27053-7_97/FIGURES/9.

[18] A. Haleem and M. Javaid, “3D scanning applications in medical field: A literature-based review,” *Clin Epidemiol Glob Health*, vol. 7, no. 2, pp. 199–210, Jun. 2019, doi: 10.1016/J.CEGH.2018.05.006.

[19] A. Paterson, “Digitisation of the splinting process: exploration and evaluation of a computer aided design approach to support additive manufacture,” Doctoral Thesis, Loughborough University, 2013.

[20] “White light vs blue light 3D scanning technologies.” Accessed: Apr. 08, 2024. [Online]. Available: https://www.capture3d.com/knowledge-center/blog/white-light-vs-blue-light-scanning

[21] X. Li *et al.*, “Polarization 3D imaging technology: a review,” 2023, *Frontiers Media SA*. doi: 10.3389/fphy.2023.1198457.

[22] E. Parrilla *et al.*, “Low-cost 3D foot scanner using a mobile app,” *Footwear Sci*, vol. 7, no. 4, pp. S26–S28, 2015, doi: 10.1080/19424280.2015.1038308.

[23] N. A. Hamzah, N. A. Abd Razak, M. S. Ab Karim, and H. Gholizadeh, “A review of history of CAD/CAM system application in the production of transtibial prosthetic socket in developing countries (from 1980 to 2019),” Dec. 01, 2021, *SAGE Publications Ltd*. doi: 10.1177/09544119211035200.

[24] M. J. Bailey-Braendgaard and P. W. Enevoldsen, “Accuracy and reliability of 3D scanning spatial data when capturing limb morphology for use within prosthetics and orthotics: A scoping review,” *Prosthetics and Orthotics*, 2022.

[25] C. Mavroidis *et al.*, “Patient specific ankle-foot orthoses using rapid prototyping,” *J Neuroeng Rehabil*, vol. 8, no. 1, 2011, doi: 10.1186/1743-0003-8-1.

[26] C. P. Agudelo-Ardila, G. C. Prada-Botía, and P. H. G. Rodrigues, “Orthotic prototype for upper limb printed in 3D: A efficient solution,” in *Journal of Physics: Conference Series*, Institute of Physics Publishing, Nov. 2019. doi: 10.1088/1742-6596/1388/1/012016.

[27] H. S. Mali and S. Vasistha, “Fabrication of customized ankle foot orthosis (AFO) by reverse engineering using fused deposition modelling,” *Advanced Manufacturing & Mechatronics Lab*, pp. 3–15, 2020, doi: 10.1007/978-981-32-9433-2_1.

[28] X. Wang, M. Jiang, Z. Zhou, J. Gou, and D. Hui, “3D printing of polymer matrix composites: A review and prospective,” *Composites Part B*, pp. 442–458, 2017, doi: 10.1016/j.compositesb.2016.11.034.

[29] O. A. Mohamed, S. H. Masood, and J. L. Bhowmik, “Optimization of fused deposition modeling process parameters: a review of current research and future prospects,” *Advanced Manufacturing*, vol. 3, pp. 42–53, 2015, doi: 10.1007/s40436-014-0097-7.

[30] J. S. Rovick, “Direct, automated fabrication of sockets for artificial limbs,” Doctoral Dissertation, Northwestern University, 1993.

[31] J. P. Kruth, X. Wang, T. Laoui, and L. Froyen, “Lasers and materials in selective laser sintering,” *Assembly Automation*, vol. 23, no. 4, pp. 357–371, 2003, Accessed: Oct. 18, 2022. [Online]. Available: http://www.emeraldinsight.com/researchregisterhttp://www.emeraldinsight.com/0144-5154.htm

[32] W. E. Rogers, R. H. Crawford, J. J. Beaman, and N. E. Walsh, “Fabrication of prosthetic sockets by selective laser sintering”.

[33] C. Cai *et al.*, “Comparative study on 3D printing of polyamide 12 by selective laser sintering and multi jet fusion,” *J Mater Process Technol*, 2021.

[34] D. Kathrotiya, A. Yusuf, R. K. Bhagchandani, and S. Gupta, “A study for the development of prosthetic foot by additive manufacturing,” *Journal of the Brazilian Society of Mechanical Sciences and Engineering*, vol. 45, no. 3, Mar. 2023, doi: 10.1007/s40430-023-04107-y.

[35] W. Ryu, Y. Choi, Y. J. Choi, and S. Lee, “Development of a lightweight prosthetic hand for patients with amputated fingers,” *Applied Sciences*, vol. 10, no. 10, May 2020, doi: 10.3390/app10103536.

[36] E. D. Lemaire and F. Johnson, “A quantitative method for comparing and evaluating manual prosthetic socket modifications,” *IEEE TRANSACTTONS ON REHABILITATION ENGINEERING*, vol. 4, no. 4, pp. 303–309, 1996.

[37] I. Atmosukarto, W. K. Leow, and Z. Huang, “Feature combination and relevance feedback for 3D model retrieval,” in *Proceedings of the 11th International Multimedia Modelling Conference*, 2005. Accessed: Jan. 23, 2023. [Online]. Available: https://ieeexplore.ieee.org/stamp/stamp.jsp?tp=&arnumber=1386011

[38] M. Kazhdan, T. Funkhouser, and S. Rusinkiewicz, “Rotation invariant spherical harmonic representation of 3D shape descriptors,” *Eurographics Symposium on Geometry Processing*, 2003.

[39] D. Zhao, Z. Lin, and X. Tang, “Laplacian PCA and its applications,” in *Proceedings of the IEEE International Conference on Computer Vision*, 2007. doi: 10.1109/ICCV.2007.4409096.

[40] J. Tedjokusumo and W. K. Leow, “Normalization and alignment of 3D objects based on bilateral symmetry planes,” in *Proceedings Part I: 13th International Multimedia Modeling Conference*, 2007, pp. 74–85.

[41] G. Barequet and S. Har-Peled, “Efficiently approximating the minimum-volume bounding box of a point set in three dimensions,” *Journal of Algorithms*, vol. 38, no. 1, pp. 91–109, Jan. 2001, doi: 10.1006/JAGM.2000.1127.

[42] C. L. Ventola, “Medical applications for 3D Printing: Current and projected uses,” *P&T*, vol. 39, no. 10, pp. 704–711, 2014, Accessed: Dec. 14, 2022. [Online]. Available: www.thingiverse.com

[43] N. J. Rosenblatt, A. Stachowiak, and C. Reddin, “Prosthetic disuse leads to lower balance confidence in a long-term user of a transtibial prosthesis,” *Adv Wound Care (New Rochelle)*, vol. 10, no. 9, pp. 529–533, Jul. 2021, doi: 10.1089/WOUND.2019.1086.

[44] N. Martelli, C. Serrano, S. Fontenay, H. Van Den Brink, J. Pineau, and P. Prognon, “Evaluation of 3D printing costs in surgery: a systematic review,” *Int J Technol Assess Health Care*, vol. 36, pp. 349–355, 2020, doi: 10.1017/S0266462320000331.

[45] D. H. Ballard, P. Mills, R. Duszak, J. A. Weisman, F. J. Rybicki, and P. K. Woodard, “Medical 3D printing cost-savings in orthopedic and maxillofacial surgery: Cost analysis of operating room time saved with 3D printed anatomic models and surgical guides,” *Acad Radiol*, vol. 27, no. 8, pp. 1103–1113, Aug. 2020, doi: 10.1016/J.ACRA.2019.08.011.

[46] K. T. Nguyen, L. Benabou, and S. Alfayad, “Systematic review of prosthetic socket fabrication using 3D printing,” in *ACM International Conference Proceeding Series*, Association for Computing Machinery, Feb. 2018, pp. 137–141. doi: 10.1145/3191477.3191506.

[47] I. Antoniac, D. Popescu, A. Zapciu, A. Antoniac, F. Miculescu, and H. Moldovan, “Magnesium filled polylactic acid (PLA) material for filament based 3D printing,” *Materials*, vol. 12, no. 719, 2019, doi: 10.3390/ma12050719.

[48] S. Pitjamit, K. Thunsiri, W. Nakkiew, T. Wongwichai, P. Pothacharoen, and W. Wattanutchariya, "The possibility of interlocking nail fabrication from FFF 3D Printing PLA/PCL/HA composites coated by local silk fibroin for canine bone fracture treatment," *Materials*, vol. 13, no. 1564, 2020, doi: 10.3390/ma13071564.

[49] V. DeStefano, S. Khan, and A. Tabada, "Applications of PLA in modern medicine," *Engineered Regeneration*, vol. 1, pp. 76–87, Jan. 2020, doi: 10.1016/J.ENGREG.2020.08.002.

[50] S. Kim, S. Yalla, S. Shetty, and N. J. Rosenblatt, "3D printed transtibial prosthetic sockets: A systematic review," *PLoS One*, vol. 17, no. 10, 2022, doi: 10.1371/JOURNAL.PONE.0275161.

[51] S. Kuciel, K. Mazur, and · Marek Hebda, "The Influence of wood and basalt fibres on mechanical, thermal and hydrothermal properties of PLA composites," *J Polym Environ*, vol. 28, pp. 1204–1215, 2020, doi: 10.1007/s10924-020-01677-z.

[52] J. C. H. Goh, P. V. S. Lee, and P. Ng, "Structural integrity of polypropylene prosthetic sockets manufactured using the polymer deposition technique," in *Proceedings of the Institution of Mechanical Engineers, Part H: Journal of Engineering in Medicine*, SAGE PublicationsSage UK: London, England, Aug. 2002, pp. 359–368. doi: 10.1243/095441102321032157.

[53] E. Stenvall *et al.*, "Additive manufacturing of prostheses using forest-based composites," *Bioengineering*, vol. 7, no. 103, 2020, doi: 10.3390/bioengineering7030103.

[54] M. Heidari-Rarani, M. Rafiee-Afarani, and A. M. Zahedi, "Mechanical characterization of FDM 3D printing of continuous carbon fiber reinforced PLA composites," *Composites Part B*, vol. 175, p. 107147, Oct. 2019, doi: 10.1016/J.COMPOSITESB.2019.107147.

[55] A. Thibodeau, "3D-printed surrogate lower limb for testing ankle-foot orthoses," 2021. doi: 10.20381/RUOR-26972.

[56] E. A. Nickel, K. J. Barrons, M. K. Owen, B. D. Hand, A. H. Hansen, and J. D. Desjardins, "Strength testing of definitive transtibial prosthetic sockets made using 3D-printing technology," *Journal of Prosthetics and Orthotics*, vol. 32, no. 4, pp. 295–300, Oct. 2020, doi: 10.1097/JPO.0000000000000294.

[57] T. Marinopoulos, S. Li, and V. V. Silberschmidt, "Structural integrity of 3D-printed prosthetic sockets: Experimental study for paediatric applications," *Journal of Materials Research and Technology*, vol. 24, pp. 2734–2742, May 2023, doi: 10.1016/j.jmrt.2023.03.192.

[58] S. Kim, S. V. Yalla, S. Shetty, and N. J. Rosenblatt, "Structural integrity of custom-designed additive manufactured prosthetic sockets compared to traditional sockets," *Results in Materials*, vol. 21, Mar. 2024, doi: 10.1016/j.rinma.2024.100549.

[59] International Organization for Standardization, *Prosthetics - structural testing of lower-limb prostheses - requirements and test methods*, Second edition 20..., vol. second edition. in International standard ; ISO 10328, vol. second edition. Geneva: ISO, 2016.

[60] J. E. Sanders, J. B. McLean, J. C. Cagle, D. W. Gardner, and K. J. Allyn, "Technical note: Computer-manufactured inserts for prosthetic sockets," *Med Eng Phys*, vol. 38, no. 8, pp. 801–806, Aug. 2016, doi: 10.1016/J.MEDENGPHY.2016.04.019.

[61] E. Nickel, K. Barrons, B. Hand, A. Cataldo, and A. Hansen, "Three-dimensional printing in prosthetics: Method for managing rapid limb volume change," *Prosthet Orthot Int*, vol. 44, no. 5, pp. 355–358, 2020, doi: 10.1177/0309364620934340.

[62] 3D Slicer, "3D slicer image computing platform." Accessed: Apr. 07, 2024. [Online]. Available: https://www.slicer.org/

[63] A. Surovas, "A digital workflow for modeling of custom dental implants," *3D Print Med*, vol. 5, no. 9, Dec. 2019, doi: 10.1186/s41205-019-0046-y.

[64] A. Lo Giudice *et al.*, "One step before 3D printing - evaluation of imaging software accuracy for 3-dimensional analysis of the mandible: A comparative study using a surface-to-surface matching technique," *Materials*, vol. 13, no. 2798, Jun. 2020, doi: 10.3390/ma13122798.

[65] H. Shetty *et al.*, "Three-dimensional semi-automated volumetric assessment of the pulp space of teeth following regenerative dental procedures," *Sci Rep*, vol. 11, no. 1, Dec. 2021, doi: 10.1038/s41598-021-01489-8.

[66] V. Boen, "Documentation/4.4/Extensions/CMFreg - Slicer Wiki." Accessed: Apr. 09, 2024. [Online]. Available: https://www.slicer.org/wiki/Documentation/4.4/Extensions/CMFreg

[67] B. Pernet, J. K. Nagel, and H. Zhang, "Compressive strength assessment of 3D printing infill patterns," in *Proceedings from the 29th CIRP Life Cycle Engineering Conference*, Elsevier B.V., 2022, pp. 682–687. doi: 10.1016/j.procir.2022.02.114.

[68] "Healthcare in Canada." Accessed: Aug. 17, 2023. [Online]. Available: https://www.worlddata.info/america/canada/health.php

[69] T. S. Keller, A. M. Weisberger, J. L. Ray, S. S. Hasan, R. G. Shiavi, and D. M. Spengler, "Relationship between vertical ground reaction force and speed during walking, slow jogging, and running," *Clinical Biomechanics*, vol. 11, no. 5, pp. 253–259, 1996.

[70] C. Feil and T. Zimmerman, "The ideal running gait: Focus on foot strike." Accessed: Jan. 17, 2024. [Online]. Available: https://www.teamchiroames.com/blog/the-ideal-running-gait-focus-on-foot-strike

[71] M. Van der Stelt, L. Verhamme, C. H. Slump, L. Brouwers, and T. J. J. Maal, "Strength testing of low-cost 3D-printed transtibial prosthetic socket," in *Proceedings of the Institution of*

Mechanical Engineers, Part H: Journal of Engineering in Medicine, SAGE Publications Ltd, Mar. 2022, pp. 367–375. doi: 10.1177/09544119211060092.

[72] R. S. Hanspal, K. Fisher, and R. Nieveen, "Prosthetic socket fit comfort score," *Disabil Rehabil*, vol. 25, no. 22, pp. 1278–1280, 2003, doi: 10.1080/09638280310001603983.

[73] D. A. Boone and K. L. Coleman, "Use of the Prosthesis Evaluation Questionnaire (PEQ)," in *SSC Proceedings*, 2006, pp. 68–79. [Online]. Available: http://journals.lww.com/jpojournal

[74] A. B. Deathe and W. C. Miller, "The L test of functional mobility: Measurement properties of a modified version of the timed 'up & go' test designed for people with lower-limb amputations," *Phys Ther*, vol. 85, no. 7, pp. 626–635, 2005, [Online]. Available: https://academic.oup.com/ptj/article/85/7/626/2804973

[75] D. Brooks, J. P. Hunter, J. Parsons, E. Livsey, J. Quirt, and M. Devlin, "Reliability of the two-minute walk test in individuals with transtibial amputation," *Arch Phys Med Rehabil*, vol. 83, no. 11, pp. 1562–1565, Nov. 2002, doi: 10.1053/apmr.2002.34600.

[76] D. Trundell, S. Le Scouiller, K. Gorni, T. Seabrook, and C. Vuillerot, "Validity and reliability of the 32-Item motor function measure in 2- to 5-year-olds with neuromuscular disorders and 2- to 25-year-olds with spinal muscular atrophy," *Neurol Ther*, vol. 9, pp. 575–584, 2020, doi: 10.6084/m9.figshare.12728270.

Appendix A: Step by Step Picture Guide to Create an Insert Model

General Workflow

Step 1: Slicer-3D set up

- Drag and drop the rectified scans of the old and new limb shape
- Center the 3D view around the models
    - Click the 3D view button at the top left of the 3D view
- Change the color of the models
    - Data tab → double click the node color for each model → choose the color

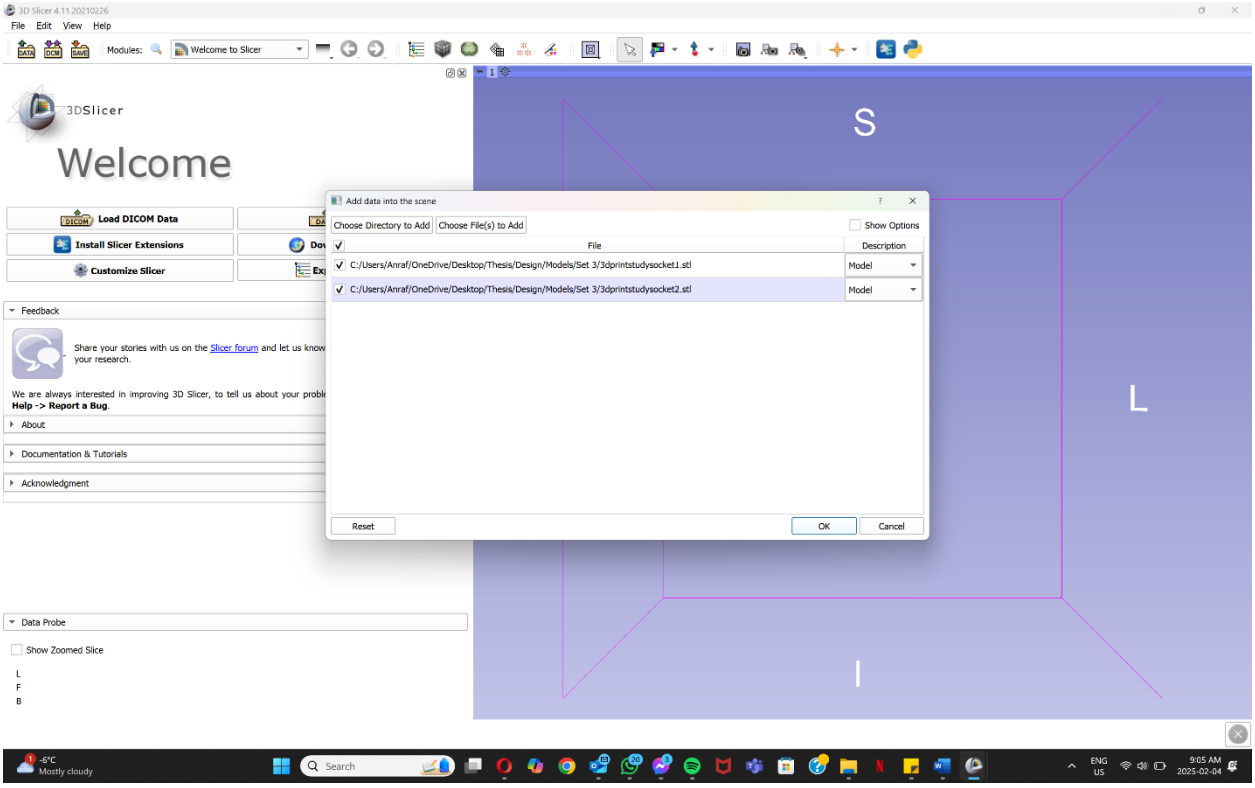

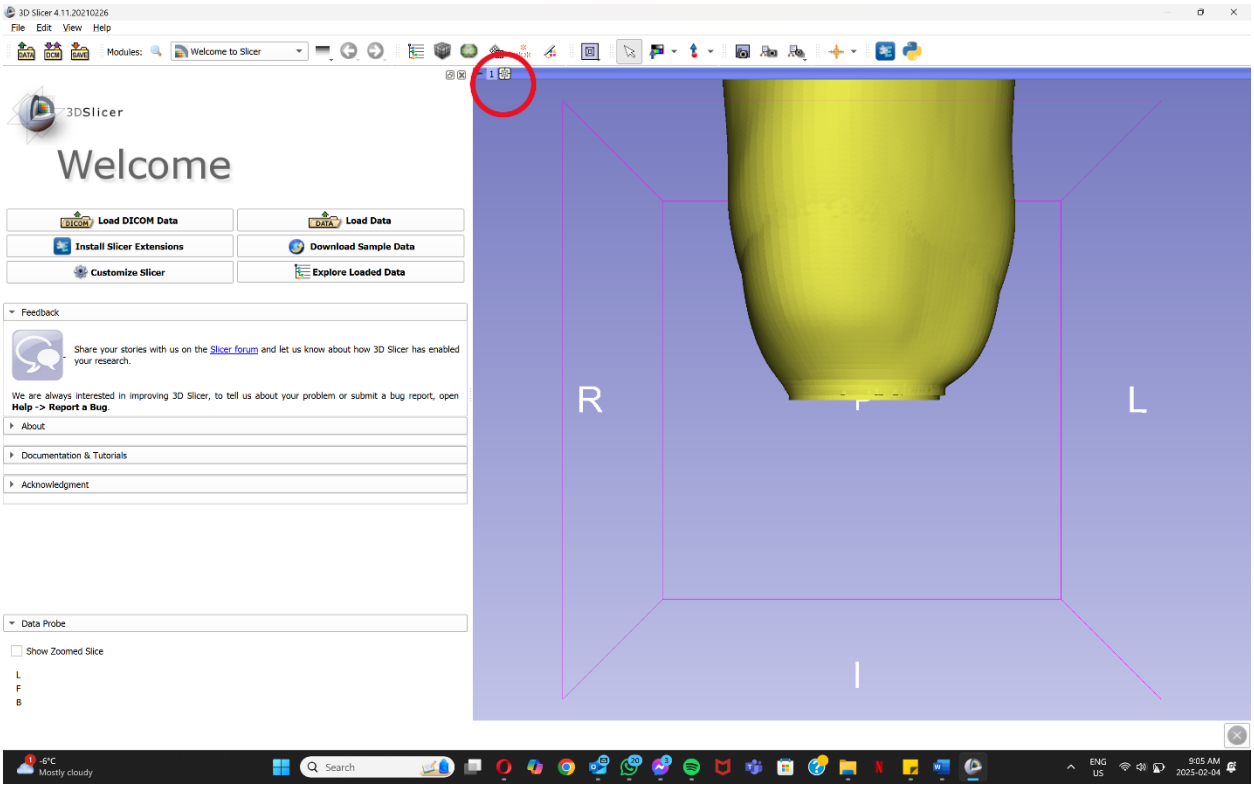
3D Slicer 4.11.20210226
File Edit View Help
Modules: Welcome to Slicer
3DSlicer
Welcome
Load DICOM Data
Load Data
Install Slicer Extensions
Download Sample Data
Customize Slicer
Explore Loaded Data
Feedback
Share your stories with us on the Slicer forum and let us know about how 3D Slicer has enabled your research.
We are always interested in improving 3D Slicer, to tell us about your problem or submit a bug report, open Help -> Report a Bug.
About
Documentation & Tutorials
Acknowledgment
Data Probe
Show Zoomed Slice
L
F
B
R
P
L
I

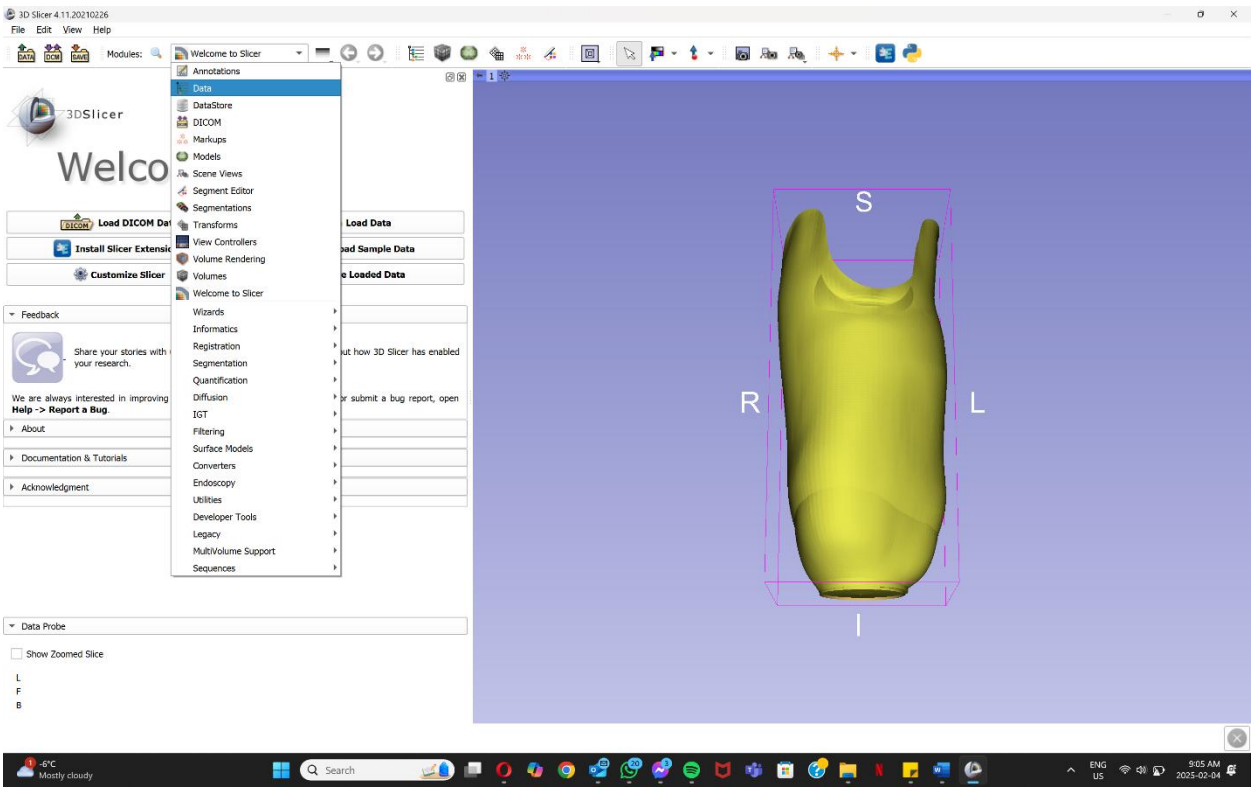
3D Slicer 4.11.20210226
File Edit View Help
Modules: Welcome to Slicer
Annotations
Data
DataStore
DICOM
Markups
Models
Scene Views
Segment Editor
Segmentations
Transforms
View Controllers
Volume Rendering
Volumes
Welcome to Slicer
Wizards
Informatics
Registration
Segmentation
Quantification
Diffusion
IGT
Filtering
Surface Models
Converters
Endoscopy
Utilities
Developer Tools
Legacy
MultiVolume Support
Sequences
3DSlicer
Data Probe
Show Zoomed Slice
S
R
L
I

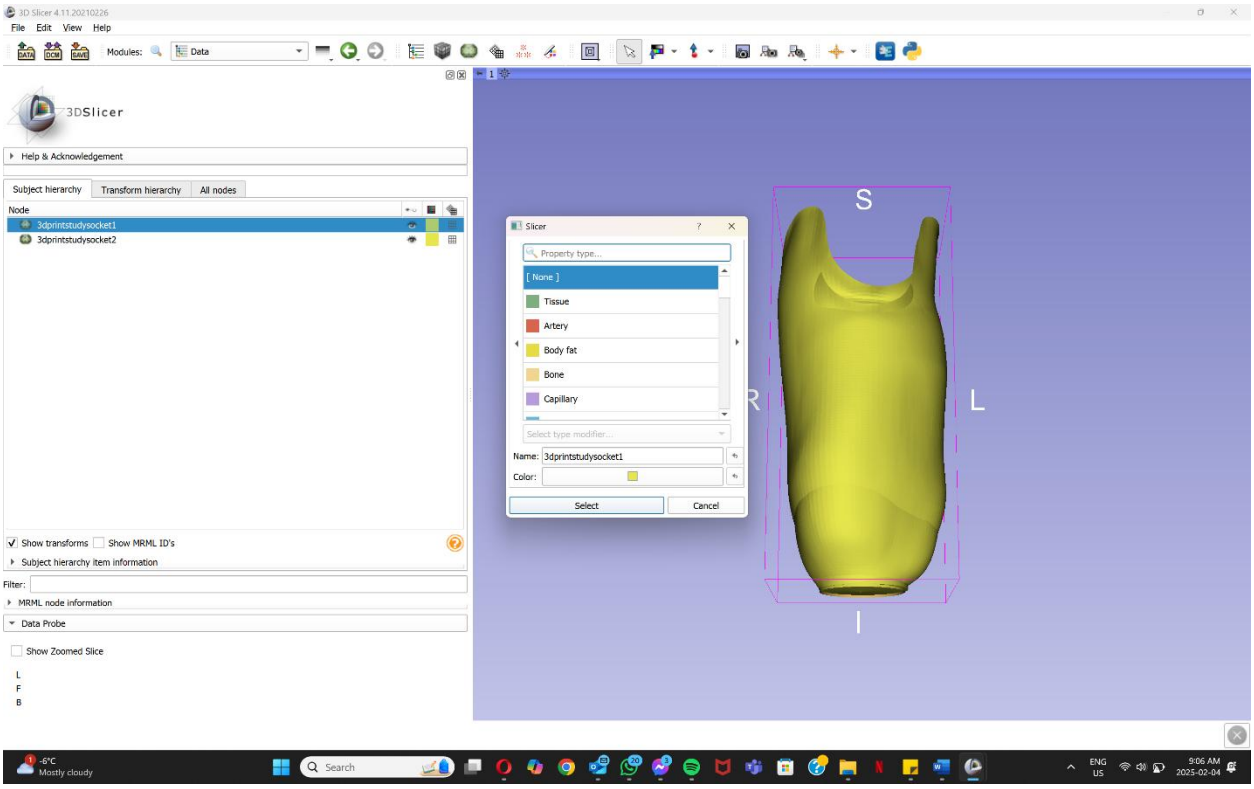

Step 2: Alignment

- Go to registration tab → CMF registration (ensure CMFreg extension is installed and enabled) → surface registration (skip to next section for fiducial registration)
    - Set fixed model to model1
    - Set moving model to model2
    - Output transfer → create new linear transfer as → 'insert transform name'
    - Output model → create new model as → 'insert model name' (socket2-registered)
    - Compute → apply
- Convert model1 and registered model to segments
    - Data tab → right click on each model → convert model to segmentation mode
- Convert segments to binary label maps
    - Right click on each segment → convert segment to binary labelmap
- Fine tune the alignment manually
    - Change the 3D view from 3D only to Four-up
    - Transform tab → Empty the transformed area → move the registered model, segment and binary label map to transformed area
    - Active Transform → create new linear transform as → 'insert transform name'
    - Use translation and rotation to fine-tune alignment as required
    - Harden the transforms in the apply transform drop-down section
- Data tab → delete the registered model segment and binary labelmap

- Data tab → right click on the registered model and rename to highlight the adjustments

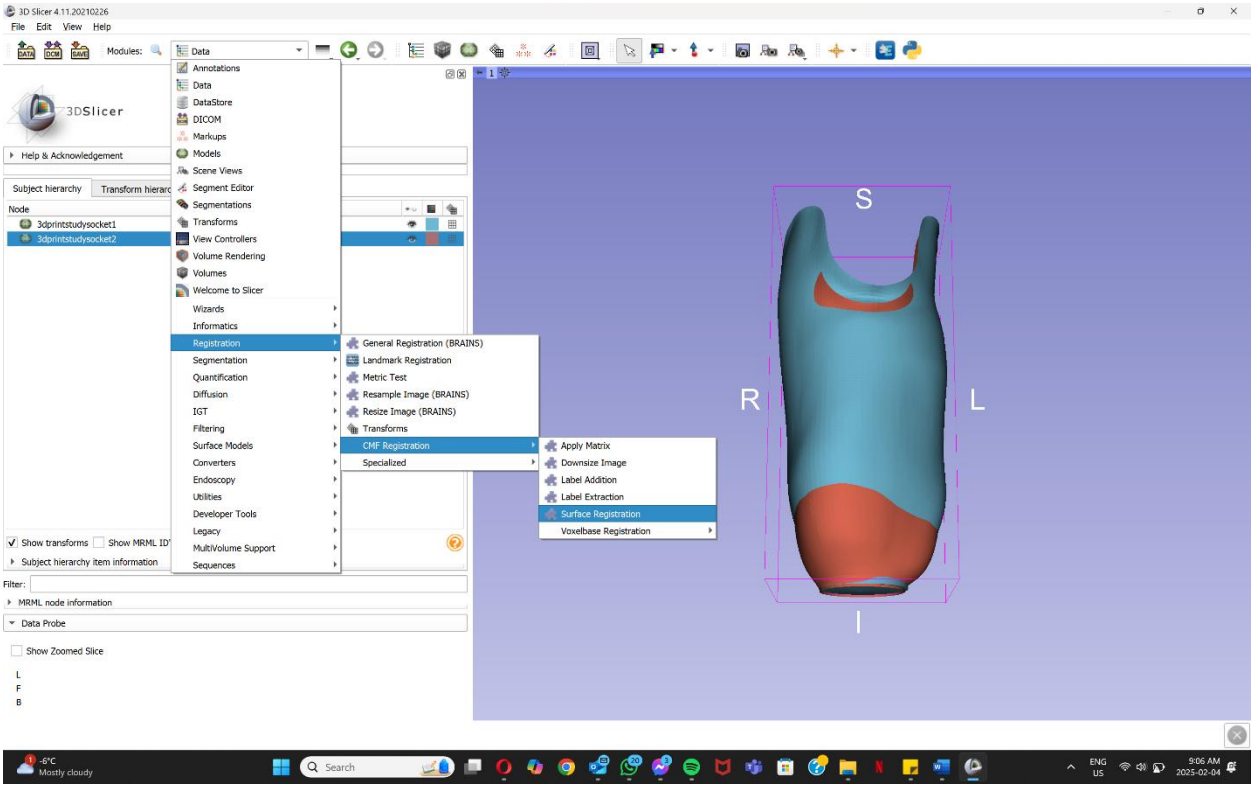

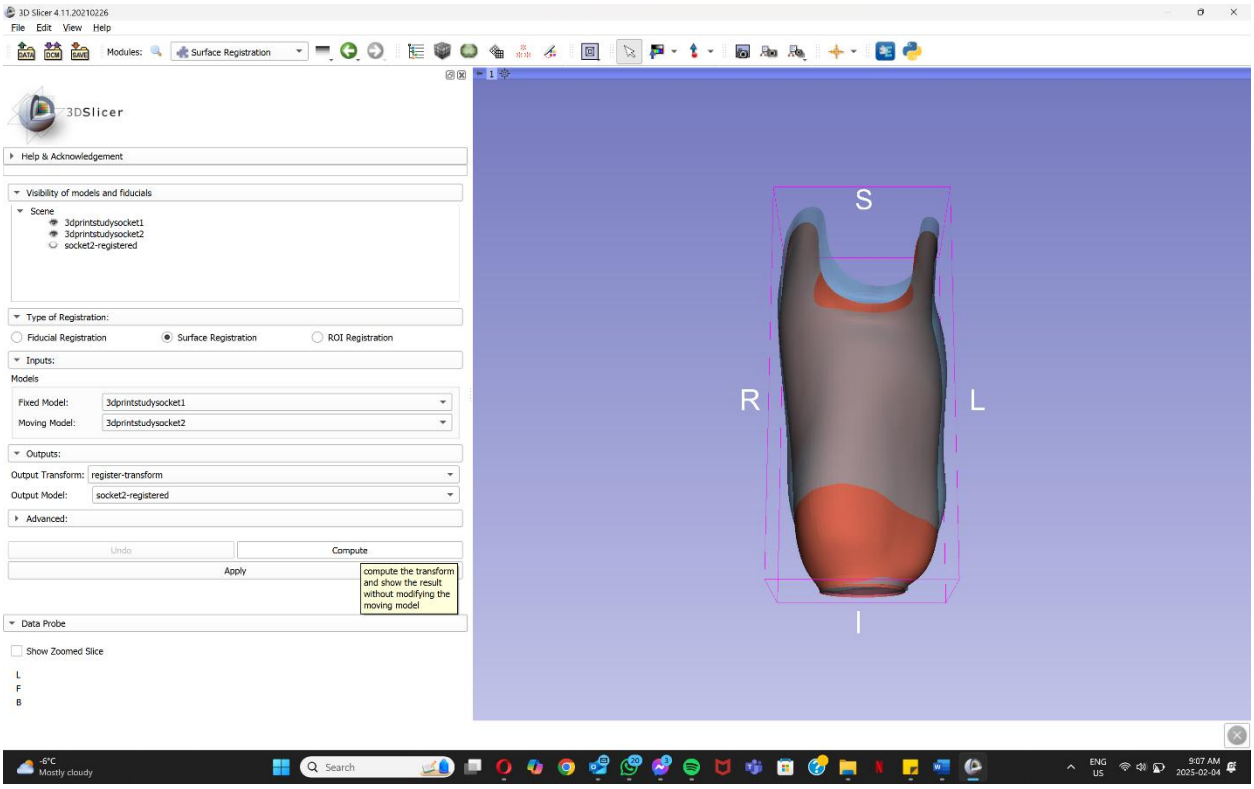
3D Slicer 4.11.20210226
File Edit View Help
Modules: Surface Registration
3DSlicer
Help & Acknowledgement
Visibility of models and fiducials
Scene
3dprintstudysocket1
3dprintstudysocket2
socket2-registered
Type of Registration:
Fiducial Registration
Surface Registration
ROI Registration
Inputs:
Models
Fixed Model: 3dprintstudysocket1
Moving Model: 3dprintstudysocket2
Outputs:
Output Transform: register-transform
Output Model: socket2-registered
Advanced:
Undo
Compute
Apply
compute the transform and show the result without modifying the moving model
Data Probe
Show Zoomed Slice
L
F
B
S
R
L
I
-6°C
Mostly cloudy
Search
ENG
US
9:07 AM
2025-02-04

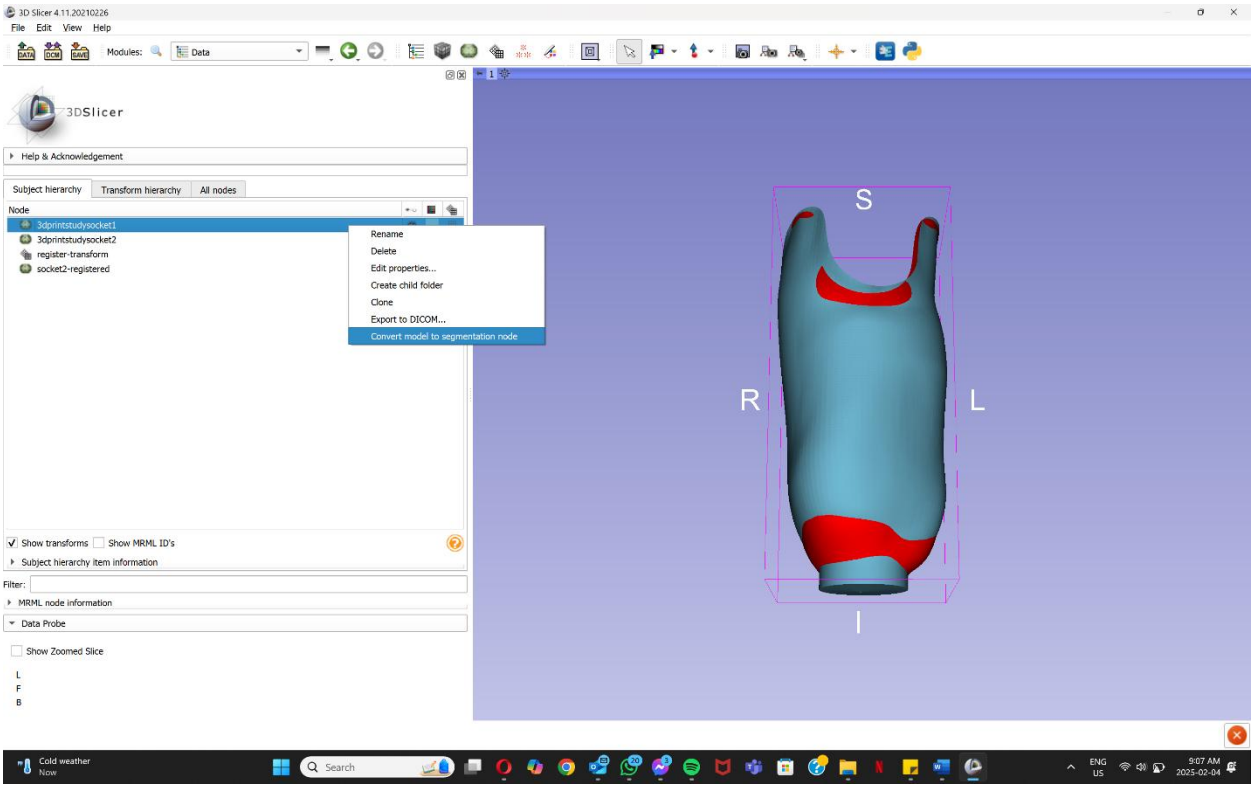
3D Slicer 4.11.20210226
File Edit View Help
Modules: Data
3DSlicer
Help & Acknowledgement
Subject hierarchy
Transform hierarchy
All nodes
Node
3dprintstudysocket1
3dprintstudysocket2
register-transform
socket2-registered
Rename
Delete
Edit properties...
Create child folder
Clone
Export to DICOM...
Convert model to segmentation node
Show transforms
Show MRML ID's
Subject hierarchy item information
Filter:
MRML node information
Data Probe
Show Zoomed Slice
L
F
B
S
R
L
I
Cold weather
Now
Search
ENG
US
9:07 AM
2025-02-04

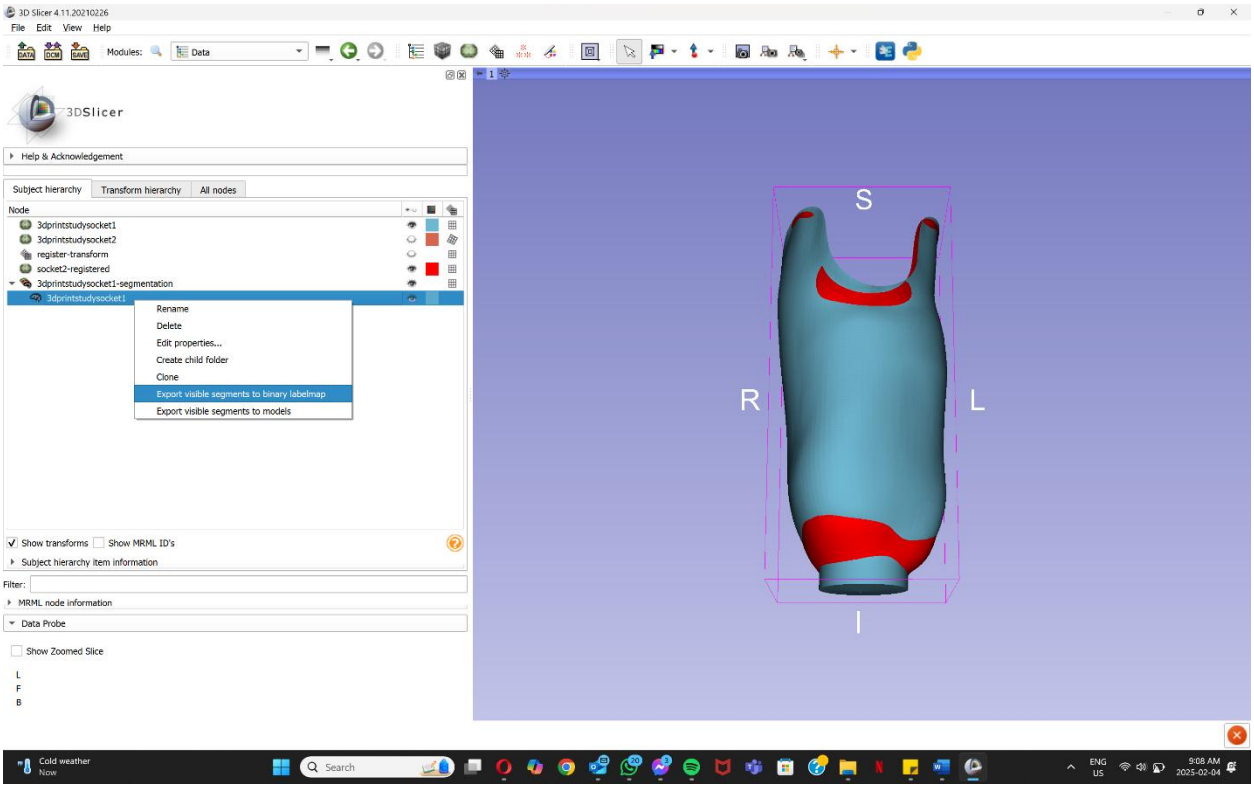
3D Slicer 4.11.20210226
File Edit View Help
Modules: Data
3DSlicer
Help & Acknowledgement
Subject hierarchy
Transform hierarchy
All nodes
Node
3dprintstudysocket1
3dprintstudysocket2
register-transform
socket2-registered
3dprintstudysocket1-segmentation
3dprintstudysocket1
Rename
Delete
Edit properties...
Create child folder
Clone
Export visible segments to binary labelmap
Export visible segments to models
Show transforms
Show MRML ID's
Subject hierarchy item information
Filter:
MRML node information
Data Probe
Show Zoomed Slice
L
F
B
S
R
L
I
Cold weather
Now
Search
ENG
US
9:08 AM
2025-02-04

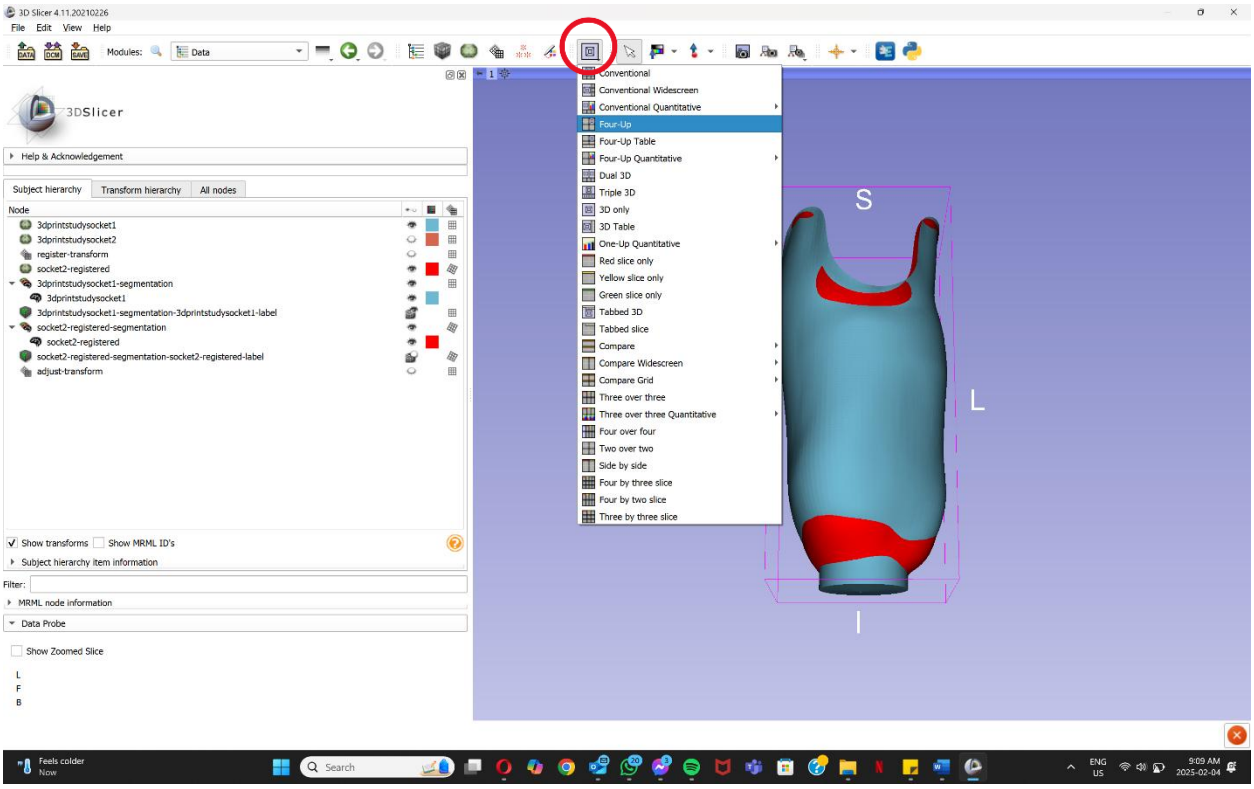
3D Slicer 4.11.20210226
File Edit View Help
Modules: Data
3DSlicer
Help & Acknowledgement
Subject hierarchy
Transform hierarchy
All nodes
Node
3dprintstudysocket1
3dprintstudysocket2
register-transform
socket2-registered
3dprintstudysocket1-segmentation
3dprintstudysocket1
3dprintstudysocket1-segmentation-3dprintstudysocket1-label
socket2-registered-segmentation
socket2-registered
socket2-registered-segmentation-socket2-registered-label
adjust-transform
Conventional
Conventional Widescreen
Conventional Quantitative
Four-Up
Four-Up Table
Four-Up Quantitative
Dual 3D
Triple 3D
3D only
3D Table
One-Up Quantitative
Red slice only
Yellow slice only
Green slice only
Tabbed 3D
Tabbed slice
Compare
Compare Widescreen
Compare Grid
Three over three
Three over three Quantitative
Four over four
Two over two
Side by side
Four by three slice
Four by two slice
Three by three slice
Show transforms
Show MRML ID's
Subject hierarchy item information
Filter:
MRML node information
Data Probe
Show Zoomed Slice
L
F
B
S
L
I
Feels colder
Now
Search
ENG
US
9:09 AM
2025-02-04

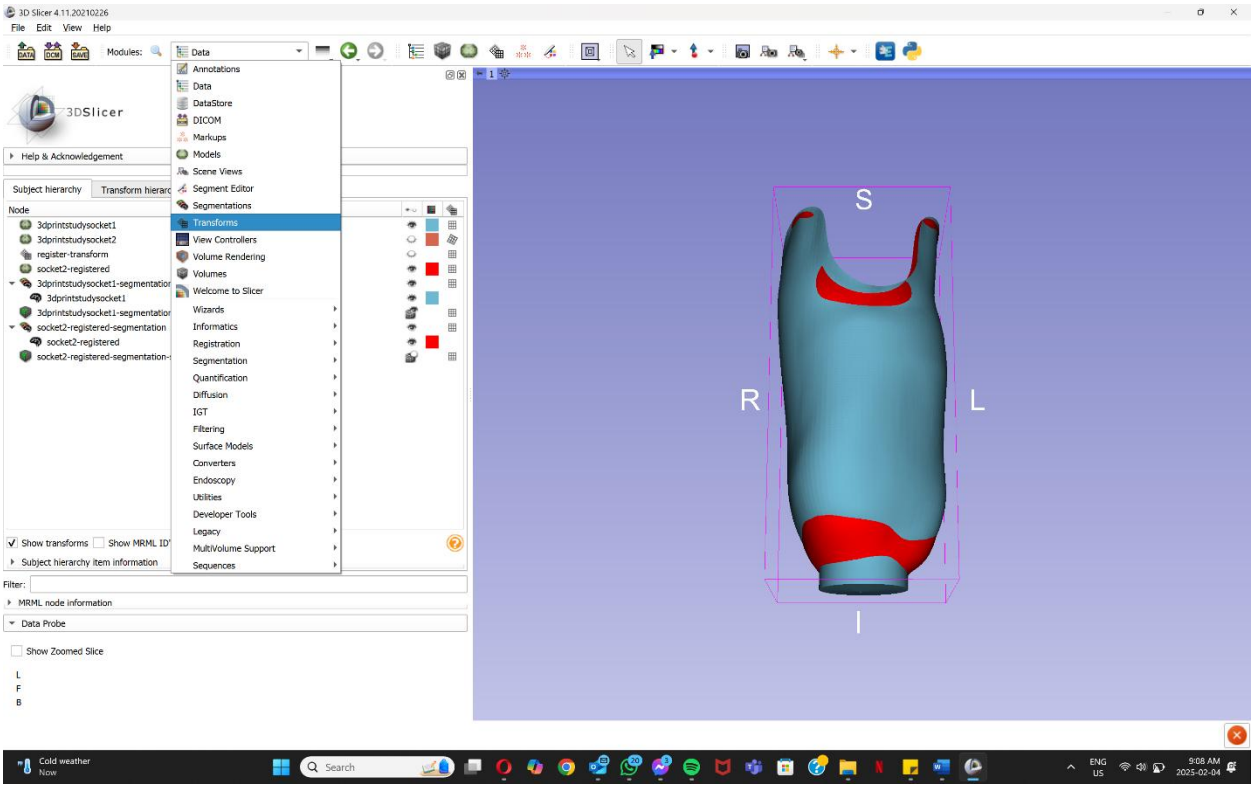
3D Slicer 4.11.20210226
File Edit View Help
Modules: Data
Annotations
Data
DataStore
DICOM
Markups
Models
Scene Views
Segment Editor
Segmentations
Transforms
View Controllers
Volume Rendering
Volumes
Welcome to Slicer
Wizards
Informatics
Registration
Segmentation
Quantification
Diffusion
IGT
Filtering
Surface Models
Converters
Endoscopy
Utilities
Developer Tools
Legacy
MultiVolume Support
Sequences
3DSlicer
Help & Acknowledgement
Subject hierarchy
Node
3dprintstudysocket1
3dprintstudysocket2
register-transform
socket2-registered
Show transforms
Subject hierarchy item information
Filter:
MRML node information
Data Probe
Show Zoomed Slice
S
R
L
I
Cold weather
Search
ENG
US
9:08 AM
2025-02-04

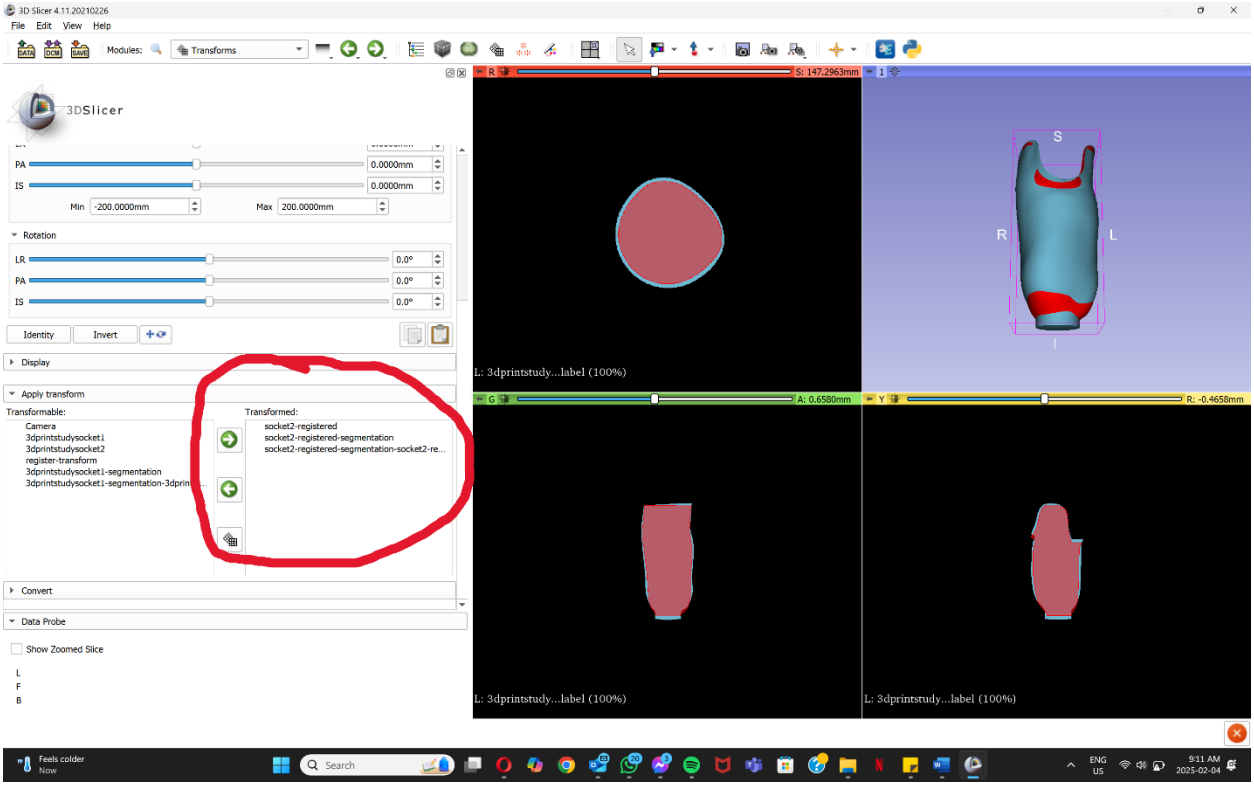
3D Slicer 4.11.20210226
File Edit View Help
Modules: Transforms
3DSlicer
PA 0.0000mm
IS 0.0000mm
Min -200.0000mm
Max 200.0000mm
Rotation
LR 0.0°
PA 0.0°
IS 0.0°
Identity
Invert
Display
Apply transform
Transformable:
Camera
3dprintstudysocket1
3dprintstudysocket2
register-transform
3dprintstudysocket1-segmentation
Transformed:
socket2-registered
socket2-registered-segmentation
socket2-registered-segmentation-socket2-re...
Convert
Data Probe
Show Zoomed Slice
S: 147.2963mm
L: 3dprintstudy...label (100%)
A: 0.6580mm
R: -0.4658mm
S
R
L
I
Feels colder
Search
ENG
US
9:11 AM
2025-02-04

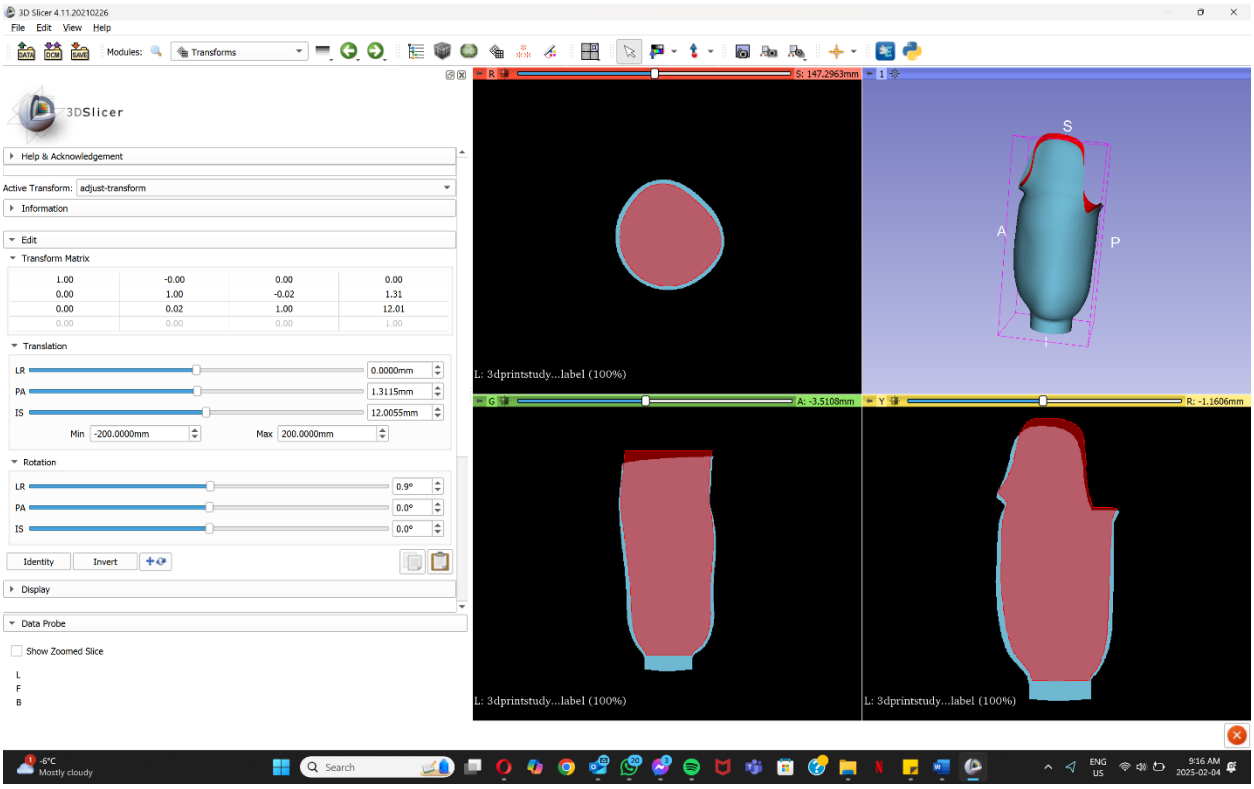
3D Slicer 4.11.20210226
File Edit View Help
Modules: Transforms
3DSlicer
Help & Acknowledgement
Active Transform: adjust-transform
Information
Edit
Transform Matrix
1.00 -0.00 0.00 0.00
0.00 1.00 -0.02 1.31
0.00 0.02 1.00 12.01
0.00 0.00 0.00 1.00
Translation
LR 0.0000mm
PA 1.3115mm
IS 12.0055mm
Min -200.0000mm Max 200.0000mm
Rotation
LR 0.9°
PA 0.0°
IS 0.0°
Identity Invert
Display
Data Probe
Show Zoomed Slice
L
F
B
S: 147.2963mm
L: 3dprintstudy...label (100%)
S
A
P
A: -3.5108mm
R: -1.1606mm
L: 3dprintstudy...label (100%)
L: 3dprintstudy...label (100%)
-6°C Mostly cloudy
Search
ENG US
9:16 AM 2025-02-04

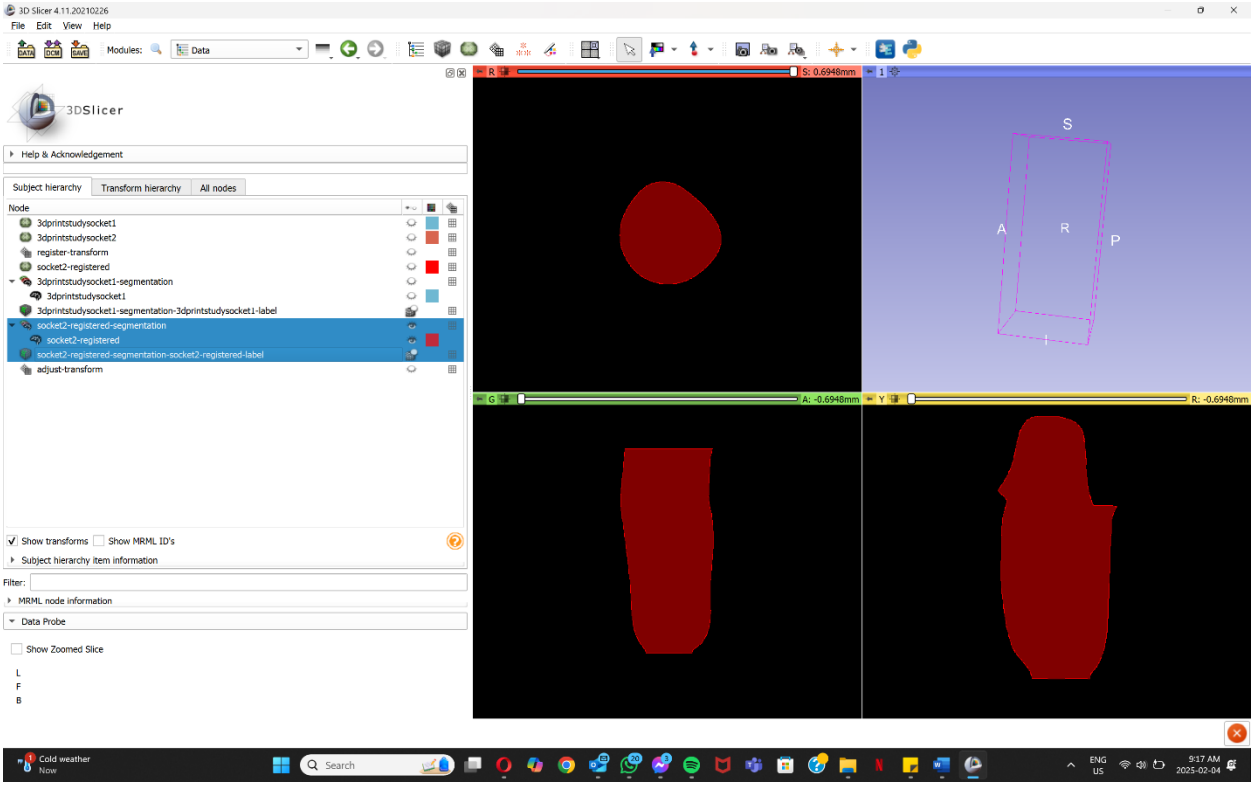
3D Slicer 4.11.20210226
File Edit View Help
Modules: Data
3DSlicer
Help & Acknowledgement
Subject hierarchy
Transform hierarchy
All nodes
Node
3dprintstudysocket1
3dprintstudysocket2
register-transform
socket2-registered
3dprintstudysocket1-segmentation
3dprintstudysocket1
3dprintstudysocket1-segmentation-3dprintstudysocket1-label
socket2-registered-segmentation
socket2-registered
socket2-registered-segmentation-socket2-registered-label
adjust-transform
Show transforms
Show MRML ID's
Subject hierarchy item information
Filter:
MRML node information
Data Probe
Show Zoomed Slice
L
F
B
S: 0.6948mm
S
A
R
P
A: -0.6948mm
R: -0.6948mm
Cold weather Now
Search
ENG US
9:17 AM 2025-02-04

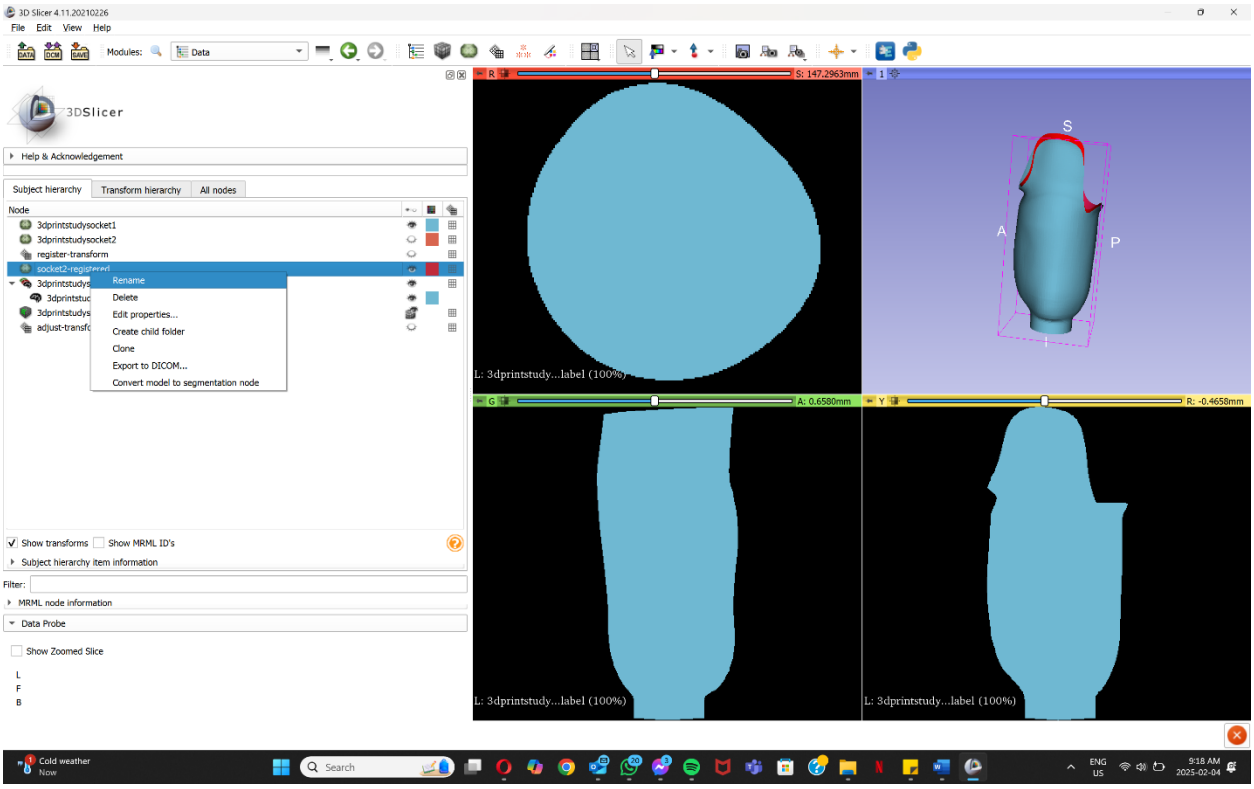

Step 3: Creating the insert

- Convert the adjusted model to segment and binary labelmap
  - Data tab → right click adjusted model → convert model to segmentation node
  - Data tab → right click segment → convert model to binary labelmap
- Fill in the models to create solid objects
  - Segment editor → set segmentation to the targeted segment → set master volume to model1 binary labelmap → smoothening → apply
    - Note this is a shortcut. Before executing this step, the models are simply a shell with no thickness. To smooth the surface, the software automatically fills in the models to create solids. Alternatively, we can use the hollow tool to give the shell a thickness followed by the fill-in tool to create a solid object
  - Repeat steps above for both model 1 and the adjusted model
- Rename segments
  - Data tab → right click the segments → rename → 'insert new segment name'
- Import both segments under the same segment folder
  - Data tab → right click adjusted filled in segment → export visible segment to model
  - Segmentations tab
    - Set active segment to model1 filled
    - Set operation to import

        - Set input type to models
        - Set input node to adjusted filled in model
        - Import
- Subtract the two segments from each other
    - Segment editor tab → set segmentation to folder with both segments → set master volume to model1 binary labelmap → logical operators → set operation to subtract → apply
        - Ensure that the larger model segment is selected in the top view while the smaller model segment is selected in the ‘subtract segment’ view
- Rename the larger model segment
    - Data tab → right click on segment → rename → ‘insert new segment name’ (insert)
    - Note, see section on filling holes if needed

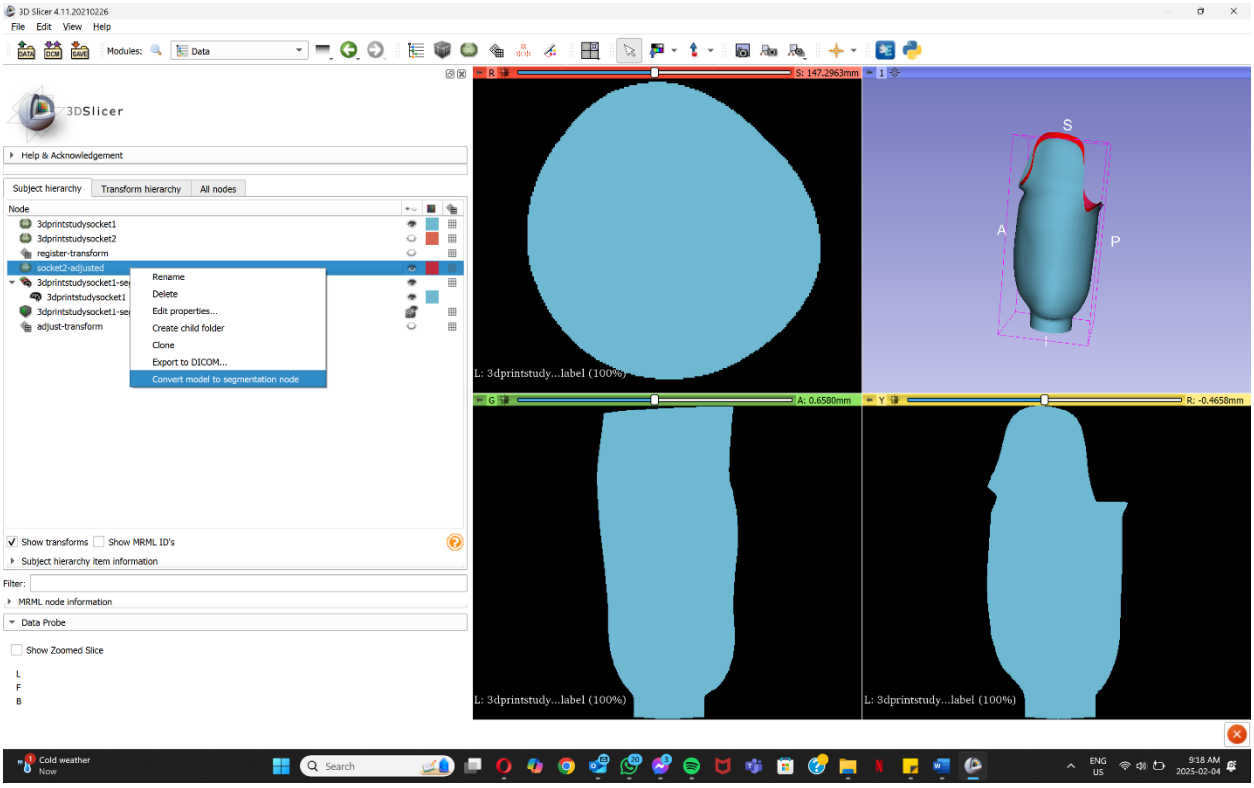

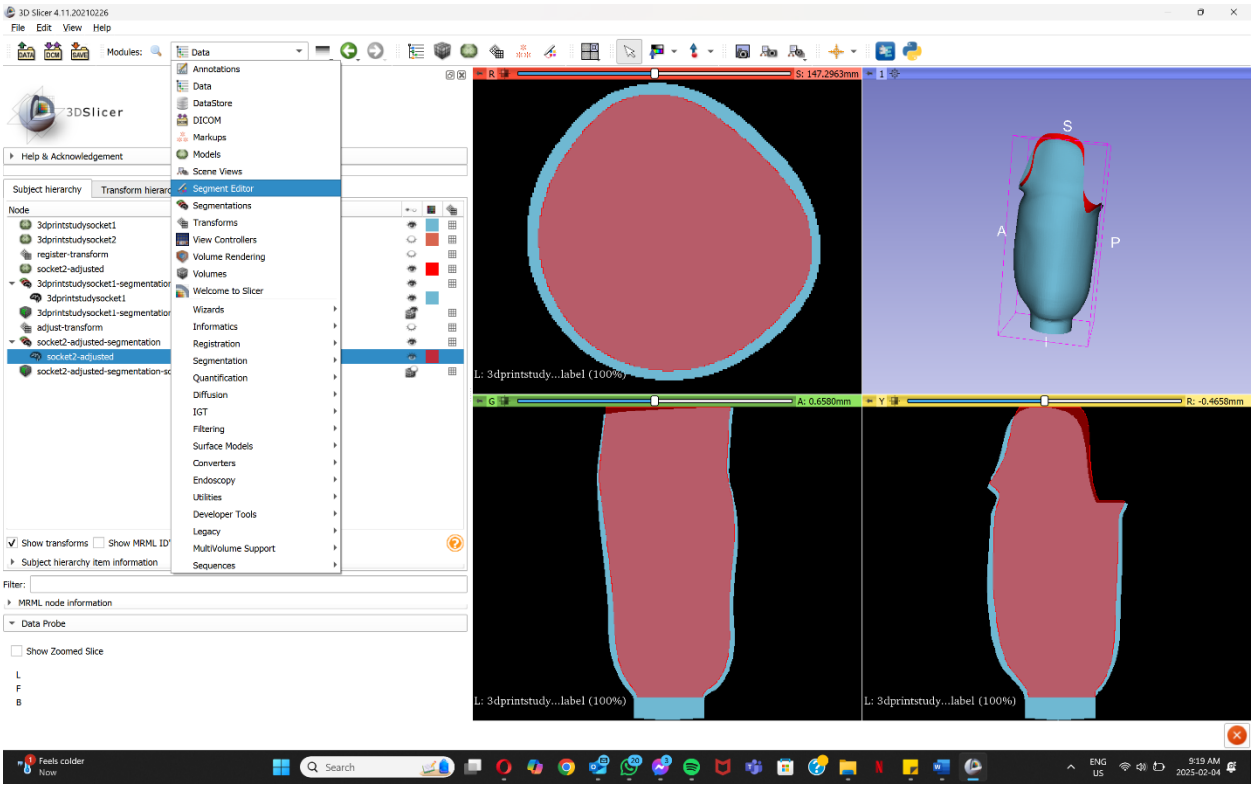
3D Slicer 4.11.20210226
File Edit View Help
Modules: Data
Annotations
Data
DataStore
DICOM
Markups
Models
Scene Views
Segment Editor
Segmentations
Transforms
View Controllers
Volume Rendering
Volumes
Welcome to Slicer
Wizards
Informatics
Registration
Segmentation
Quantification
Diffusion
IGT
Filtering
Surface Models
Converters
Endoscopy
Utilities
Developer Tools
Legacy
MultiVolume Support
Sequences
3DSlicer
Help & Acknowledgement
Subject hierarchy
Node
3dprintstudysocket1
3dprintstudysocket2
register-transform
socket2-adjusted
3dprintstudysocket1-segmentation
adjust-transform
socket2-adjusted-segmentation
Show transforms
Subject hierarchy item information
Filter:
MRML node information
Data Probe
Show Zoomed Slice
L
F
B
S: 147.2963mm
S
A
P
I
L: 3dprintstudy...label (100%)
A: 0.6580mm
R: -0.4658mm
Feels colder
Now
Search
ENG
US
9:19 AM
2025-02-04

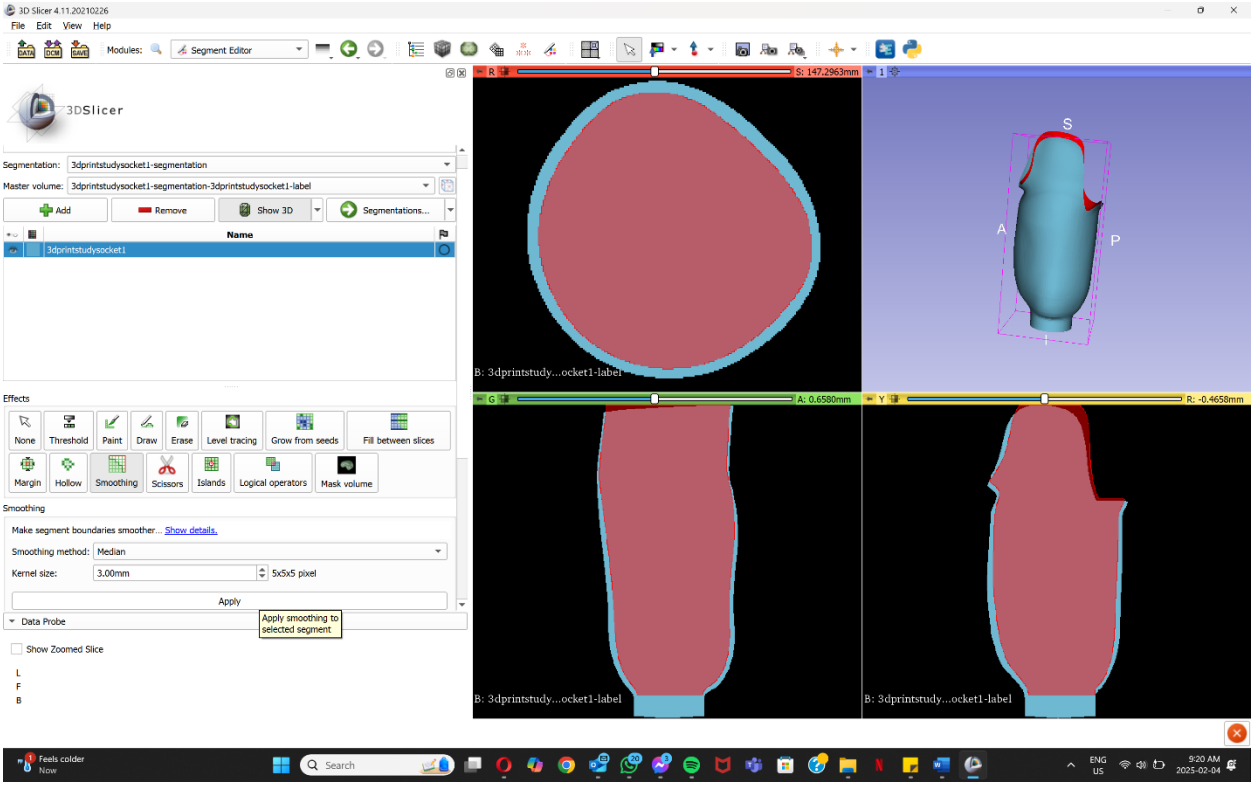
3D Slicer 4.11.20210226
File Edit View Help
Modules: Segment Editor
3DSlicer
Segmentation: 3dprintstudysocket1-segmentation
Master volume: 3dprintstudysocket1-segmentation-3dprintstudysocket1-label
Add
Remove
Show 3D
Segmentations...
Name
3dprintstudysocket1
Effects
None
Threshold
Paint
Draw
Erase
Level tracing
Grow from seeds
Fill between slices
Margin
Hollow
Smoothing
Scissors
Islands
Logical operators
Mask volume
Smoothing
Make segment boundaries smoother... Show details.
Smoothing method: Median
Kernel size: 3.00mm
5x5x5 pixel
Apply
Apply smoothing to selected segment
Data Probe
Show Zoomed Slice
L
F
B
S: 147.2963mm
S
A
P
I
B: 3dprintstudy...ocket1-label
A: 0.6580mm
R: -0.4658mm
Feels colder
Now
Search
ENG
US
9:20 AM
2025-02-04

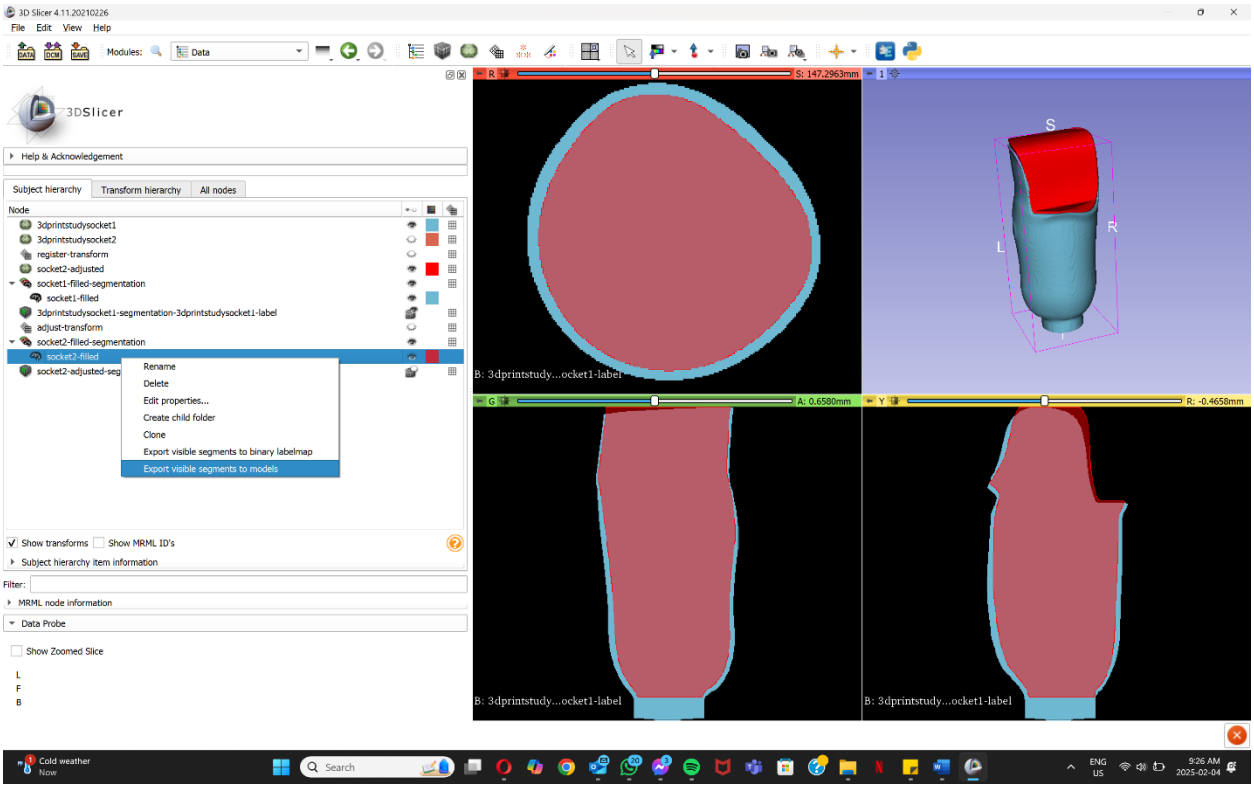
3D Slicer 4.11.20210226
File Edit View Help
Modules: Data
3DSlicer
Help & Acknowledgement
Subject hierarchy
Transform hierarchy
All nodes
Node
3dprintstudysocket1
3dprintstudysocket2
register-transform
socket2-adjusted
socket1-filled-segmentation
socket1-filled
3dprintstudysocket1-segmentation-3dprintstudysocket1-label
adjust-transform
socket2-filled-segmentation
socket2-filled
socket2-adjusted-seg
Rename
Delete
Edit properties...
Create child folder
Clone
Export visible segments to binary labelmap
Export visible segments to models
Show transforms
Show MRML ID's
Subject hierarchy item information
Filter:
MRML node information
Data Probe
Show Zoomed Slice
L
F
B
S: 147.2963mm
B: 3dprintstudy...ocket1-label
A: 0.6580mm
R: -0.4658mm
Cold weather
Now
Search
ENG
US
9:26 AM
2025-02-04

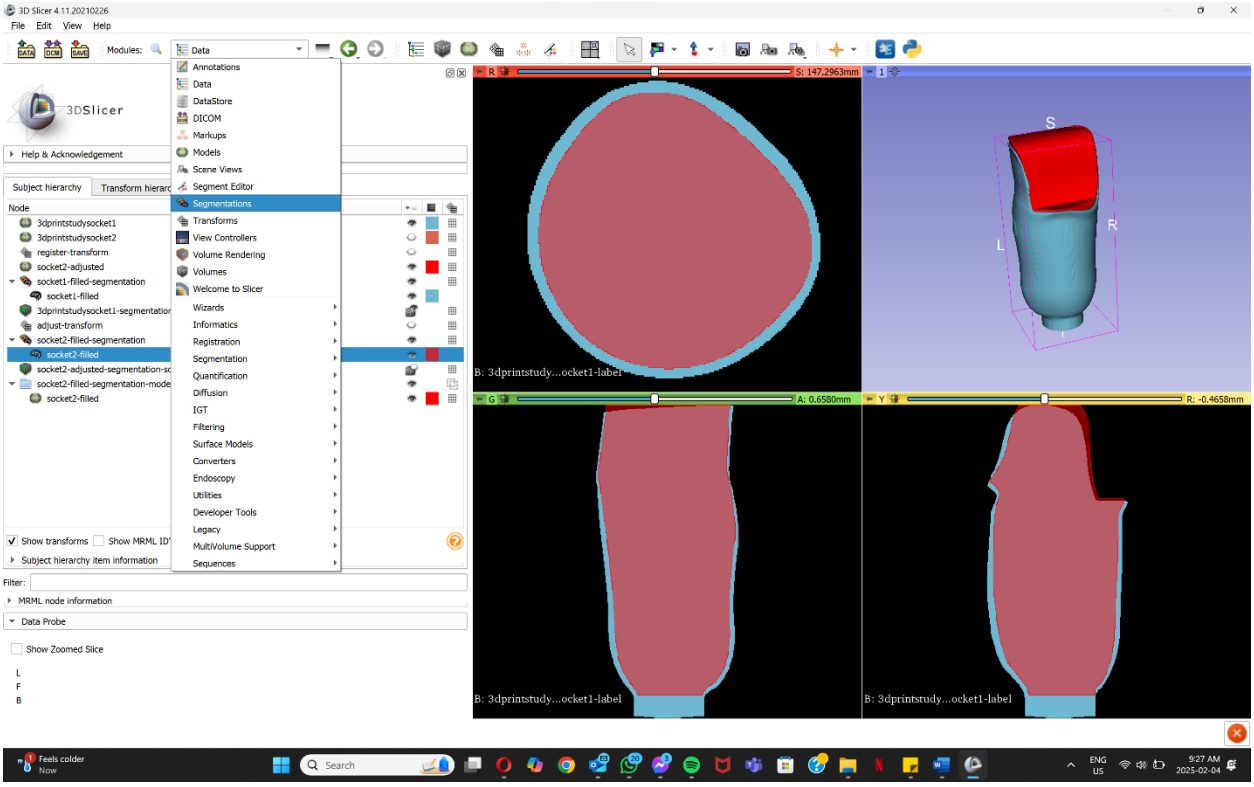
3D Slicer 4.11.20210226
File Edit View Help
Modules: Data
Annotations
Data
DataStore
DICOM
Markups
Models
Scene Views
Segment Editor
Segmentations
Transforms
View Controllers
Volume Rendering
Volumes
Welcome to Slicer
Wizards
Informatics
Registration
Segmentation
Quantification
Diffusion
IGT
Filtering
Surface Models
Converters
Endoscopy
Utilities
Developer Tools
Legacy
MultiVolume Support
Sequences
3DSlicer
Help & Acknowledgement
Subject hierarchy
Node
socket2-filled
Show transforms
Subject hierarchy item information
Filter:
MRML node information
Data Probe
Show Zoomed Slice
L
F
B
S: 147.2963mm
B: 3dprintstudy...ocket1-label
A: 0.6580mm
R: -0.4658mm
Feels colder
Now
Search
ENG
US
9:27 AM
2025-02-04

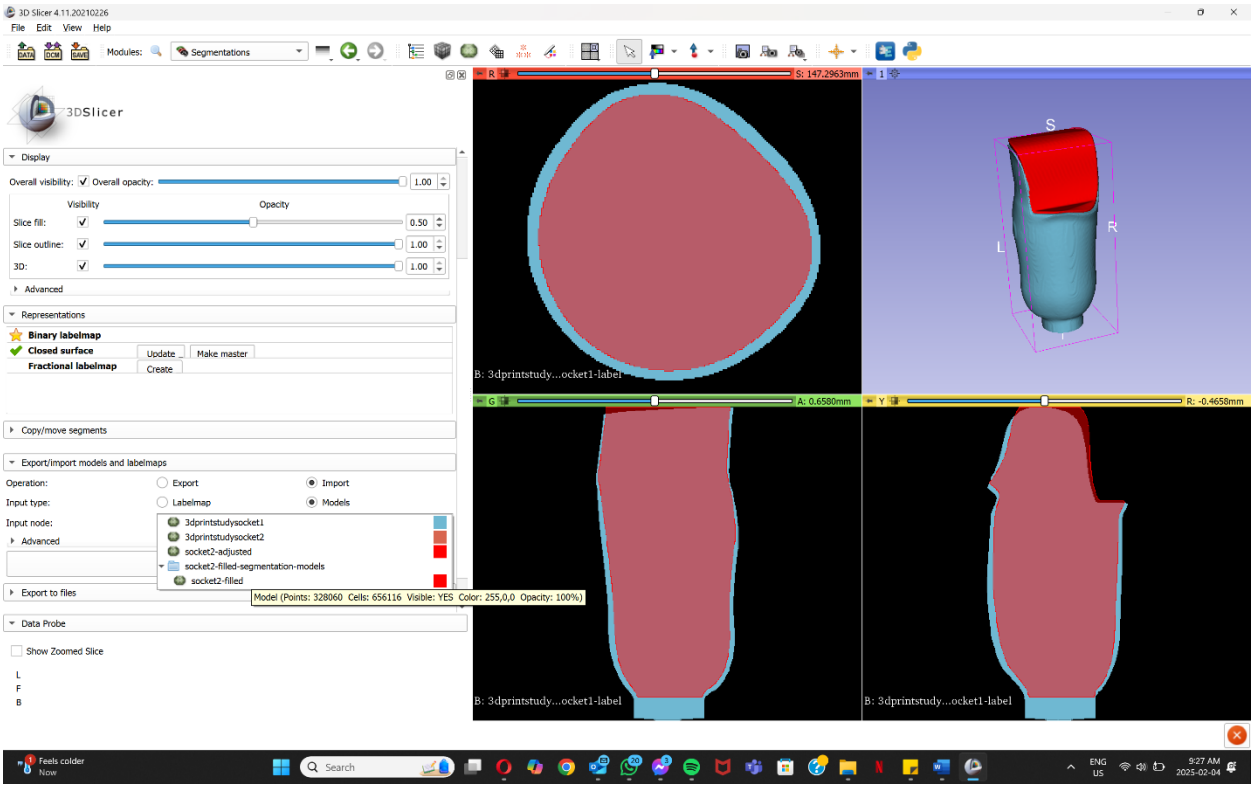
3D Slicer 4.11.20210226
File Edit View Help
Modules: Segmentations
3DSlicer
Display
Overall visibility: Overall opacity: 1.00
Visibility Opacity
Slice fill: 0.50
Slice outline: 1.00
3D: 1.00
Advanced
Representations
Binary labelmap
Closed surface
Fractional labelmap
Update Make master
Create
Copy/move segments
Export/import models and labelmaps
Operation: Export Import
Input type: Labelmap Models
Input node:
Advanced
3dprintstudysocket1
3dprintstudysocket2
socket2-adjusted
socket2-filled-segmentation-models
socket2-filled
Export to files
Model (Points: 328060 Cells: 656116 Visible: YES Color: 255,0,0 Opacity: 100%)
Data Probe
Show Zoomed Slice
L
F
B
S: 147.2963mm
B: 3dprintstudy...ocket1-label
A: 0.6580mm
R: -0.4658mm
Feels colder
Now
Search
ENG
US
9:27 AM
2025-02-04

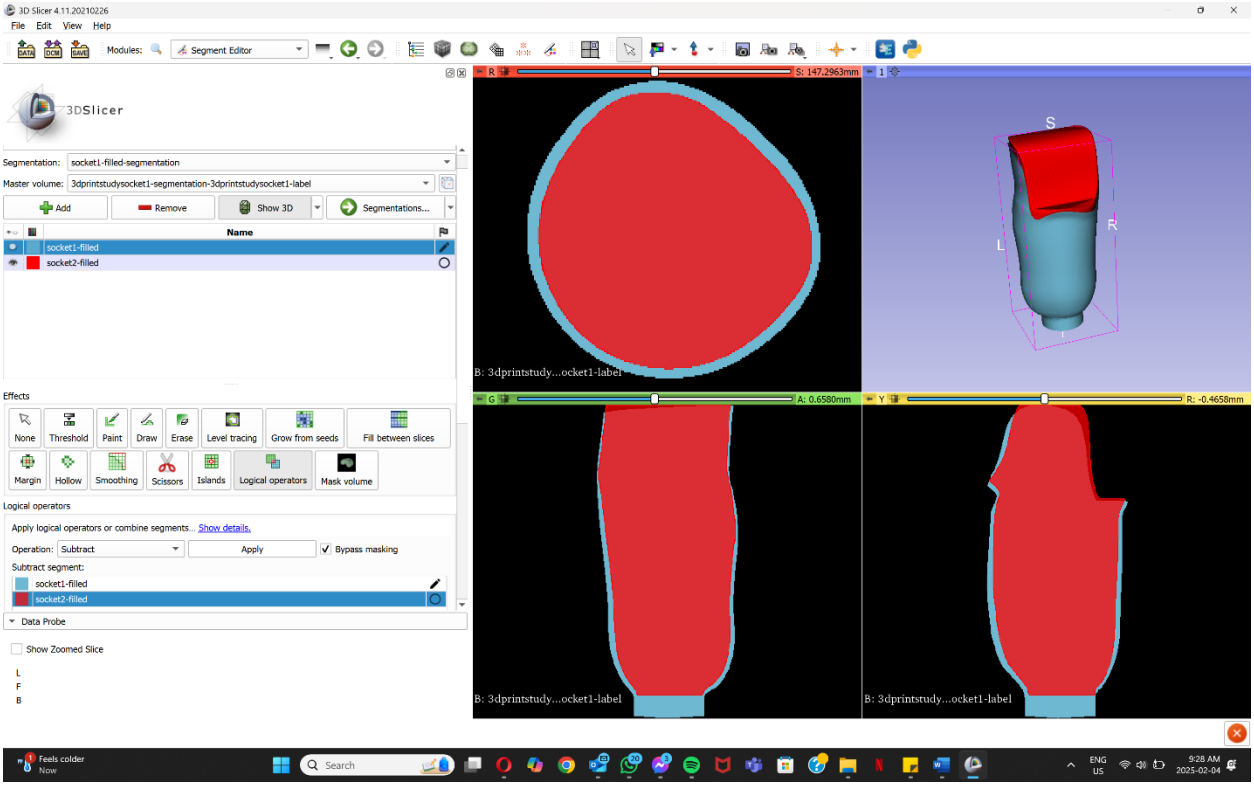
3D Slicer 4.11.20210226
File Edit View Help
Modules: Segment Editor
3DSlicer
Segmentation: socket1-filled-segmentation
Master volume: 3dprintstudysocket1-segmentation-3dprintstudysocket1-label
Add Remove Show 3D Segmentations...
Name
socket1-filled
socket2-filled
Effects
None Threshold Paint Draw Erase Level tracing Grow from seeds Fill between slices
Margin Hollow Smoothing Scissors Islands Logical operators Mask volume
Logical operators
Apply logical operators or combine segments... Show details.
Operation: Subtract Apply Bypass masking
Subtract segment:
socket1-filled
socket2-filled
Data Probe
Show Zoomed Slice
L
F
B
S: 147.2963mm
B: 3dprintstudy...ocket1-label
A: 0.6580mm
R: -0.4658mm
Feels colder
Now
Search
ENG
US
9:28 AM
2025-02-04

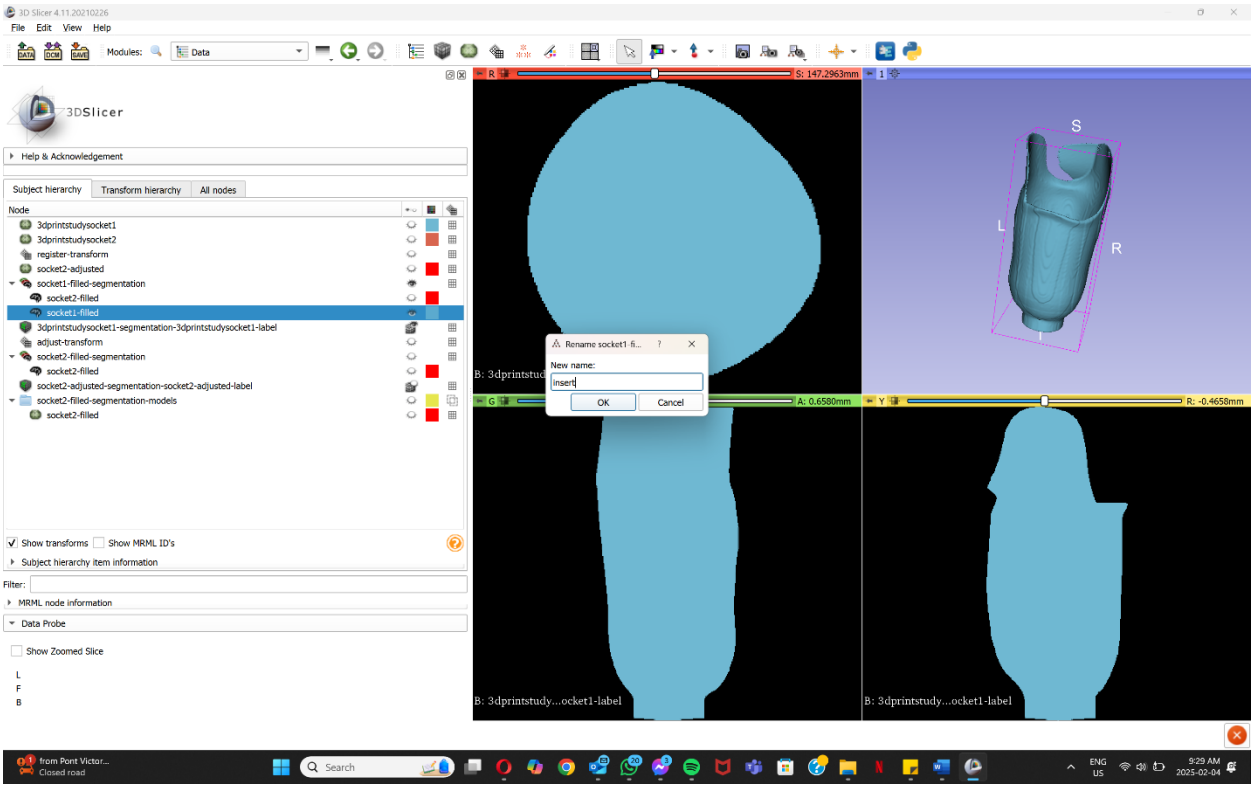

Step 4: Trim excess shapes

- Segment editor tab → scissors → set operation to erase inside → set shape to free-form, circle or rectangle as required
    - Note: it might be beneficial to change views between 3D and four-up as needed. To get fine control over sliced views in four-up view, convert segment to binary labelmap
- Rename segment
    - Data tab → right click on the segment → rename → ‘insert new segment name’

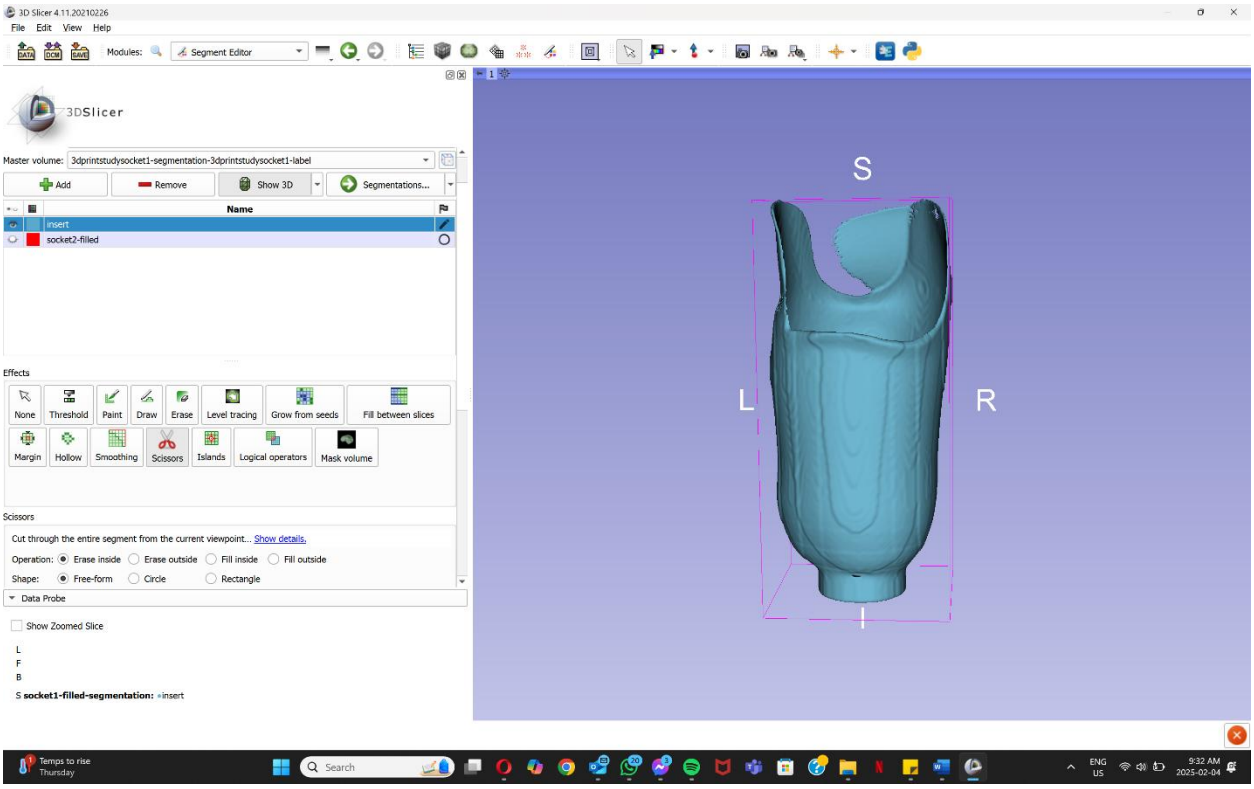
3D Slicer 4.11.20210226
File Edit View Help
Modules: Segment Editor
3DSlicer
Master volume: 3dprintstudysocket1-segmentation-3dprintstudysocket1-label
Add Remove Show 3D Segmentations...
Name
insert
socket2-filled
Effects
None Threshold Paint Draw Erase Level tracing Grow from seeds Fill between slices
Margin Hollow Smoothing Scissors Islands Logical operators Mask volume
Scissors
Cut through the entire segment from the current viewpoint... Show details.
Operation: Erase inside Erase outside Fill inside Fill outside
Shape: Free-form Circle Rectangle
Data Probe
Show Zoomed Slice
L
F
B
S socket1-filled-segmentation: insert
S
L
R
I
Temps to rise
Thursday
Search
ENG
US
9:32 AM
2025-02-04

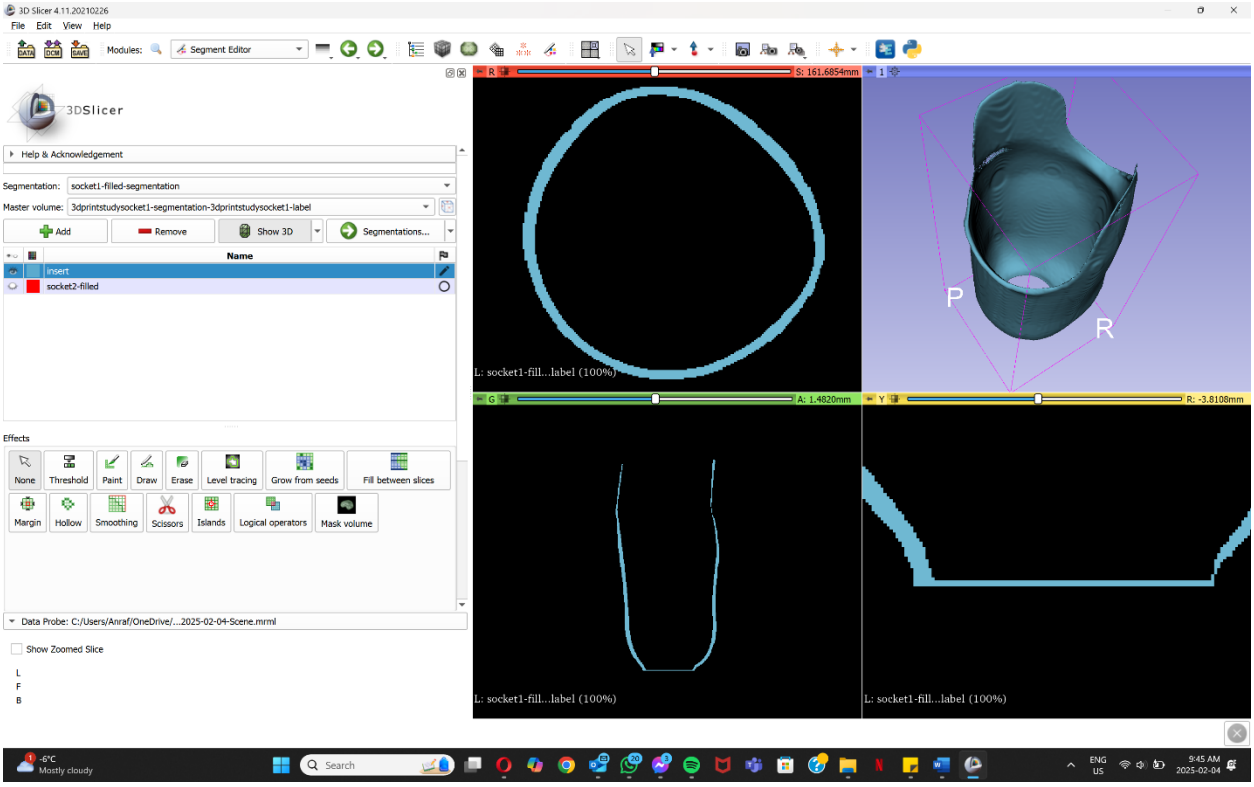
3D Slicer 4.11.20210226
File Edit View Help
Modules: Segment Editor
3DSlicer
Help & Acknowledgement
Segmentation: socket1-filled-segmentation
Master volume: 3dprintstudysocket1-segmentation-3dprintstudysocket1-label
Add Remove Show 3D Segmentations...
Name
insert
socket2-filled
Effects
None Threshold Paint Draw Erase Level tracing Grow from seeds Fill between slices
Margin Hollow Smoothing Scissors Islands Logical operators Mask volume
Data Probe: C:/Users/Anraf/OneDrive/...2025-02-04-Scene.mrml
Show Zoomed Slice
L
F
B
S: 161.6854mm
L: socket1-fill...label (100%)
P
R
A: 1.4820mm
R: -3.8108mm
L: socket1-fill...label (100%)
L: socket1-fill...label (100%)
-6°C
Mostly cloudy
Search
ENG
US
9:45 AM
2025-02-04

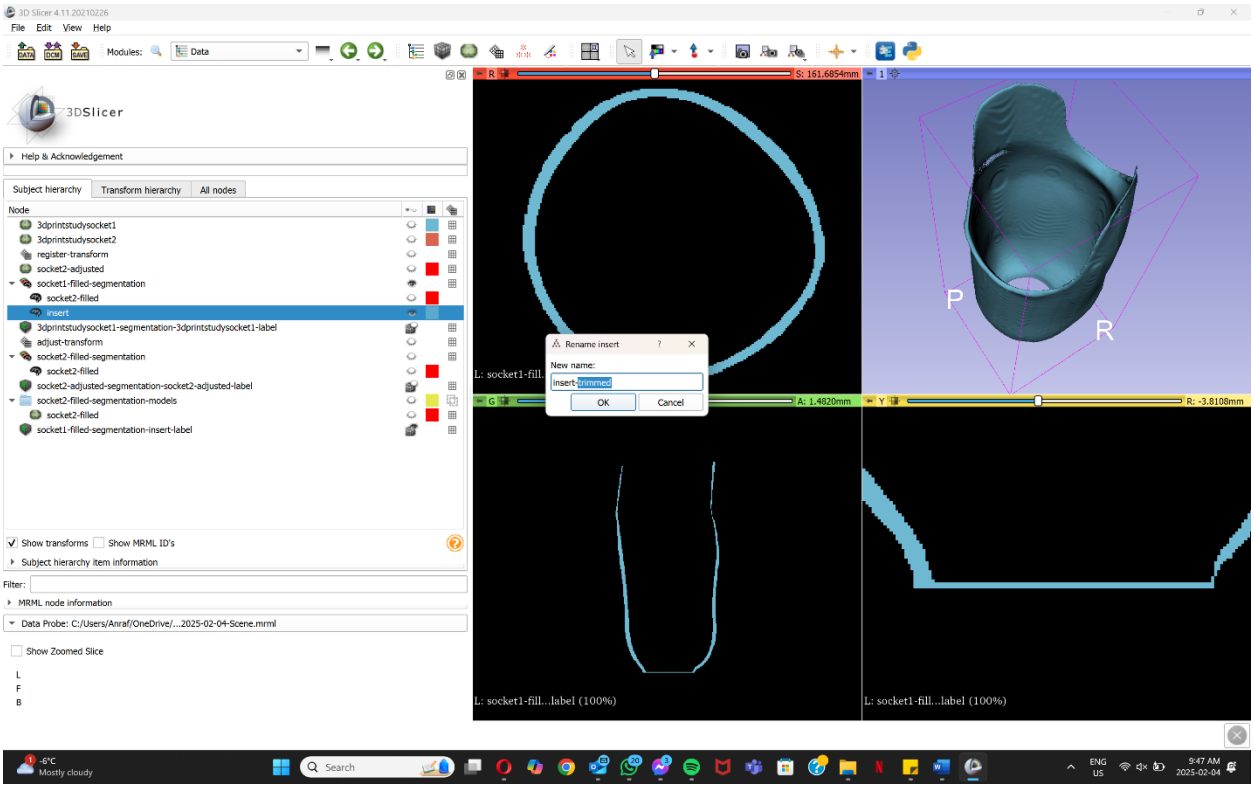

Step 5: Smooth model

- Convert new segment to model and export as an STL
    - Data tab → right click on trimmed segment → export visible segment to model
    - Save data → set file format of insert model to ‘STL’ → set directory as required → save
- Launch Fusion360
- Insert dropdown → insert mesh → find the insert model in the directory
- Mesh tab → modify dropdown → smooth → select the mesh → ok
- File → export

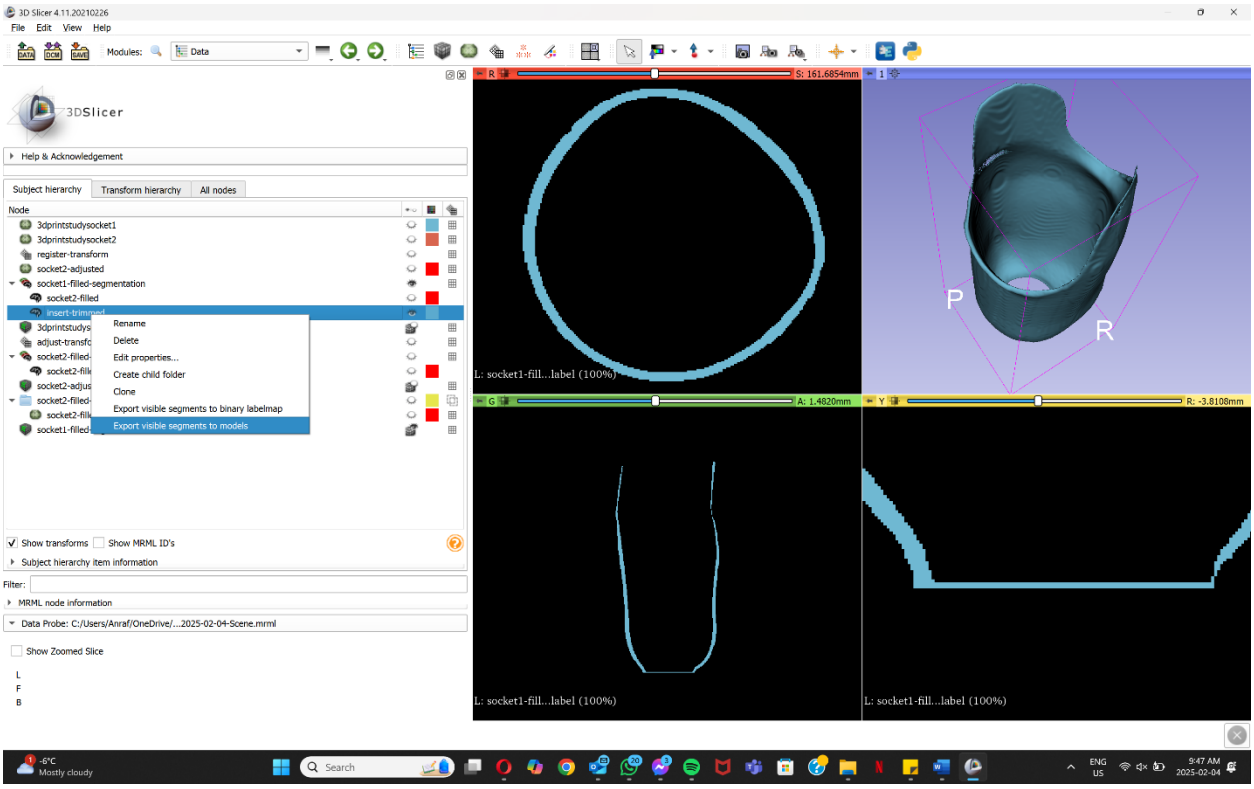
3D Slicer 4.11.20210226
File Edit View Help
Modules: Data
3DSlicer
Help & Acknowledgement
Subject hierarchy
Transform hierarchy
All nodes
Node
3dprintstudysocket1
3dprintstudysocket2
register-transform
socket2-adjusted
socket1-filled-segmentation
socket2-filled
insert-trimmed
Rename
Delete
Edit properties...
Create child folder
Clone
Export visible segments to binary labelmap
Export visible segments to models
Show transforms
Show MRML ID's
Subject hierarchy item information
Filter:
MRML node information
Data Probe: C:/Users/Anraf/OneDrive/...2025-02-04-Scene.mrml
Show Zoomed Slice
L
F
B
L: socket1-fill...label (100%)
P
R
Search
ENG
US
9:47 AM
2025-02-04

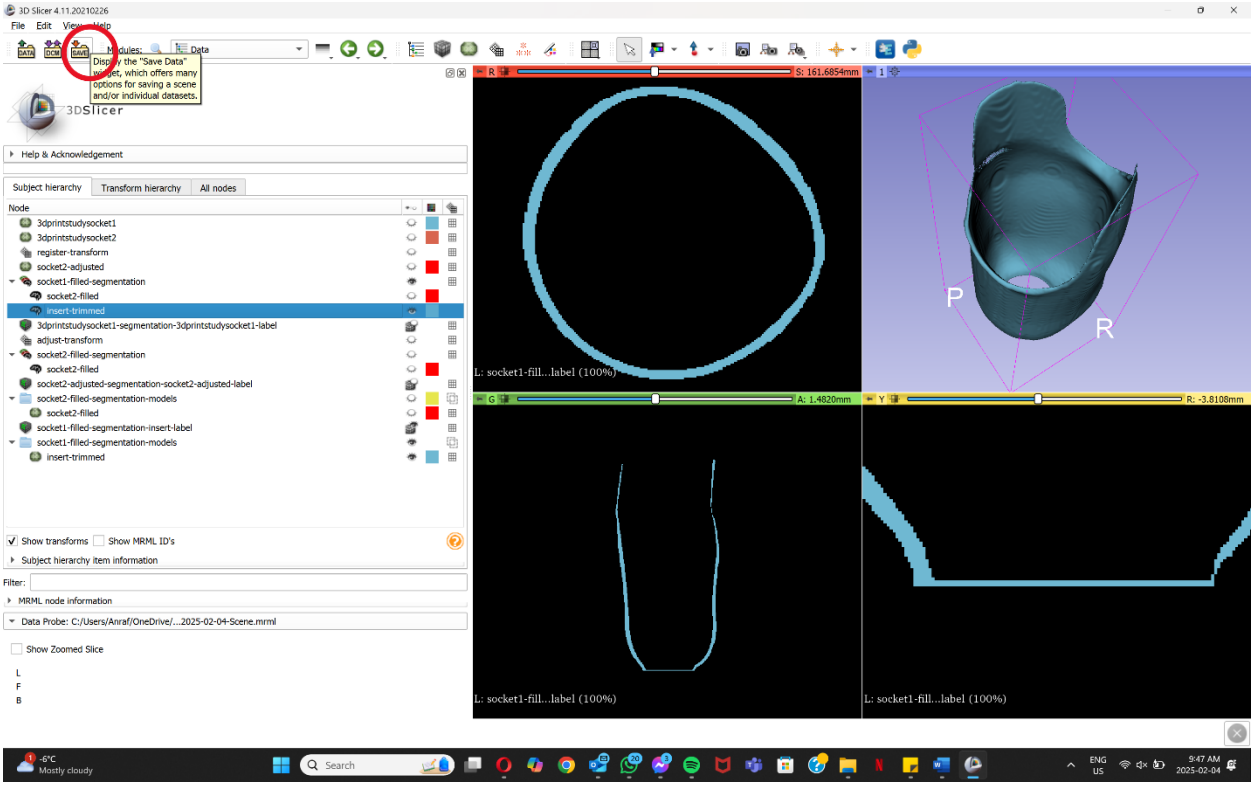
3D Slicer 4.11.20210226
File Edit View Help
Display the "Save Data" widget, which offers many options for saving a scene and/or individual datasets.
3DSlicer
Help & Acknowledgement
Subject hierarchy
Transform hierarchy
All nodes
Node
3dprintstudysocket1
3dprintstudysocket2
register-transform
socket2-adjusted
socket1-filled-segmentation
socket2-filled
insert-trimmed
3dprintstudysocket1-segmentation-3dprintstudysocket1-label
adjust-transform
socket2-filled-segmentation
socket2-filled
socket2-adjusted-segmentation-socket2-adjusted-label
socket2-filled-segmentation-models
socket2-filled
socket1-filled-segmentation-insert-label
socket1-filled-segmentation-models
insert-trimmed
Show transforms
Show MRML ID's
Subject hierarchy item information
Filter:
MRML node information
Data Probe: C:/Users/Anraf/OneDrive/...2025-02-04-Scene.mrml
Show Zoomed Slice
L
F
B
L: socket1-fill...label (100%)
P
R
Search
ENG
US
9:47 AM
2025-02-04

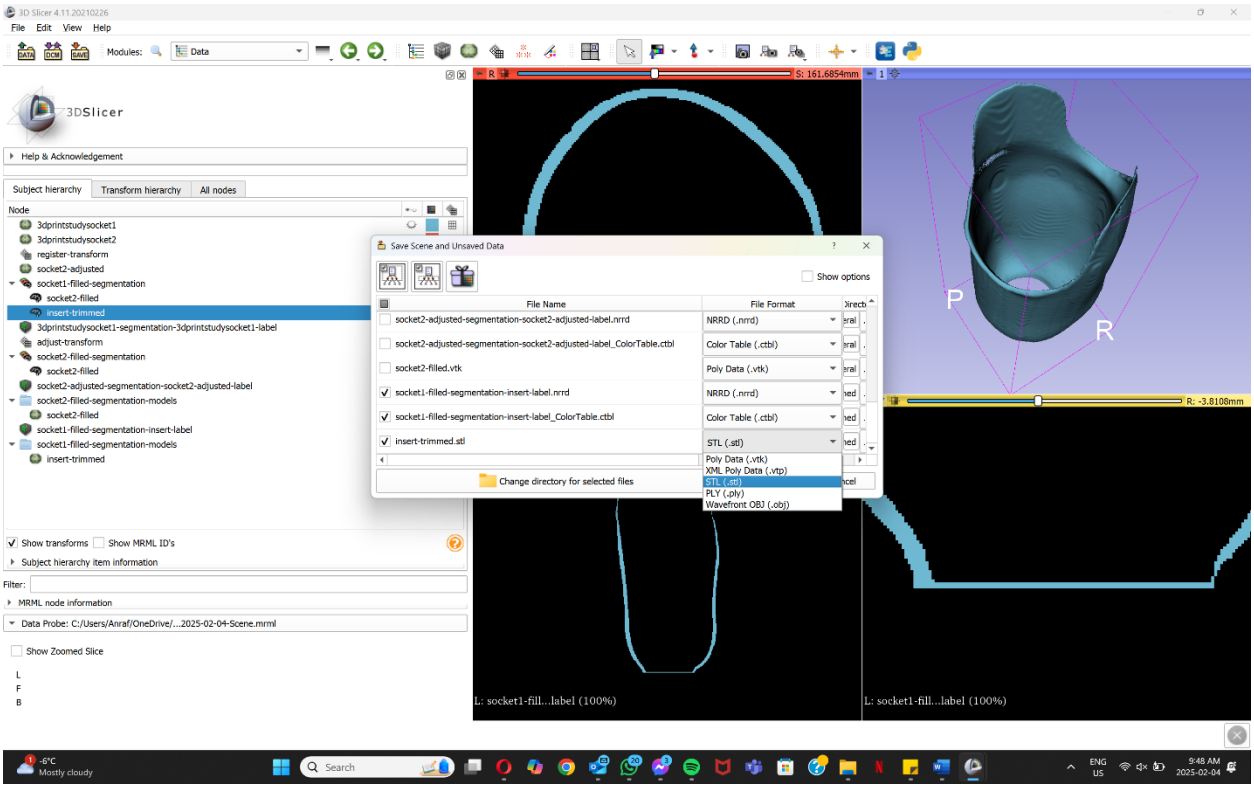
3D Slicer 4.11.20210226
File Edit View Help
Modules: Data
3DSlicer
Help & Acknowledgement
Subject hierarchy
Transform hierarchy
All nodes
Node
3dprintstudysocket1
3dprintstudysocket2
register-transform
socket2-adjusted
socket1-filled-segmentation
socket2-filled
insert-trimmed
3dprintstudysocket1-segmentation-3dprintstudysocket1-label
adjust-transform
socket2-filled-segmentation
socket2-filled
socket2-adjusted-segmentation-socket2-adjusted-label
socket2-filled-segmentation-models
socket2-filled
socket1-filled-segmentation-insert-label
socket1-filled-segmentation-models
insert-trimmed
Show transforms
Show MRML ID's
Subject hierarchy item information
Filter:
MRML node information
Data Probe: C:/Users/Anraf/OneDrive/...2025-02-04-Scene.mrml
Show Zoomed Slice
L
F
B
Save Scene and Unsaved Data
Show options
File Name
File Format
socket2-adjusted-segmentation-socket2-adjusted-label.nrrd
NRRD (.nrrd)
socket2-adjusted-segmentation-socket2-adjusted-label_ColorTable.ctbl
Color Table (.ctbl)
socket2-filled.vtk
Poly Data (.vtk)
socket1-filled-segmentation-insert-label.nrrd
NRRD (.nrrd)
socket1-filled-segmentation-insert-label_ColorTable.ctbl
Color Table (.ctbl)
insert-trimmed.stl
STL (.stl)
Poly Data (.vtk)
XML Poly Data (.vtp)
STL (.stl)
PLY (.ply)
Wavefront OBJ (.obj)
Change directory for selected files
S: 161.6854mm
R: -3.8108mm
P
R
L: socket1-fill...label (100%)
L: socket1-fill...label (100%)
-6°C
Mostly cloudy
Search
ENG
US
9:48 AM
2025-02-04

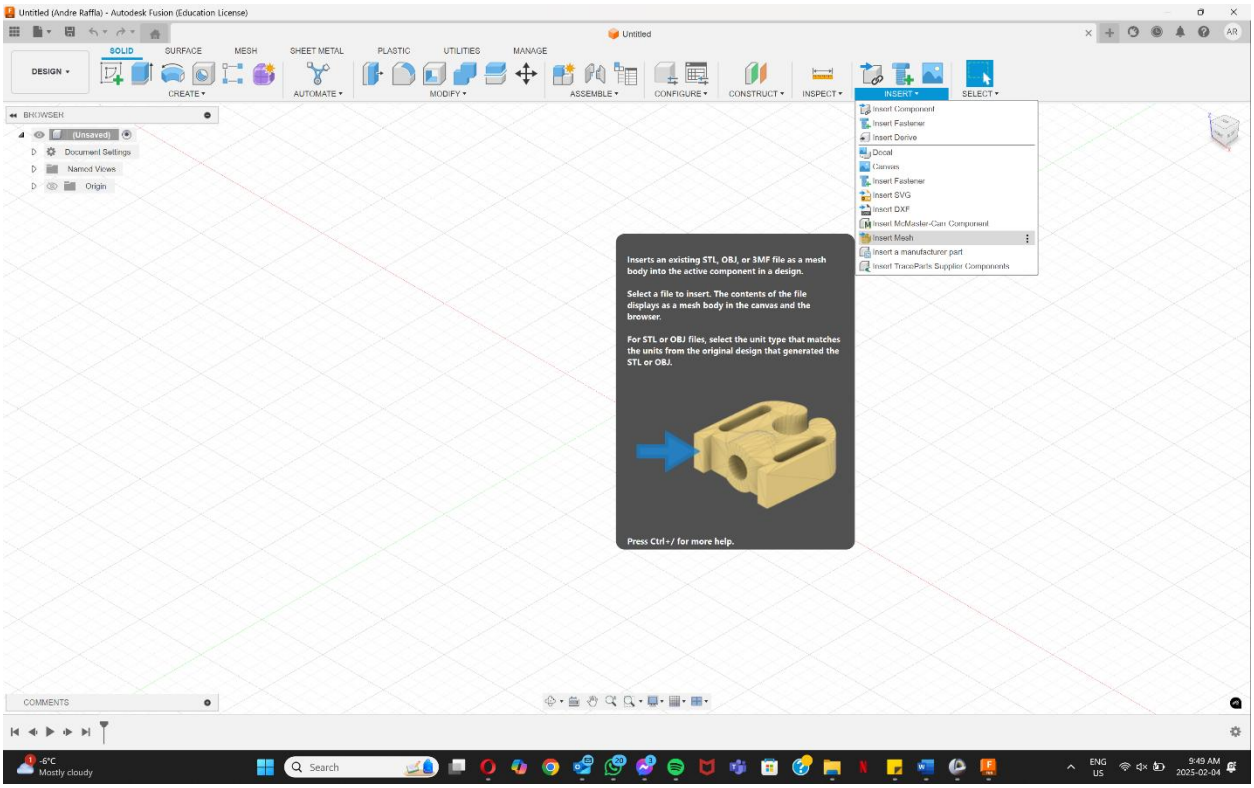
Untitled (Andre Raffla) - Autodesk Fusion (Education License)
Untitled
DESIGN
SOLID
SURFACE
MESH
SHEET METAL
PLASTIC
UTILITIES
MANAGE
CREATE
AUTOMATE
MODIFY
ASSEMBLE
CONFIGURE
CONSTRUCT
INSPECT
INSERT
SELECT
BROWSER
(Unsaved)
Document Settings
Named Views
Origin
Insert Component
Insert Fastener
Insert Derive
Decal
Canvas
Insert Fastener
Insert SVG
Insert DXF
Insert McMaster-Carr Component
Insert Mesh
Insert a manufacturer part
Insert TraceParts Supplier Components
Inserts an existing STL, OBJ, or 3MF file as a mesh body into the active component in a design.
Select a file to insert. The contents of the file displays as a mesh body in the canvas and the browser.
For STL or OBJ files, select the unit type that matches the units from the original design that generated the STL or OBJ.
Press Ctrl+/ for more help.
COMMENTS
-6°C
Mostly cloudy
Search
ENG
US
9:49 AM
2025-02-04

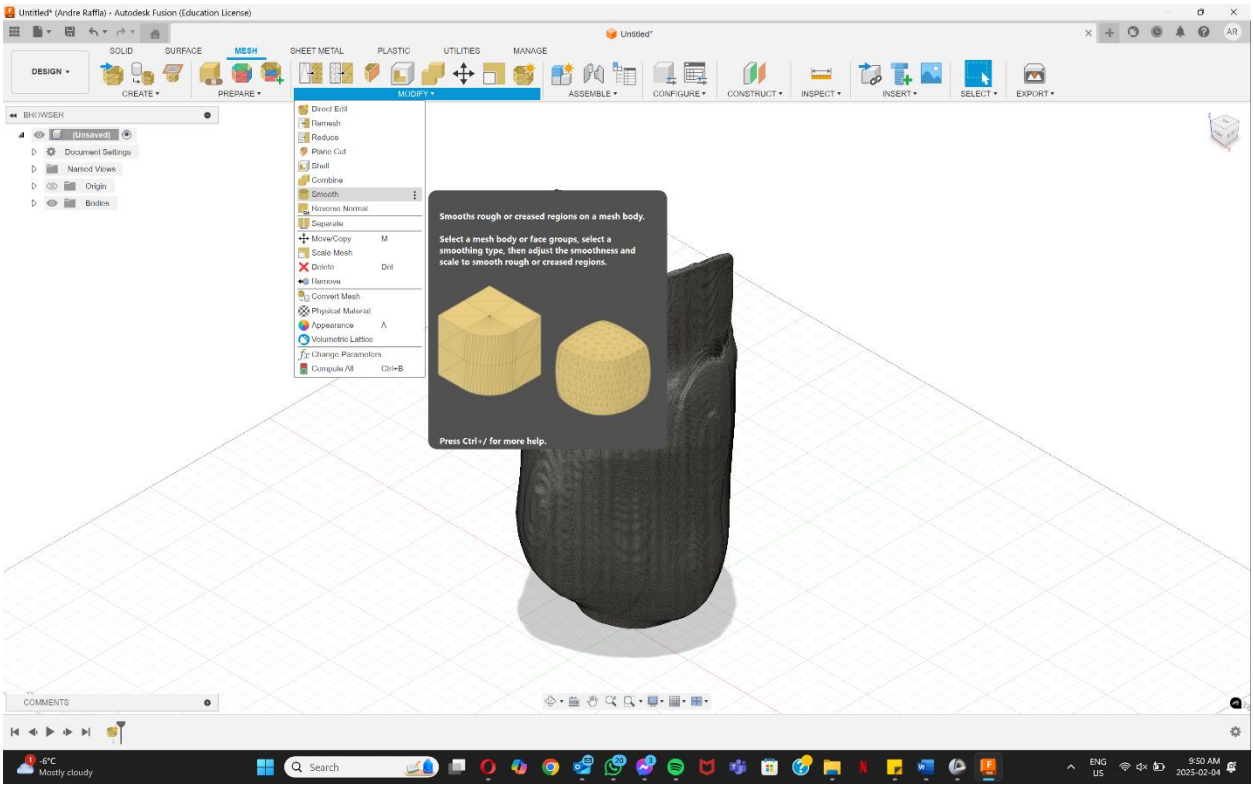
Untitled* (Andre Raffla) - Autodesk Fusion (Education License)
Untitled*
SOLID
SURFACE
MESH
SHEET METAL
PLASTIC
UTILITIES
MANAGE
DESIGN
CREATE
PREPARE
MODIFY
ASSEMBLE
CONFIGURE
CONSTRUCT
INSPECT
INSERT
SELECT
EXPORT
BROWSER
(Unsaved)
Document Settings
Named Views
Origin
Bodies
Direct Edit
Remesh
Reduce
Plane Cut
Shell
Combine
Smooth
Reverse Normal
Separate
Move/Copy M
Scale Mesh
Delete Del
Remove
Convert Mesh
Physical Material
Appearance A
Volumetric Lattice
Change Parameters
Compute All Ctrl+B
Smooths rough or creased regions on a mesh body.
Select a mesh body or face groups, select a smoothing type, then adjust the smoothness and scale to smooth rough or creased regions.
Press Ctrl+/ for more help.
COMMENTS
-6°C
Mostly cloudy
Search
ENG
US
9:50 AM
2025-02-04

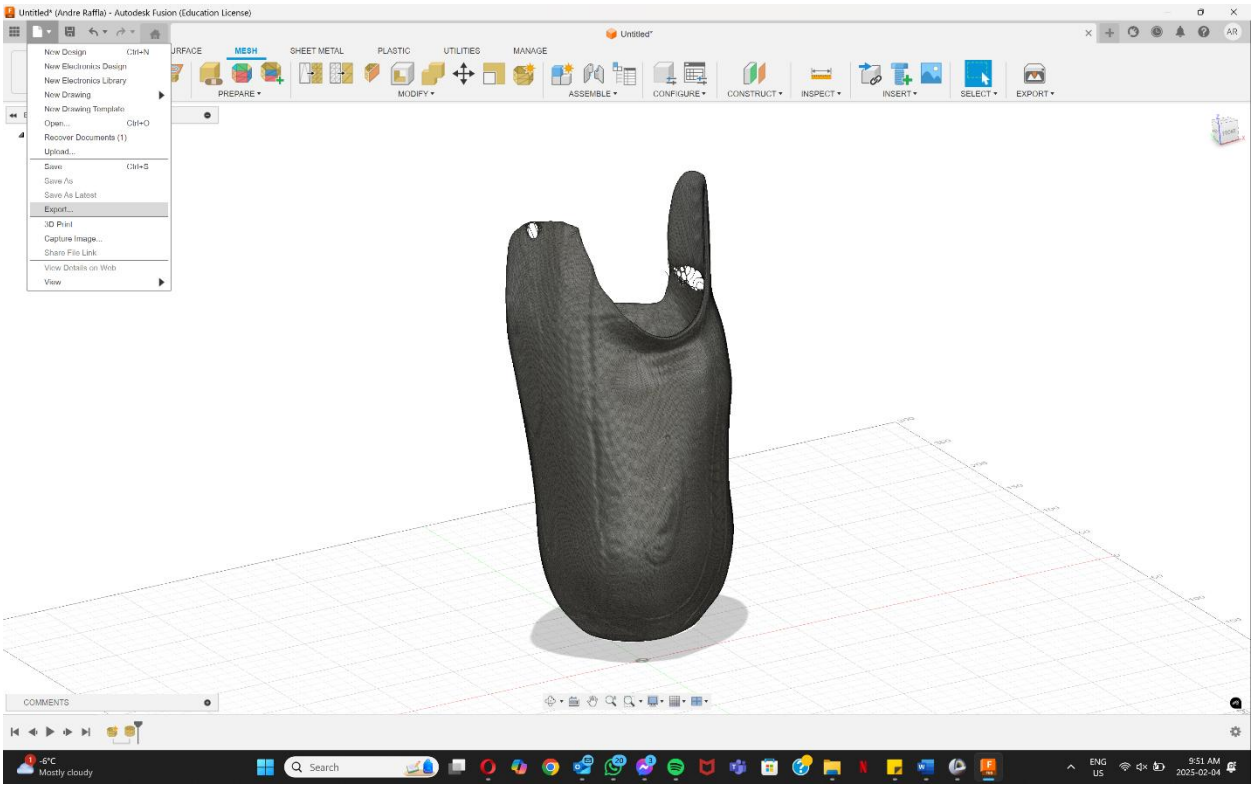
Untitled* (Andre Raffla) - Autodesk Fusion (Education License)
Untitled*
New Design Ctrl+N
New Electronics Design
New Electronics Library
New Drawing
New Drawing Template
Open... Ctrl+O
Recover Documents (1)
Upload...
Save Ctrl+S
Save As
Save As Latest
Export...
3D Print
Capture Image...
Share File Link
View Details on Web
View
MESH
PREPARE
MODIFY
ASSEMBLE
CONFIGURE
CONSTRUCT
INSPECT
INSERT
SELECT
EXPORT
COMMENTS
-6°C
Mostly cloudy
Search
ENG
US
9:51 AM
2025-02-04

Fiducial (Landmark) Registration

- Go to registration tab → CMF registration (ensure CMFreg extension is installed and enabled) → surface registration
    - Set type of registration to ‘fiducial registration’
    - Set fixed model to model1
    - Set moving model to model2
    - Set fixed landmarks list to ‘create new markupsfiducial as’ → ‘insert markups name’
    - Set moving landmarks list to ‘create new markupsfiducial as’ → ‘insert markups name’
    - Use the ‘add landmark’ drop down to place landmarks for both moving and fixed models
    - Output transfer → create new linear transfer as → ‘insert transform name’
    - Output model → create new model as → ‘insert model name’ (socket2-registered)
    - Compute → apply

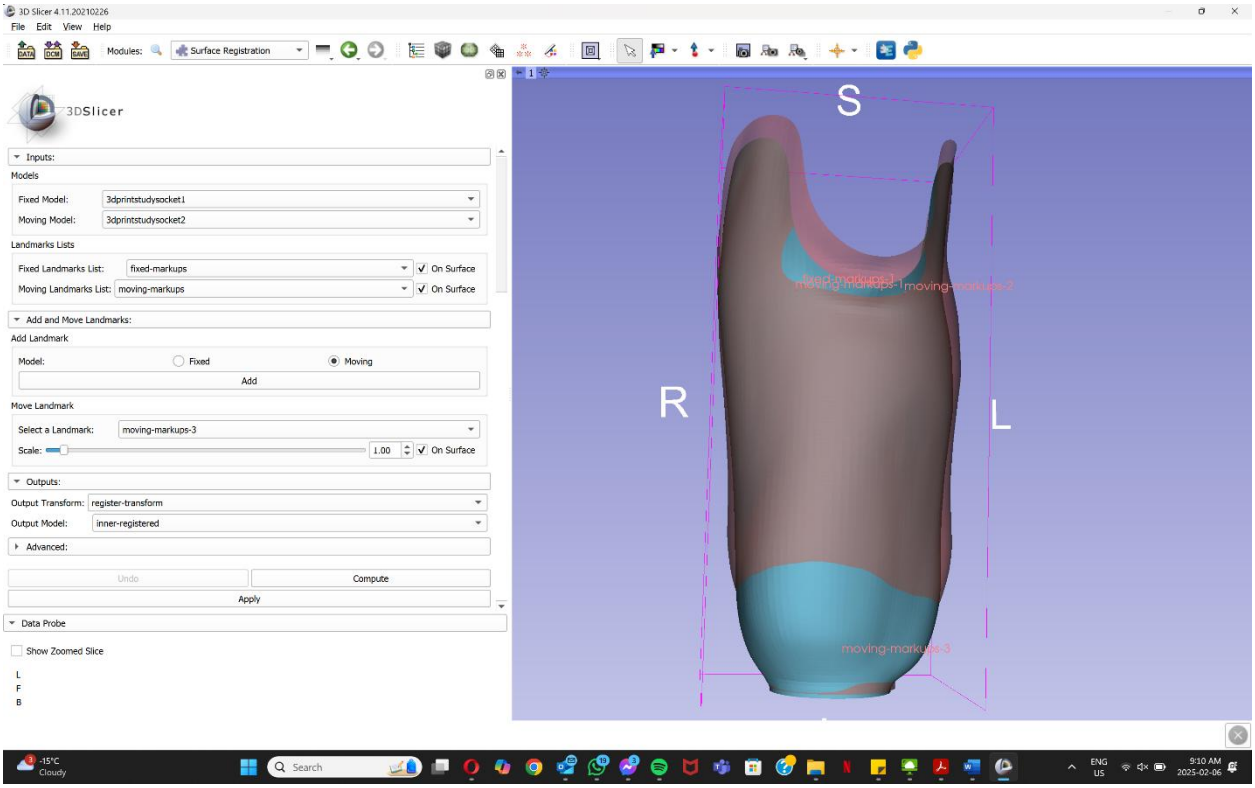

Filling Holes

- Data tab → right click on model 1 (larger model) → convert to segmentation node → right click on segmentation → convert to binary labelmaps
- Create a shell of the outside layer with a thickness of 0.7 mm
    - Segment editor tab
        - set segmentation to model 1 segmentation
        - set master volume to model 1 binary labelmap
        - set effects to hollow
        - set current segment as outside
        - set shell thickness to 0.7 mm
        - apply
- Data tab → right click on model 1 segmentation → rename → 'insert new segment name' (model 1 - hollow)
- Data tab → right click on model 1 – hollow segmentation → export visible segments to model
- Segmentation tab
    - set active segmentation to insert segmentation
    - set operation to import
    - set input type to model
    - set input node to model 1 – hollow
    - import
- Add the two segments to each other
    - Segment editor tab → set segmentation to folder with both segments → set master volume to model1 binary labelmap → logical operators → set operation to add → apply
        - Ensure that the insert model segment is selected in the top view while the model 1 - hollow segment is selected in the 'add segment' view

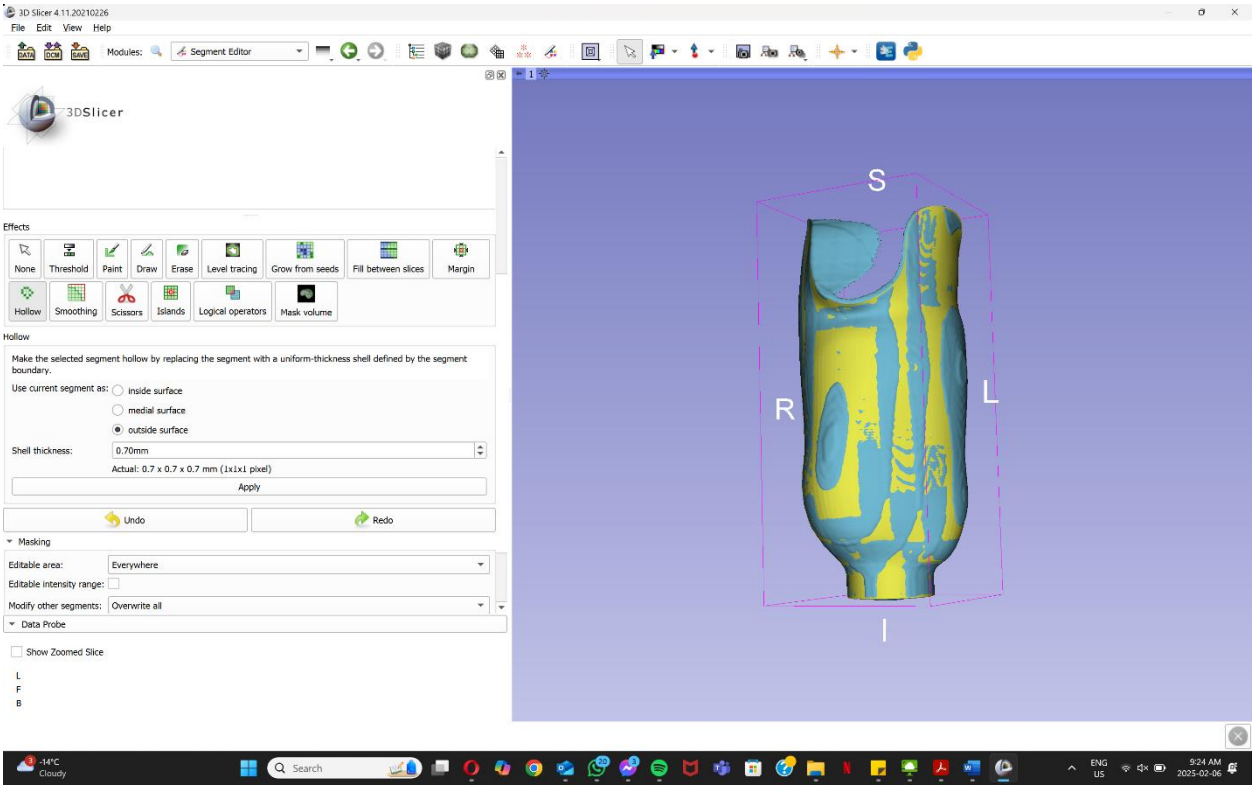
3D Slicer 4.11.20210226
File Edit View Help
Modules: Segment Editor
3DSlicer
Effects
None Threshold Paint Draw Erase Level tracing Grow from seeds Fill between slices Margin
Hollow Smoothing Scissors Islands Logical operators Mask volume
Hollow
Make the selected segment hollow by replacing the segment with a uniform-thickness shell defined by the segment boundary.
Use current segment as: inside surface
medial surface
outside surface
Shell thickness: 0.70mm
Actual: 0.7 x 0.7 x 0.7 mm (1x1x1 pixel)
Apply
Undo Redo
Masking
Editable area: Everywhere
Editable intensity range:
Modify other segments: Overwrite all
Data Probe
Show Zoomed Slice
L
F
B
S
R
L
I
-14°C Cloudy
Search
ENG US
9:24 AM 2025-02-06

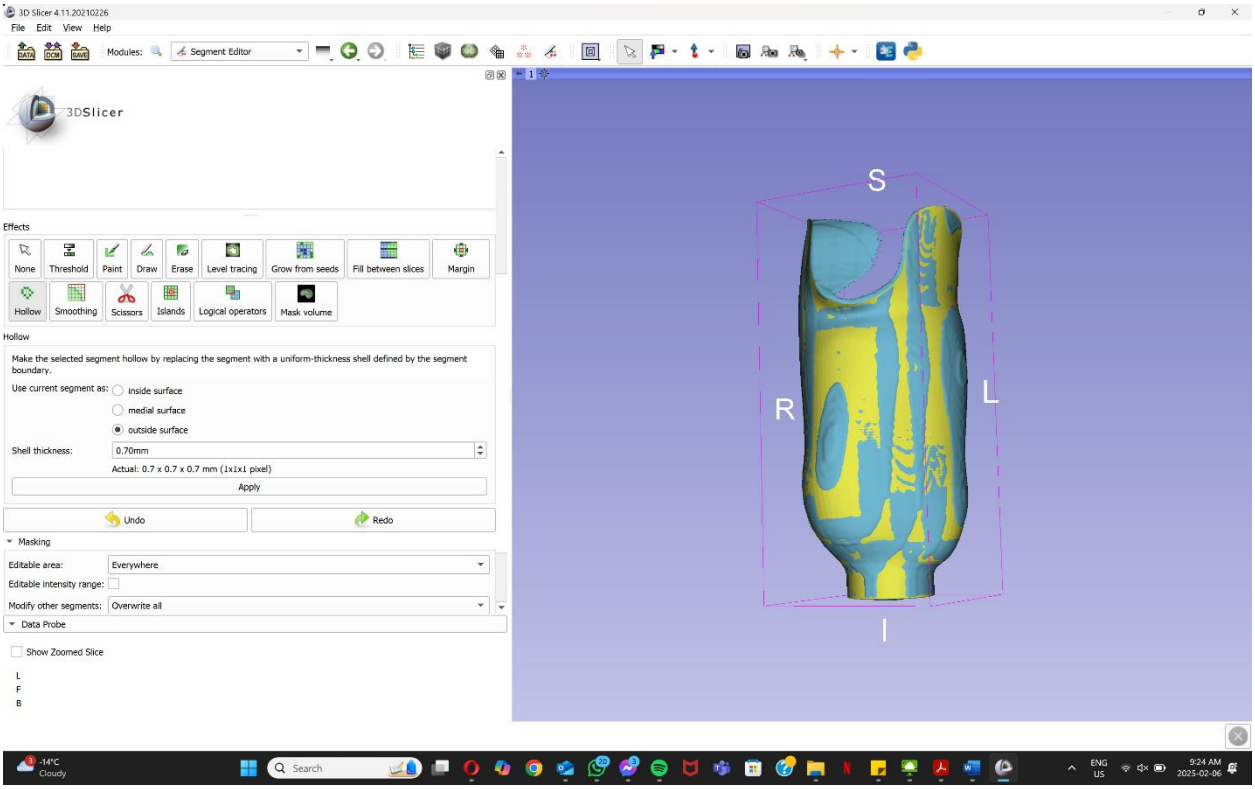
3D Slicer 4.11.20210226
File Edit View Help
Modules: Segment Editor
3DSlicer
Effects
None Threshold Paint Draw Erase Level tracing Grow from seeds Fill between slices Margin
Hollow Smoothing Scissors Islands Logical operators Mask volume
Hollow
Make the selected segment hollow by replacing the segment with a uniform-thickness shell defined by the segment boundary.
Use current segment as: inside surface
medial surface
outside surface
Shell thickness: 0.70mm
Actual: 0.7 x 0.7 x 0.7 mm (1x1x1 pixel)
Apply
Undo Redo
Masking
Editable area: Everywhere
Editable intensity range:
Modify other segments: Overwrite all
Data Probe
Show Zoomed Slice
L
F
B
S
R
L
I
-14°C Cloudy
Search
ENG US
9:24 AM 2025-02-06

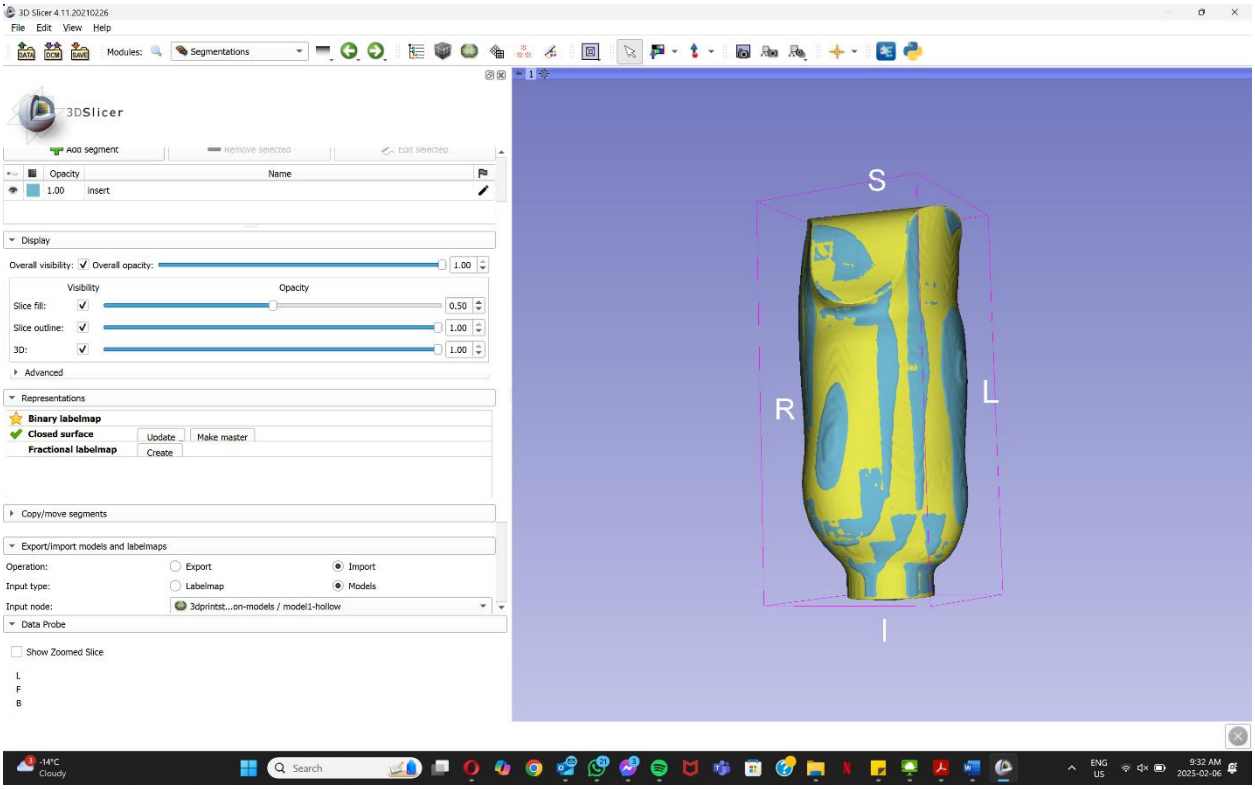
3D Slicer 4.11.20210226
File Edit View Help
Modules: Segmentations
3DSlicer
Add segment
Remove selected
Edit selected
Opacity
Name
1.00
insert
Display
Overall visibility:
Overall opacity:
1.00
Visibility
Opacity
Slice fill:
0.50
Slice outline:
1.00
3D:
1.00
Advanced
Representations
Binary labelmap
Closed surface
Fractional labelmap
Update
Make master
Create
Copy/move segments
Export/import models and labelmaps
Operation:
Export
Import
Input type:
Labelmap
Models
Input node:
3dprintst...on-models / model1-hollow
Data Probe
Show Zoomed Slice
L
F
B
S
R
L
I
-14°C
Cloudy
Search
ENG
US
9:32 AM
2025-02-06

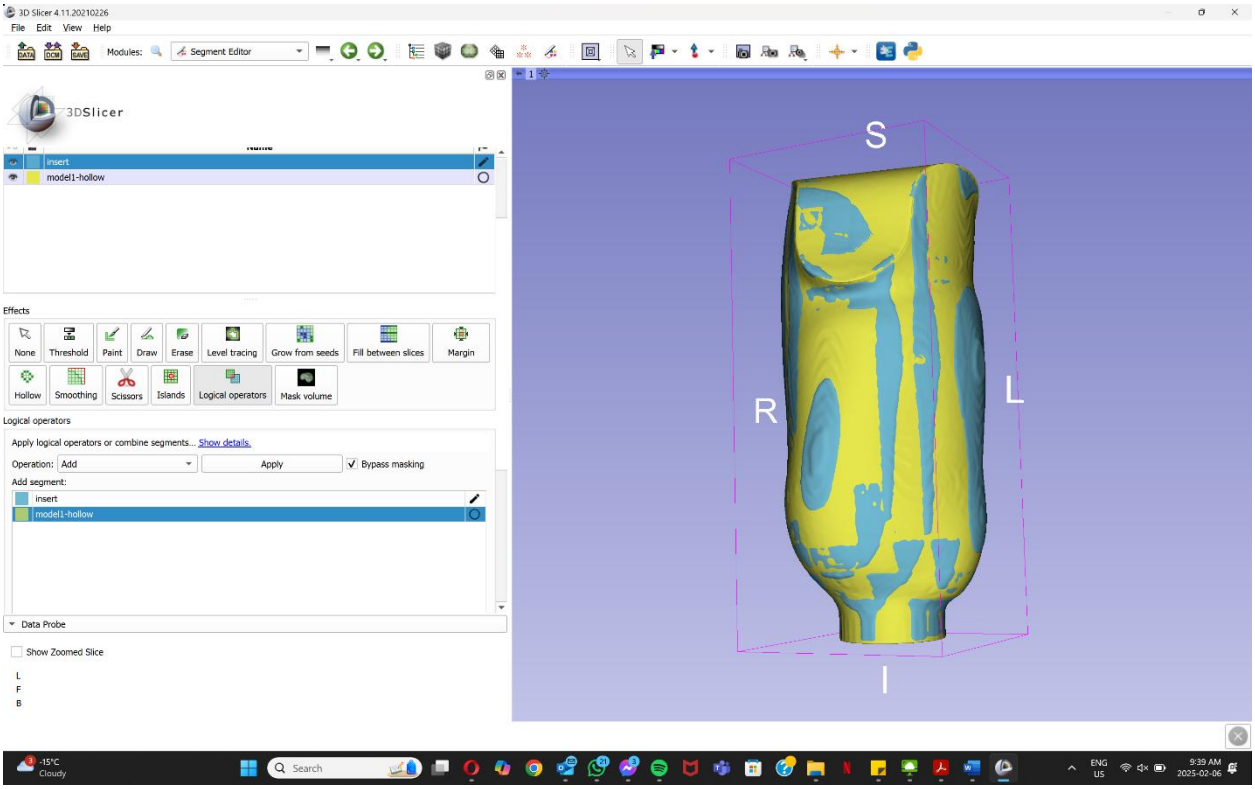
3D Slicer 4.11.20210226
File Edit View Help
Modules: Segment Editor
3DSlicer
insert
model1-hollow
Effects
None
Threshold
Paint
Draw
Erase
Level tracing
Grow from seeds
Fill between slices
Margin
Hollow
Smoothing
Scissors
Islands
Logical operators
Mask volume
Logical operators
Apply logical operators or combine segments... Show details.
Operation: Add
Apply
Bypass masking
Add segment:
insert
model1-hollow
Data Probe
Show Zoomed Slice
L
F
B
S
R
L
I
-15°C
Cloudy
Search
ENG
US
9:39 AM
2025-02-06

Appendix B: 3D Print Settings

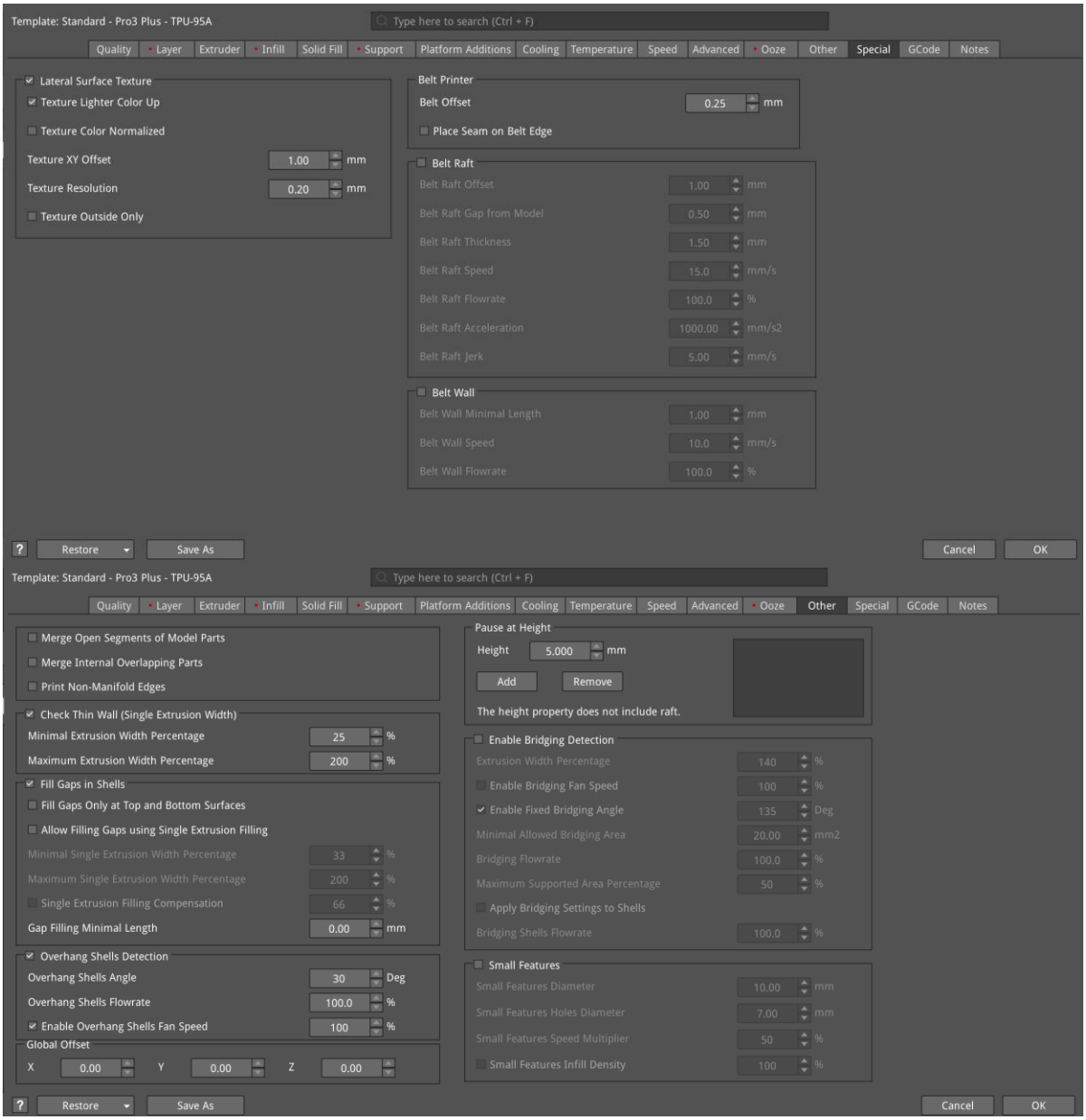

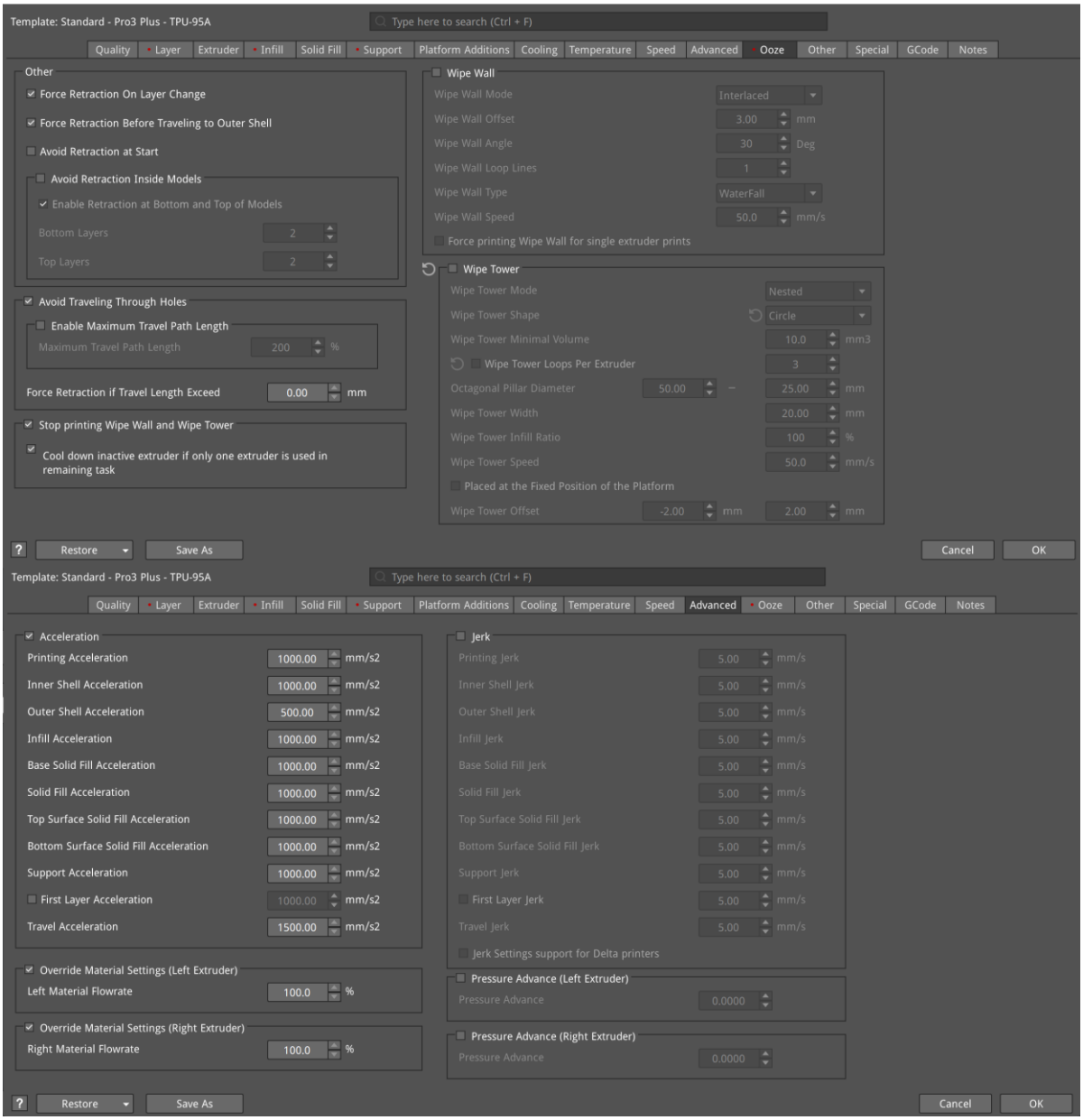
Template: Standard - Pro3 Plus - TPU-95A
Type here to search (Ctrl + F)
Quality
Layer
Extruder
Infill
Solid Fill
Support
Platform Additions
Cooling
Temperature
Speed
Advanced
Ooze
Other
Special
GCode
Notes
Other
Force Retraction On Layer Change
Force Retraction Before Traveling to Outer Shell
Avoid Retraction at Start
Avoid Retraction Inside Models
Enable Retraction at Bottom and Top of Models
Bottom Layers
Top Layers
Avoid Traveling Through Holes
Enable Maximum Travel Path Length
Maximum Travel Path Length
Force Retraction if Travel Length Exceed
Stop printing Wipe Wall and Wipe Tower
Cool down inactive extruder if only one extruder is used in remaining task
Wipe Wall
Wipe Wall Mode
Interlaced
Wipe Wall Offset
Wipe Wall Angle
Wipe Wall Loop Lines
Wipe Wall Type
WaterFall
Wipe Wall Speed
Force printing Wipe Wall for single extruder prints
Wipe Tower
Wipe Tower Mode
Nested
Wipe Tower Shape
Circle
Wipe Tower Minimal Volume
Wipe Tower Loops Per Extruder
Octagonal Pillar Diameter
Wipe Tower Width
Wipe Tower Infill Ratio
Wipe Tower Speed
Placed at the Fixed Position of the Platform
Wipe Tower Offset
Restore
Save As
Cancel
OK
Template: Standard - Pro3 Plus - TPU-95A
Type here to search (Ctrl + F)
Quality
Layer
Extruder
Infill
Solid Fill
Support
Platform Additions
Cooling
Temperature
Speed
Advanced
Ooze
Other
Special
GCode
Notes
Acceleration
Printing Acceleration
Inner Shell Acceleration
Outer Shell Acceleration
Infill Acceleration
Base Solid Fill Acceleration
Solid Fill Acceleration
Top Surface Solid Fill Acceleration
Bottom Surface Solid Fill Acceleration
Support Acceleration
First Layer Acceleration
Travel Acceleration
Override Material Settings (Left Extruder)
Left Material Flowrate
Override Material Settings (Right Extruder)
Right Material Flowrate
Jerk
Printing Jerk
Inner Shell Jerk
Outer Shell Jerk
Infill Jerk
Base Solid Fill Jerk
Solid Fill Jerk
Top Surface Solid Fill Jerk
Bottom Surface Solid Fill Jerk
Support Jerk
First Layer Jerk
Travel Jerk
Jerk Settings support for Delta printers
Pressure Advance (Left Extruder)
Pressure Advance
Pressure Advance (Right Extruder)
Pressure Advance
Restore
Save As
Cancel
OK

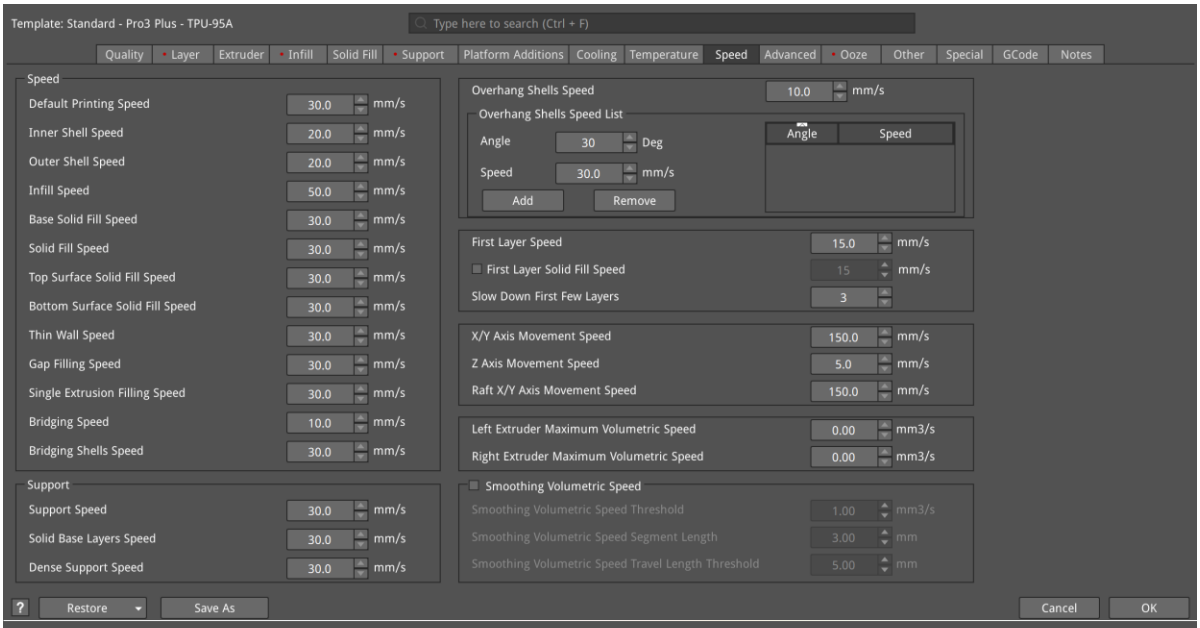
Template: Standard - Pro3 Plus - TPU-95A
Type here to search (Ctrl + F)
Quality
Layer
Extruder
Infill
Solid Fill
Support
Platform Additions
Cooling
Temperature
Speed
Advanced
Ooze
Other
Special
GCode
Notes
Speed
Default Printing Speed 30.0 mm/s
Inner Shell Speed 20.0 mm/s
Outer Shell Speed 20.0 mm/s
Infill Speed 50.0 mm/s
Base Solid Fill Speed 30.0 mm/s
Solid Fill Speed 30.0 mm/s
Top Surface Solid Fill Speed 30.0 mm/s
Bottom Surface Solid Fill Speed 30.0 mm/s
Thin Wall Speed 30.0 mm/s
Gap Filling Speed 30.0 mm/s
Single Extrusion Filling Speed 30.0 mm/s
Bridging Speed 10.0 mm/s
Bridging Shells Speed 30.0 mm/s
Support
Support Speed 30.0 mm/s
Solid Base Layers Speed 30.0 mm/s
Dense Support Speed 30.0 mm/s
Overhang Shells Speed 10.0 mm/s
Overhang Shells Speed List
Angle 30 Deg
Speed 30.0 mm/s
Add
Remove
Angle
Speed
First Layer Speed 15.0 mm/s
First Layer Solid Fill Speed 15 mm/s
Slow Down First Few Layers 3
X/Y Axis Movement Speed 150.0 mm/s
Z Axis Movement Speed 5.0 mm/s
Raft X/Y Axis Movement Speed 150.0 mm/s
Left Extruder Maximum Volumetric Speed 0.00 mm3/s
Right Extruder Maximum Volumetric Speed 0.00 mm3/s
Smoothing Volumetric Speed
Smoothing Volumetric Speed Threshold 1.00 mm3/s
Smoothing Volumetric Speed Segment Length 3.00 mm
Smoothing Volumetric Speed Travel Length Threshold 5.00 mm
Restore
Save As
Cancel
OK

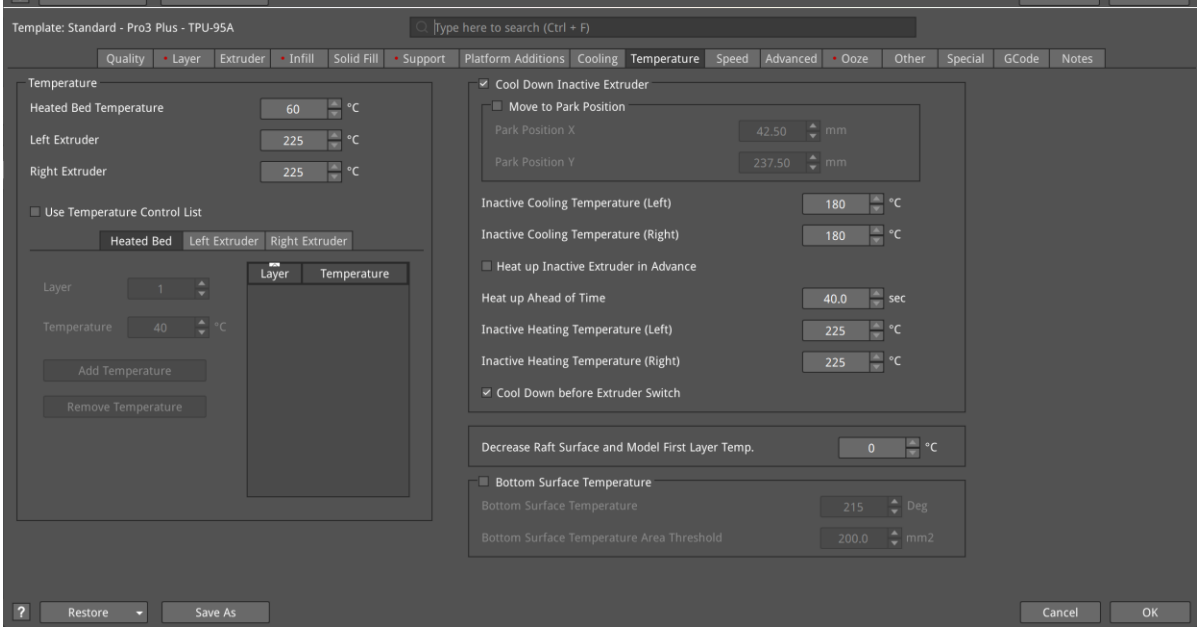
Template: Standard - Pro3 Plus - TPU-95A
Type here to search (Ctrl + F)
Quality
Layer
Extruder
Infill
Solid Fill
Support
Platform Additions
Cooling
Temperature
Speed
Advanced
Ooze
Other
Special
GCode
Notes
Temperature
Heated Bed Temperature 60 °C
Left Extruder 225 °C
Right Extruder 225 °C
Use Temperature Control List
Heated Bed
Left Extruder
Right Extruder
Layer
Temperature
Layer 1
Temperature 40 °C
Add Temperature
Remove Temperature
Cool Down Inactive Extruder
Move to Park Position
Park Position X 42.50 mm
Park Position Y 237.50 mm
Inactive Cooling Temperature (Left) 180 °C
Inactive Cooling Temperature (Right) 180 °C
Heat up Inactive Extruder in Advance
Heat up Ahead of Time 40.0 sec
Inactive Heating Temperature (Left) 225 °C
Inactive Heating Temperature (Right) 225 °C
Cool Down before Extruder Switch
Decrease Raft Surface and Model First Layer Temp. 0 °C
Bottom Surface Temperature
Bottom Surface Temperature 215 Deg
Bottom Surface Temperature Area Threshold 200.0 mm2
Restore
Save As
Cancel
OK

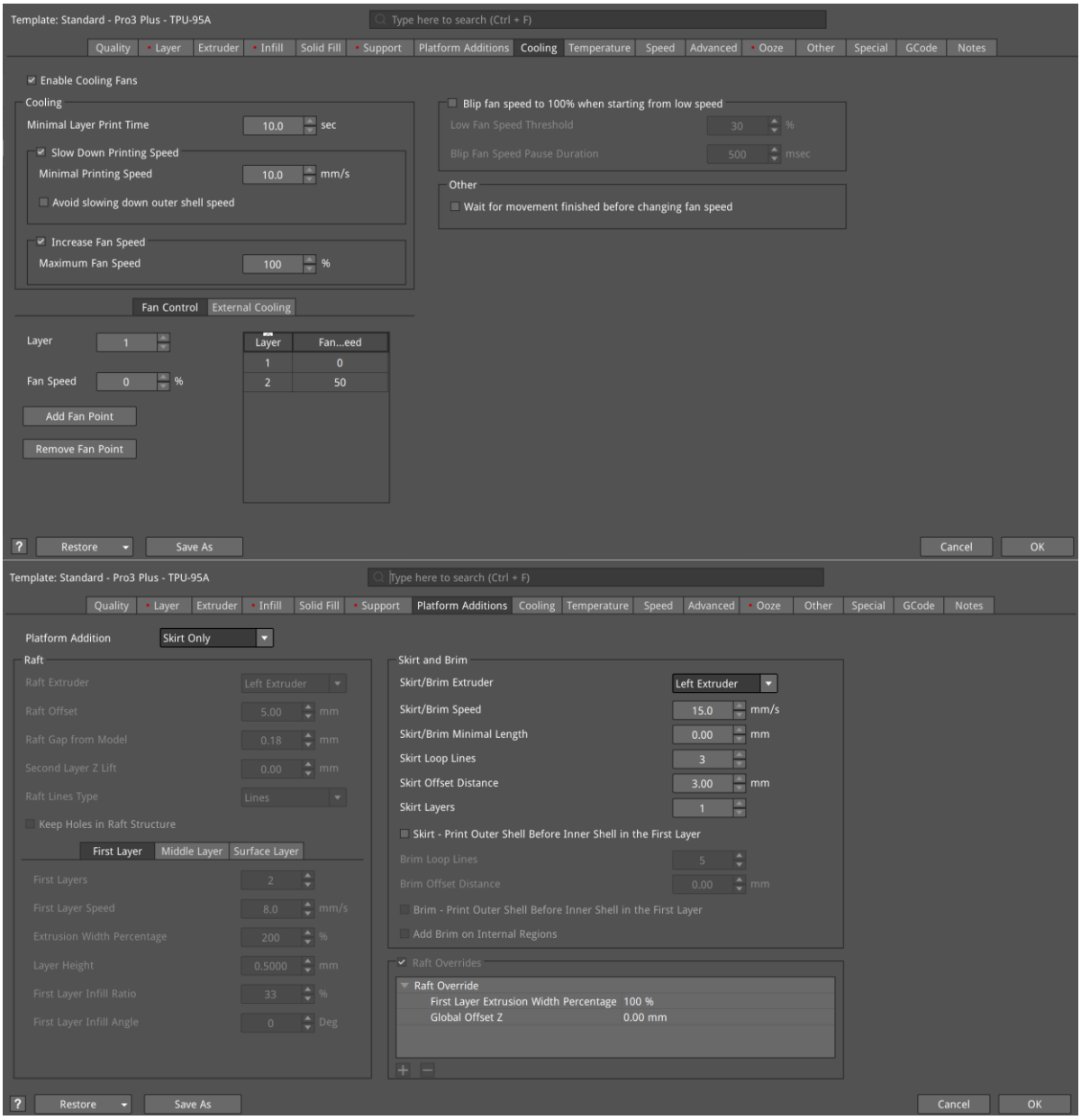
Template: Standard - Pro3 Plus - TPU-95A
Type here to search (Ctrl + F)
Quality
Layer
Extruder
Infill
Solid Fill
Support
Platform Additions
Cooling
Temperature
Speed
Advanced
Ooze
Other
Special
GCode
Notes
Enable Cooling Fans
Cooling
Minimal Layer Print Time
10.0
sec
Slow Down Printing Speed
Minimal Printing Speed
10.0
mm/s
Avoid slowing down outer shell speed
Increase Fan Speed
Maximum Fan Speed
100
%
Blip fan speed to 100% when starting from low speed
Low Fan Speed Threshold
30
%
Blip Fan Speed Pause Duration
500
msec
Other
Wait for movement finished before changing fan speed
Fan Control
External Cooling
Layer
1
Fan Speed
0
%
Add Fan Point
Remove Fan Point
Layer
Fan...eed
1
0
2
50
Restore
Save As
Cancel
OK
Template: Standard - Pro3 Plus - TPU-95A
Type here to search (Ctrl + F)
Quality
Layer
Extruder
Infill
Solid Fill
Support
Platform Additions
Cooling
Temperature
Speed
Advanced
Ooze
Other
Special
GCode
Notes
Platform Addition
Skirt Only
Raft
Raft Extruder
Left Extruder
Raft Offset
5.00
mm
Raft Gap from Model
0.18
mm
Second Layer Z Lift
0.00
mm
Raft Lines Type
Lines
Keep Holes in Raft Structure
First Layer
Middle Layer
Surface Layer
First Layers
2
First Layer Speed
8.0
mm/s
Extrusion Width Percentage
200
%
Layer Height
0.5000
mm
First Layer Infill Ratio
33
%
First Layer Infill Angle
0
Deg
Skirt and Brim
Skirt/Brim Extruder
Left Extruder
Skirt/Brim Speed
15.0
mm/s
Skirt/Brim Minimal Length
0.00
mm
Skirt Loop Lines
3
Skirt Offset Distance
3.00
mm
Skirt Layers
1
Skirt - Print Outer Shell Before Inner Shell in the First Layer
Brim Loop Lines
5
Brim Offset Distance
0.00
mm
Brim - Print Outer Shell Before Inner Shell in the First Layer
Add Brim on Internal Regions
Raft Overrides
Raft Override
First Layer Extrusion Width Percentage
100 %
Global Offset Z
0.00 mm
Restore
Save As
Cancel
OK

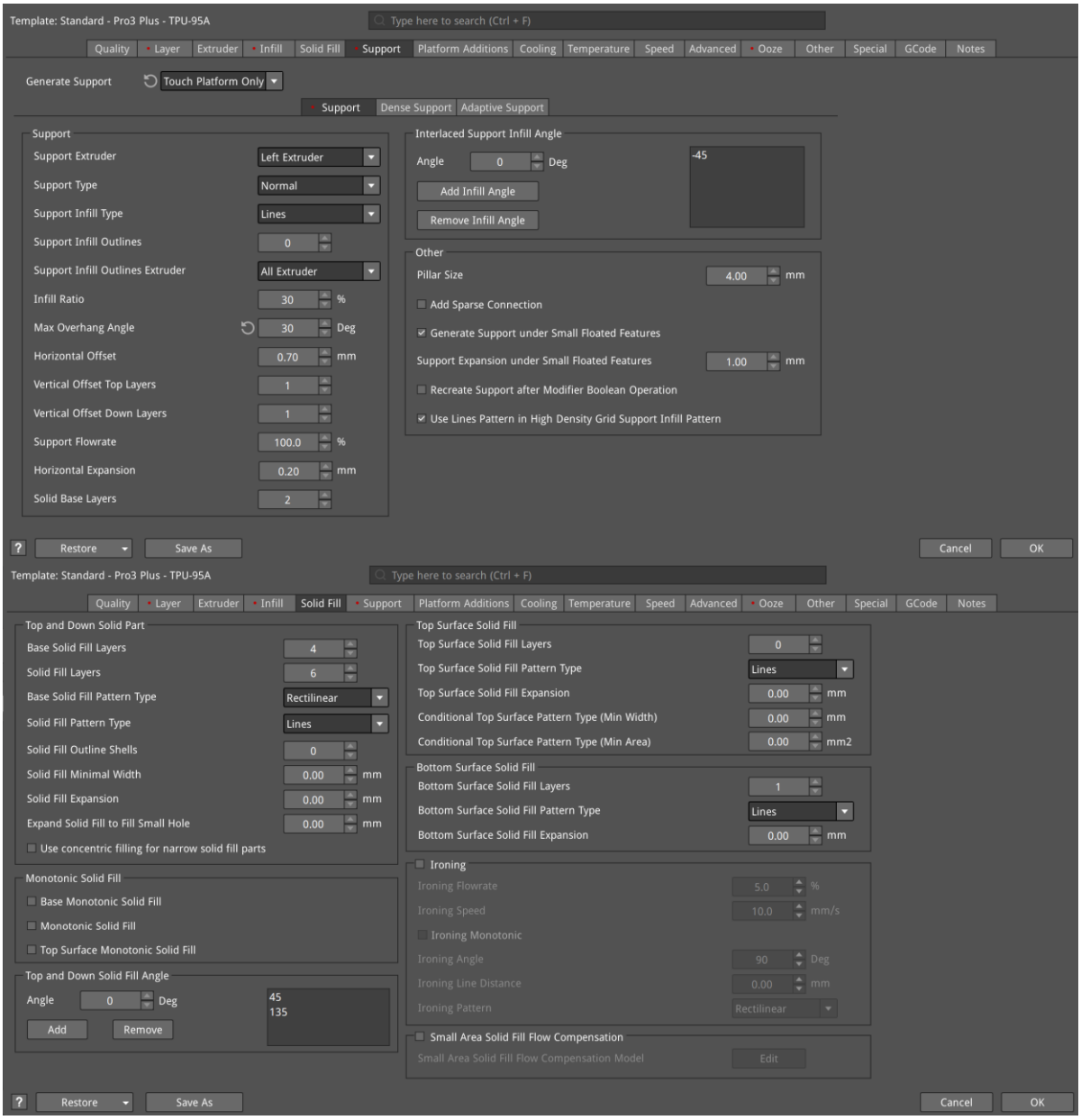
Template: Standard - Pro3 Plus - TPU-95A
Type here to search (Ctrl + F)
Quality
Layer
Extruder
Infill
Solid Fill
Support
Platform Additions
Cooling
Temperature
Speed
Advanced
Ooze
Other
Special
GCode
Notes
Generate Support
Touch Platform Only
Support
Dense Support
Adaptive Support
Support
Support Extruder
Left Extruder
Support Type
Normal
Support Infill Type
Lines
Support Infill Outlines
0
Support Infill Outlines Extruder
All Extruder
Infill Ratio
30
%
Max Overhang Angle
30
Deg
Horizontal Offset
0.70
mm
Vertical Offset Top Layers
1
Vertical Offset Down Layers
1
Support Flowrate
100.0
%
Horizontal Expansion
0.20
mm
Solid Base Layers
2
Interlaced Support Infill Angle
Angle
0
Deg
Add Infill Angle
Remove Infill Angle
-45
Other
Pillar Size
4.00
mm
Add Sparse Connection
Generate Support under Small Floated Features
Support Expansion under Small Floated Features
1.00
mm
Recreate Support after Modifier Boolean Operation
Use Lines Pattern in High Density Grid Support Infill Pattern
Restore
Save As
Cancel
OK
Template: Standard - Pro3 Plus - TPU-95A
Type here to search (Ctrl + F)
Quality
Layer
Extruder
Infill
Solid Fill
Support
Platform Additions
Cooling
Temperature
Speed
Advanced
Ooze
Other
Special
GCode
Notes
Top and Down Solid Part
Base Solid Fill Layers
4
Solid Fill Layers
6
Base Solid Fill Pattern Type
Rectilinear
Solid Fill Pattern Type
Lines
Solid Fill Outline Shells
0
Solid Fill Minimal Width
0.00
mm
Solid Fill Expansion
0.00
mm
Expand Solid Fill to Fill Small Hole
0.00
mm
Use concentric filling for narrow solid fill parts
Monotonic Solid Fill
Base Monotonic Solid Fill
Monotonic Solid Fill
Top Surface Monotonic Solid Fill
Top and Down Solid Fill Angle
Angle
0
Deg
Add
Remove
45
135
Top Surface Solid Fill
Top Surface Solid Fill Layers
0
Top Surface Solid Fill Pattern Type
Lines
Top Surface Solid Fill Expansion
0.00
mm
Conditional Top Surface Pattern Type (Min Width)
0.00
mm
Conditional Top Surface Pattern Type (Min Area)
0.00
mm2
Bottom Surface Solid Fill
Bottom Surface Solid Fill Layers
1
Bottom Surface Solid Fill Pattern Type
Lines
Bottom Surface Solid Fill Expansion
0.00
mm
Ironing
Ironing Flowrate
5.0
%
Ironing Speed
10.0
mm/s
Ironing Monotonic
Ironing Angle
90
Deg
Ironing Line Distance
0.00
mm
Ironing Pattern
Rectilinear
Small Area Solid Fill Flow Compensation
Small Area Solid Fill Flow Compensation Model
Edit
Restore
Save As
Cancel
OK

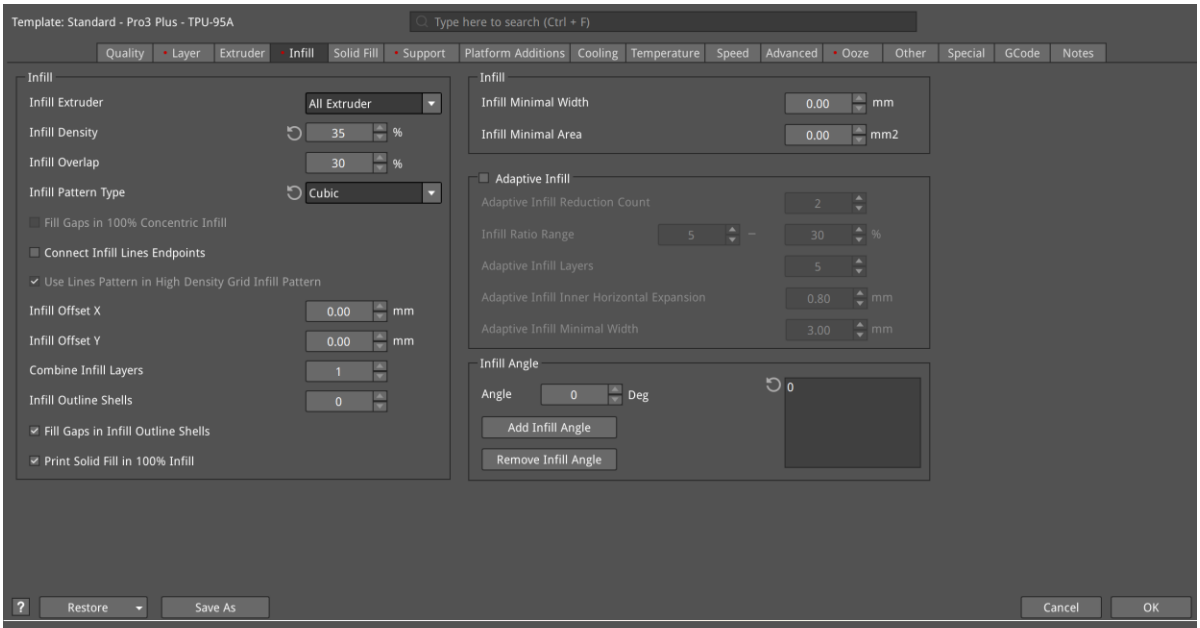
Template: Standard - Pro3 Plus - TPU-95A
Type here to search (Ctrl + F)
Quality
Layer
Extruder
Infill
Solid Fill
Support
Platform Additions
Cooling
Temperature
Speed
Advanced
Ooze
Other
Special
GCode
Notes
Infill
Infill Extruder
All Extruder
Infill Density
35
%
Infill Overlap
30
%
Infill Pattern Type
Cubic
Fill Gaps in 100% Concentric Infill
Connect Infill Lines Endpoints
Use Lines Pattern in High Density Grid Infill Pattern
Infill Offset X
0.00
mm
Infill Offset Y
0.00
mm
Combine Infill Layers
1
Infill Outline Shells
0
Fill Gaps in Infill Outline Shells
Print Solid Fill in 100% Infill
Infill
Infill Minimal Width
0.00
mm
Infill Minimal Area
0.00
mm2
Adaptive Infill
Adaptive Infill Reduction Count
2
Infill Ratio Range
5
30
%
Adaptive Infill Layers
5
Adaptive Infill Inner Horizontal Expansion
0.80
mm
Adaptive Infill Minimal Width
3.00
mm
Infill Angle
Angle
0
Deg
0
Add Infill Angle
Remove Infill Angle
Restore
Save As
Cancel
OK

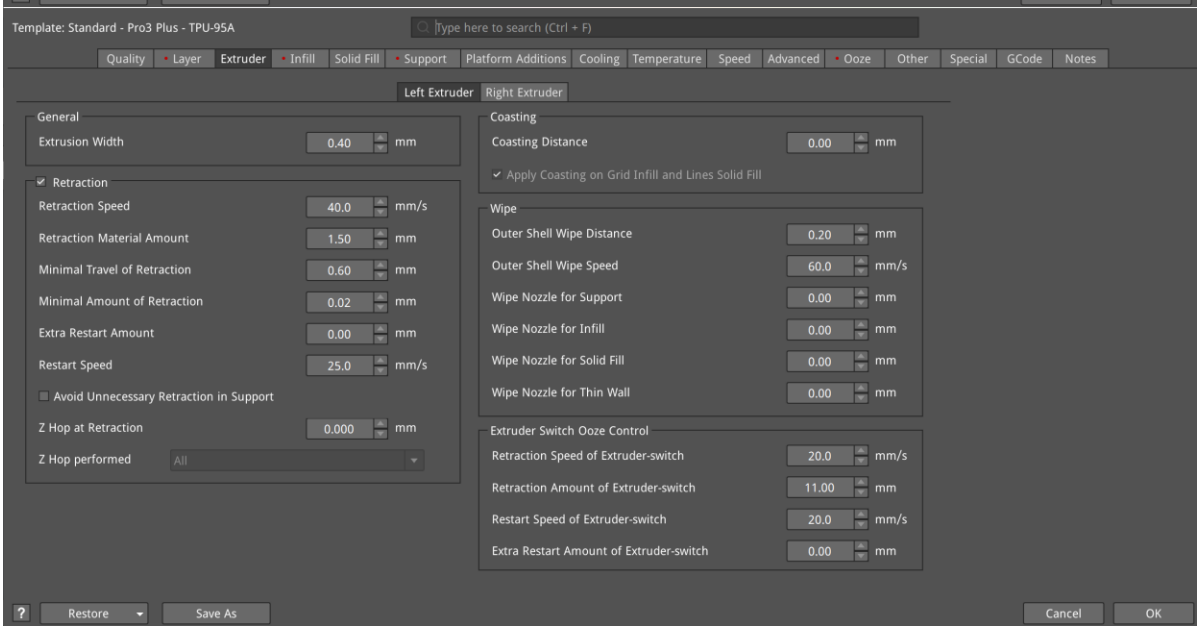
Template: Standard - Pro3 Plus - TPU-95A
Type here to search (Ctrl + F)
Quality
Layer
Extruder
Infill
Solid Fill
Support
Platform Additions
Cooling
Temperature
Speed
Advanced
Ooze
Other
Special
GCode
Notes
Left Extruder
Right Extruder
General
Extrusion Width
0.40
mm
Retraction
Retraction Speed
40.0
mm/s
Retraction Material Amount
1.50
mm
Minimal Travel of Retraction
0.60
mm
Minimal Amount of Retraction
0.02
mm
Extra Restart Amount
0.00
mm
Restart Speed
25.0
mm/s
Avoid Unnecessary Retraction in Support
Z Hop at Retraction
0.000
mm
Z Hop performed
All
Coasting
Coasting Distance
0.00
mm
Apply Coasting on Grid Infill and Lines Solid Fill
Wipe
Outer Shell Wipe Distance
0.20
mm
Outer Shell Wipe Speed
60.0
mm/s
Wipe Nozzle for Support
0.00
mm
Wipe Nozzle for Infill
0.00
mm
Wipe Nozzle for Solid Fill
0.00
mm
Wipe Nozzle for Thin Wall
0.00
mm
Extruder Switch Ooze Control
Retraction Speed of Extruder-switch
20.0
mm/s
Retraction Amount of Extruder-switch
11.00
mm
Restart Speed of Extruder-switch
20.0
mm/s
Extra Restart Amount of Extruder-switch
0.00
mm
Restore
Save As
Cancel
OK

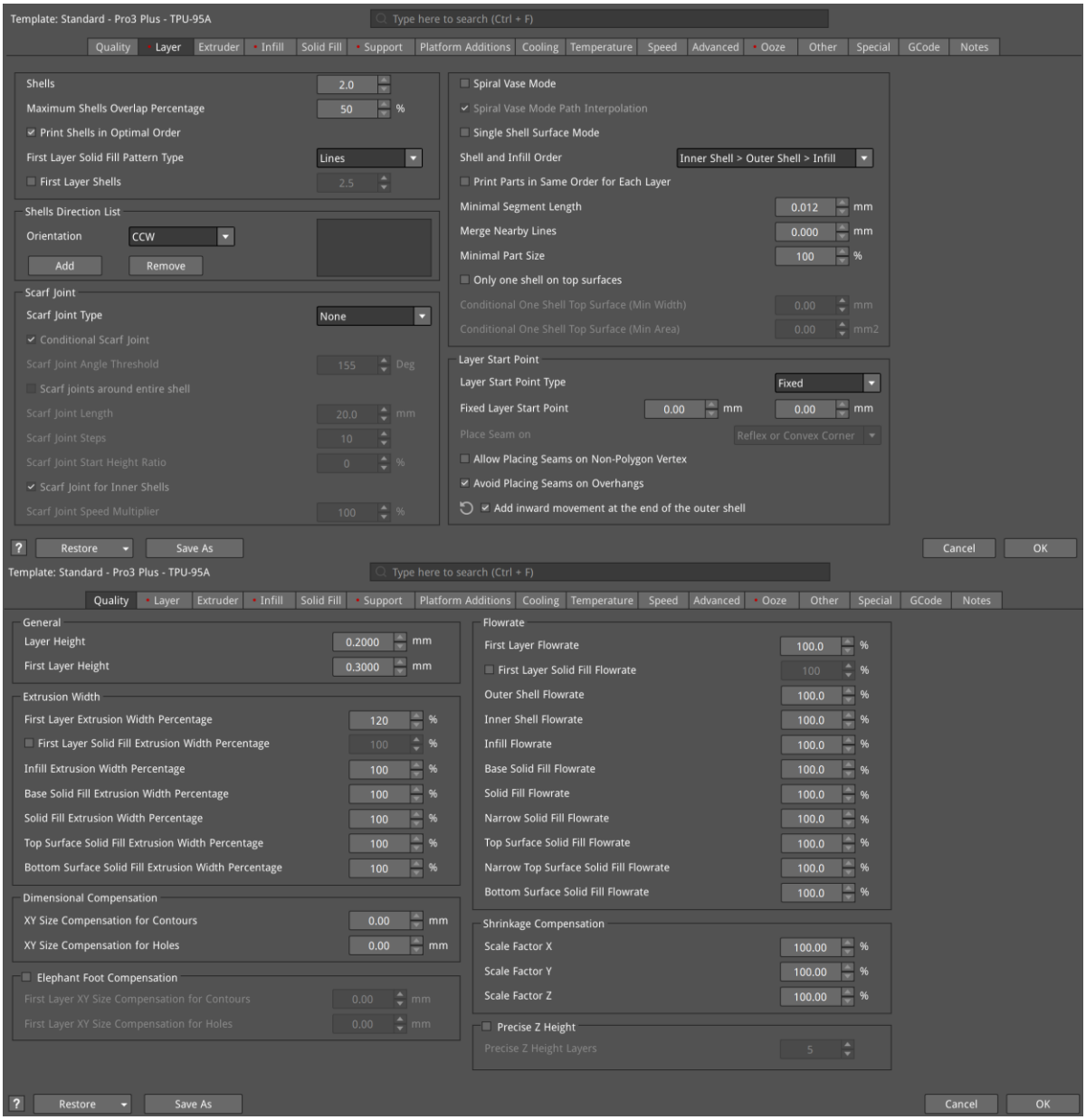
Template: Standard - Pro3 Plus - TPU-95A
Type here to search (Ctrl + F)
Quality
Layer
Extruder
Infill
Solid Fill
Support
Platform Additions
Cooling
Temperature
Speed
Advanced
Ooze
Other
Special
GCode
Notes
Shells
2.0
Maximum Shells Overlap Percentage
50
%
Print Shells in Optimal Order
First Layer Solid Fill Pattern Type
Lines
First Layer Shells
2.5
Shells Direction List
Orientation
CCW
Add
Remove
Scarf Joint
Scarf Joint Type
None
Conditional Scarf Joint
Scarf Joint Angle Threshold
155
Deg
Scarf joints around entire shell
Scarf Joint Length
20.0
mm
Scarf Joint Steps
10
Scarf Joint Start Height Ratio
0
%
Scarf Joint for Inner Shells
Scarf Joint Speed Multiplier
100
%
Spiral Vase Mode
Spiral Vase Mode Path Interpolation
Single Shell Surface Mode
Shell and Infill Order
Inner Shell > Outer Shell > Infill
Print Parts in Same Order for Each Layer
Minimal Segment Length
0.012
mm
Merge Nearby Lines
0.000
mm
Minimal Part Size
100
%
Only one shell on top surfaces
Conditional One Shell Top Surface (Min Width)
0.00
mm
Conditional One Shell Top Surface (Min Area)
0.00
mm2
Layer Start Point
Layer Start Point Type
Fixed
Fixed Layer Start Point
0.00
mm
0.00
mm
Place Seam on
Reflex or Convex Corner
Allow Placing Seams on Non-Polygon Vertex
Avoid Placing Seams on Overhangs
Add inward movement at the end of the outer shell
Restore
Save As
Cancel
OK
Template: Standard - Pro3 Plus - TPU-95A
Type here to search (Ctrl + F)
Quality
Layer
Extruder
Infill
Solid Fill
Support
Platform Additions
Cooling
Temperature
Speed
Advanced
Ooze
Other
Special
GCode
Notes
General
Layer Height
0.2000
mm
First Layer Height
0.3000
mm
Extrusion Width
First Layer Extrusion Width Percentage
120
%
First Layer Solid Fill Extrusion Width Percentage
100
%
Infill Extrusion Width Percentage
100
%
Base Solid Fill Extrusion Width Percentage
100
%
Solid Fill Extrusion Width Percentage
100
%
Top Surface Solid Fill Extrusion Width Percentage
100
%
Bottom Surface Solid Fill Extrusion Width Percentage
100
%
Dimensional Compensation
XY Size Compensation for Contours
0.00
mm
XY Size Compensation for Holes
0.00
mm
Elephant Foot Compensation
First Layer XY Size Compensation for Contours
0.00
mm
First Layer XY Size Compensation for Holes
0.00
mm
Flowrate
First Layer Flowrate
100.0
%
First Layer Solid Fill Flowrate
100
%
Outer Shell Flowrate
100.0
%
Inner Shell Flowrate
100.0
%
Infill Flowrate
100.0
%
Base Solid Fill Flowrate
100.0
%
Solid Fill Flowrate
100.0
%
Narrow Solid Fill Flowrate
100.0
%
Top Surface Solid Fill Flowrate
100.0
%
Narrow Top Surface Solid Fill Flowrate
100.0
%
Bottom Surface Solid Fill Flowrate
100.0
%
Shrinkage Compensation
Scale Factor X
100.00
%
Scale Factor Y
100.00
%
Scale Factor Z
100.00
%
Precise Z Height
Precise Z Height Layers
5
Restore
Save As
Cancel
OK

Appendix C: Jig Drawings

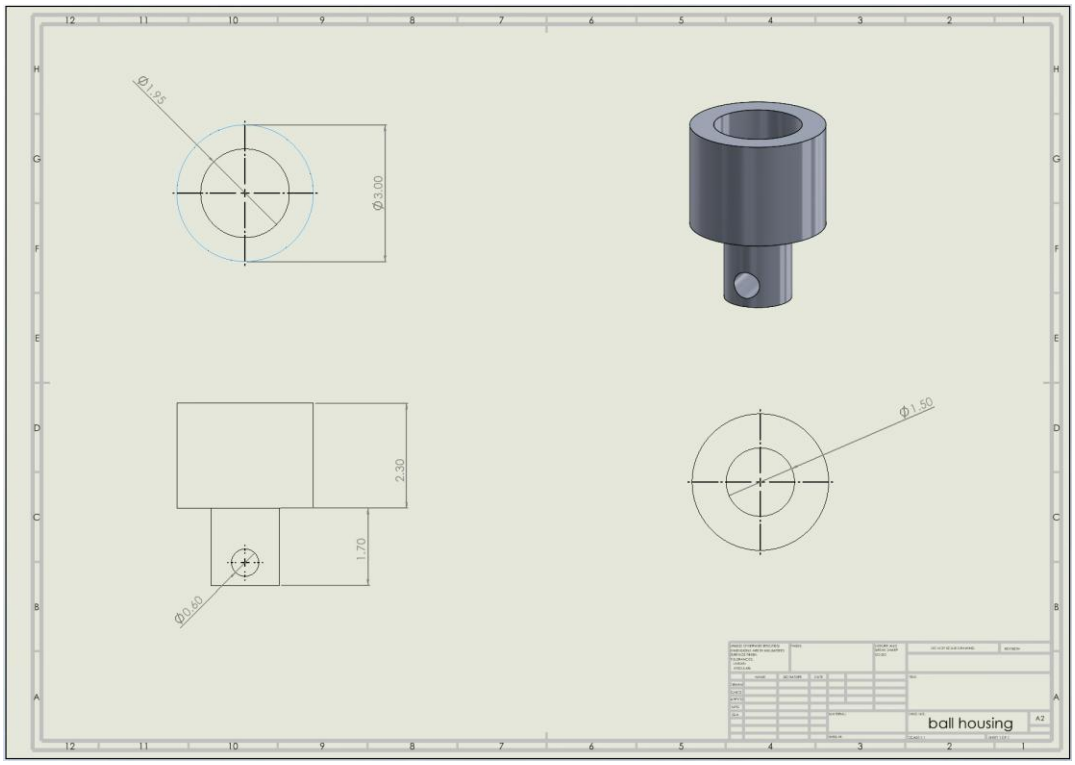

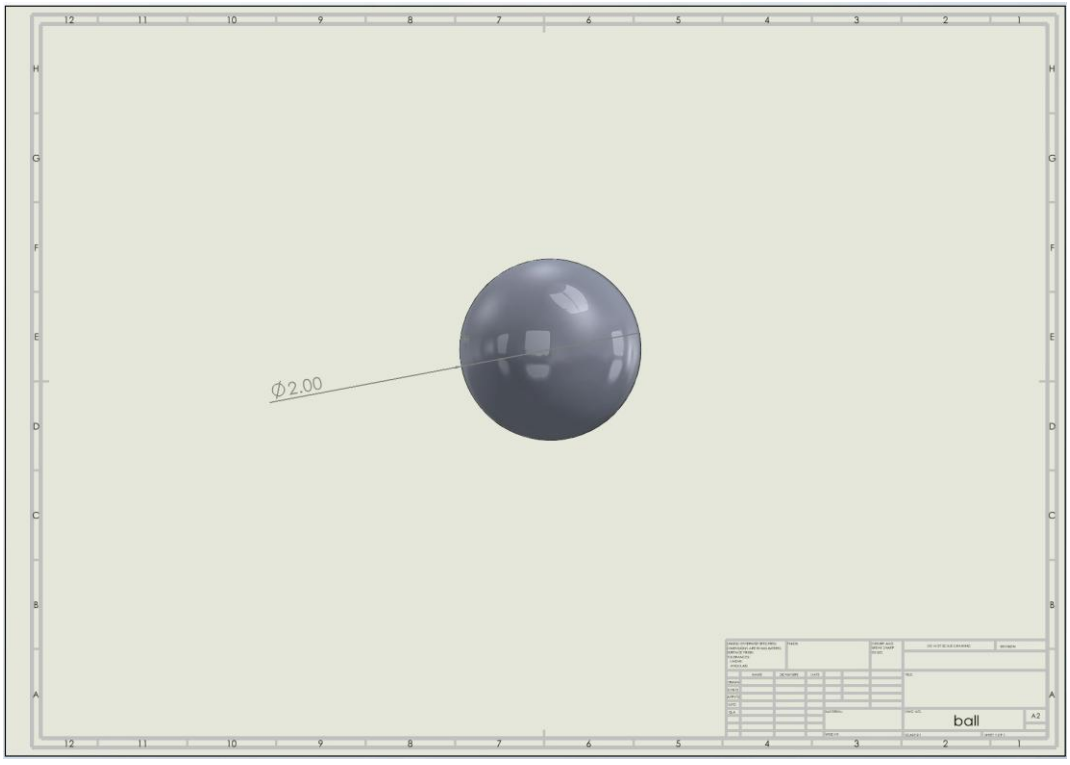

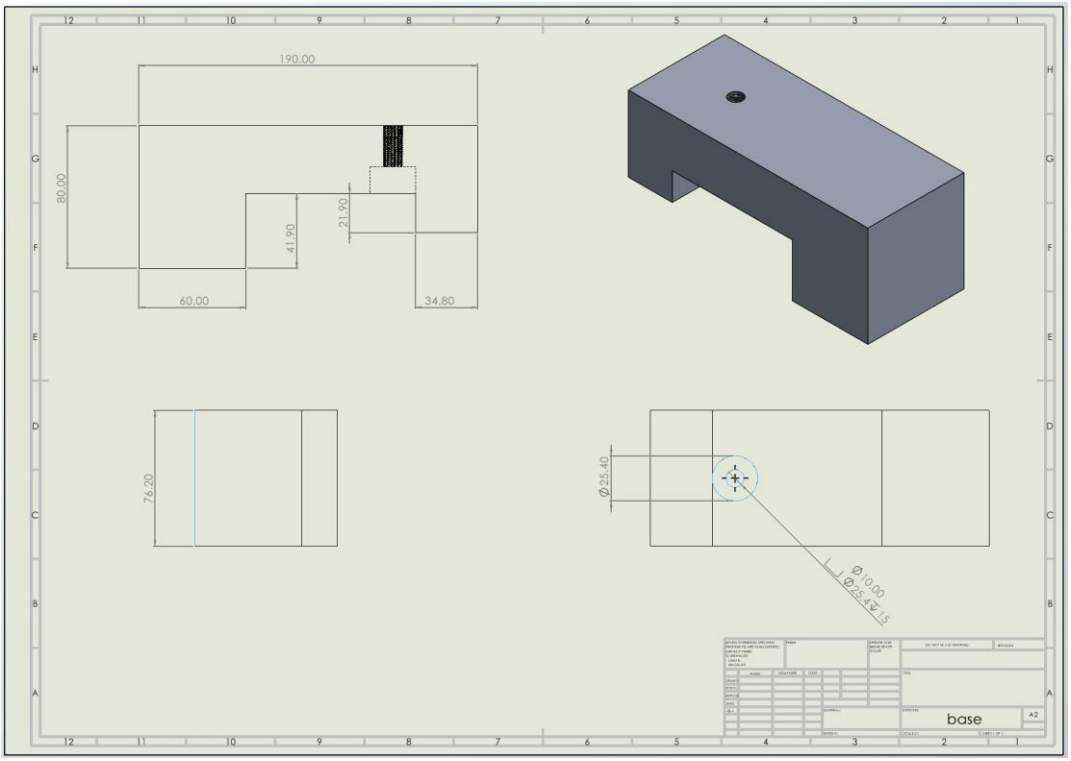

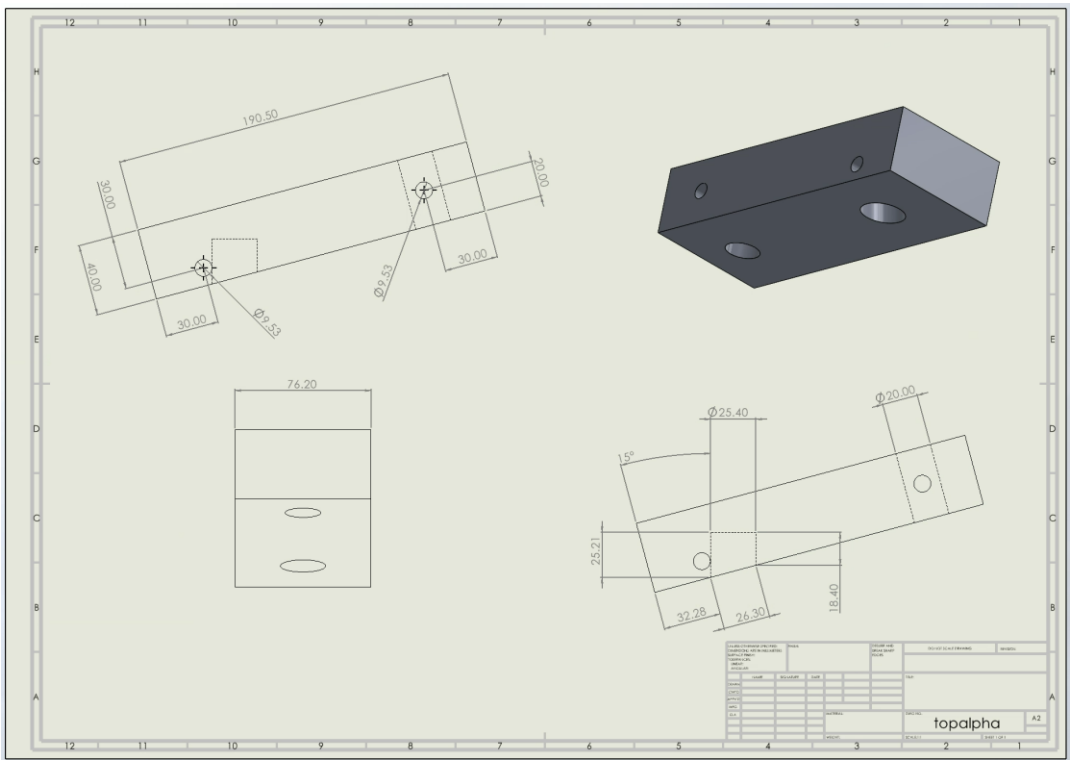

* Note: lockpin position is inaccurate in drawings. Position was adjusted by the machinist to center the corresponding hole

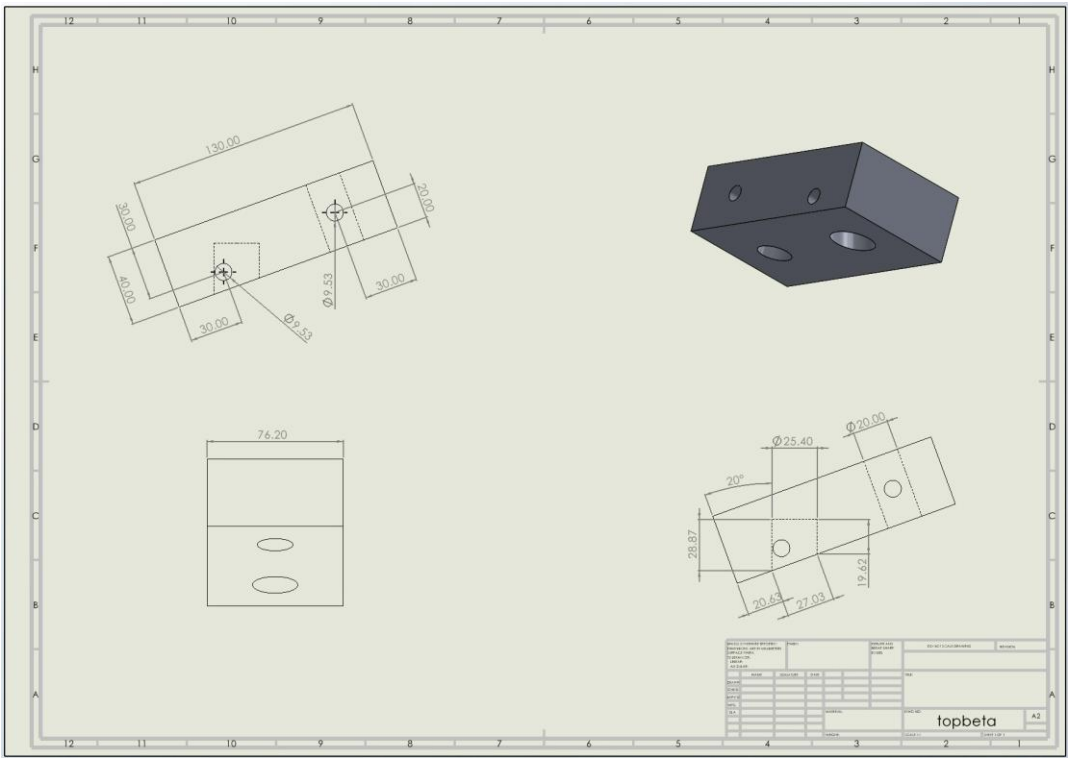

* Note: lockpin position is inaccurate in drawings. Position was adjusted by the machinist to center the corresponding hole